ULTRASONIC MACHINING OF TUNGSTEN CARBIDE, STELLITE AND DIAMOND

A thesis submitted
in fulfillment of the requirements
for the award of the degree
of

DOCTOR OF PHILOSOPHY

By

VINOD KUMAR
(Regn. No. 9030555)

DEPARTMENT OF MECHANICAL ENGINEERING
THAPAR UNIVERSITY
PATIALA-147004, INDIA
2009

CERTIFICATE

It is certified that the work presented in the thesis entitled **"ULTRASONIC MACHINING OF TUNGSTEN CARBIDE, STELLITE AND DIAMOND",** being submitted by Mr. Vinod Kumar, to the Department of Mechanical Engineering, Thapar University Patiala, in fulfillment of the degree of **DOCTOR OF PHILOSOPHY**, is a record of bonafide research work carried out by him under my guidance and supervision. The matter presented in this thesis has not been submitted either in part or full to any other university or institute for the award of any degree.

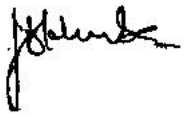

(Dr. J.S.Khamba)
(Supervisor)
Professor of Mechanical Engineering
University College of Engineering
Punjabi University Patiala (PB)-147002

PREFACE

This research work was carried out by the author under the guidance of Dr. J. S. Khamba, Professor of Mechanical Engineering, University College of Engineering, Punjabi University, Patiala (PB) (India). Ultrasonic drilling machine (SONIC-MILL, Albuquerque, USA), surface roughness measuring instrument (Perthometer, M4Pi), lathe tool Dynamometer (Kisteler), lathe tool (Kirolosakar),weighing machine and other facilities available in the Department of Mechanical Engineering, Thapar University, Patiala were used for this research work. Also some other equipments like scanning electron microscope (Jeol, Japan) available at sophisticated analytical insumentation facility, central instrumentation laboratory, Punjab University, Chandigarh were used for the investigation of ultrasonically machined samples.

Several research papers were published out of this research work. The list of international journals / international conferences in which the research papers find place is given below:

1. Kumar Vinod, Khamba J.S.(2008), Statistical analysis of experimental parameters in ultrasonic machining of tungsten carbide using taguchi approach, Journal of the American Ceramic Society, (*Blackwell publishers*) 91[1] pp. 92-96.
2. Kumar Vinod, Khamba J.S.(2006),Experimental investigation of ultrasonic machining of alumina-based ceramic composite, Journal of the American Ceramic Society, (*Blackwell publishers*) 89[8] pp. 2413-2417.
3. Kumar Vinod, Khamba J.S.(2009), An investigation into the ultrasonic machining of Co-based super alloy using the taguchi approach, International Journal of Machining and Machinability of Materials, (Inderscience Publishers) – (Accepted for publication)
4. Kumar Vinod, Khamba J.S.(2008), Optimization of tool wear rate in ultrasonic machining of tungsten carbide using taguchi methodology, Journal of Machining and Forming Technologies, (Inderscience Publishers) – (Communicated)
5. Kumar Vinod, Khamba J.S.(2005),Ultrasonic machining (USM) and its application to the machining of tough materials-a review; Proceedings of International Conference on Materials, Product Design and manufacturing (*ICMPM*), BIT Coimbtore, India in association with North Carolina State A & T University, Greensboro, USA, Dec 12-15, pp. 313-318.

6. Kumar Vinod,Khamba J.S.(2008),Optimization and modelling of process parameters in ultrasonic machining process,Proceedings of International Conference on Processing and Fabrication of Advanced Materials XVII (PFAM XVII) IIT , Delhi, Co-sponsored by American Society for Materials International ,USA and Centre for Tribology,California,USA, December 15-17, pp. 242-252.

(Vinod kumar)

ACKNOWLEDGEMENT

I am highly grateful to the authorities of Thapar University, Patiala for providing this opportunity to carry out the present research work. I acknowledge with deep sense of gratitude & humility, the inspiring help and guidance rendered by my supervisor, Dr. J.S.Khamba, Professor of Mechanical Engineering, University College of Engineering, Punjabi University, Patiala (PB) for his interest and encouragement throughout the research programme. His deep insight into the problem and ability to provide constructive suggestions have been of immense value in improving the quality of my research work at all stages.

Heartful thanks are due to Dr. Abhijit Mukherjee (Director, Thapar University, Patiala) and Dr.K.K.Raina (Dy. Director, Thapar University, Patiala) for their encouragement and support during this research work. The author expresses deep sense of gratitude to Dr. Susheel Mittal (Dean, Research and Sponsored Projects, Thapar University, Patiala) and Dr. S.K.Mohapatra, Professor & Head, Department of Mechanical Engineering, Thapar University, Patiala, who have been a source of inspiration and guidance, for persuing this work.

I am thankful to Mr. V.K. Singal, General Manager, Advanced Training Institute, Patiala for providing the facility for experiments during my research work at different stages. I acknowledge my thanks to Professor Tilak Bhardwaj, Director Sophisticated Analytical Insumentation Facility, Central Instrumentation Laboratory, Punjab University Chandigarh for providing the testing facilities for the machined surface.

The author wishes to thank Mr. Trilok Singh, Mr. Sukhdev Chand, Mr. Sohan Lal (Lab Superintendents, Machine Tool Lab and CAD Lab) Department of Mechanical Engineering, Thapar University, Patiala for providing all the possible assistance and co-operation during the course of experimental work.The author shall remain indebted to Mr. Charlie Wilhite (SONIC-MILL, Albuquerque, NM) for their technical advice. I am also thankful to the authors whose research has helped me a lot.

I express my gratitude to my wife Neelam, daughter Ritika and other family members for their patience, personal sacrifices and support throughout the research project. My firm faith in the almighty god has led me to face all the problems with a smile, and helped me to cross all the bridges which came my way during this journey of success. I would like to thank god for not letting me down at the time of crisis and showing me the silver lining in the dark clouds.

Last, but not the least, my parents deserve special mention for their love, affection and blessings showered on me to undertake and successfully complete this research work leading to Ph.D. degree.

Date: 17-11-2009 (**Vinod Kumar)**

Place: Patiala

ABSTRACT

This thesis presents an experimental and theoretical analysis of ultrasonic machining (USM) process with respect to machining characteristics and material properties of the work piece. Experimental work has been conducted on tungsten carbide, stellite and poly-crystalline diamond. Titanium alloys (TITAN 12, TITAN 15 and TITAN 31) have been used as the tool materials and aluminium oxide, silicon carbide and boron carbide as the abrasive slurries. The machine used for the experiments was ultrasonic drilling machine (SONIC-MILL, Albuquerque, USA). The data compiled during the experimentation has been used to get the responses in respect of material removal rate (MRR), surface roughness (SR) and tool wear rate (TWR). Further, the results have been modeled for their application in manufacturing industry.

In this investigation, the mathematical models considering the material properties have been employed to study the effects of operating parameters such as: power rating, abrasive slurry concentration, grit size of abrasive particles, type of abrasive slurry, tool material and work material .The model formulated in this work has been found to be much simpler in comparison to FEM and the results show an improved correlation with the experimental data. Moreover, the models developed have been capable of predicting the measure of performance for the USM process.

For USM processes, graphical representation of MRR, TWR and SR with operating parameters has been shown and compared with available existing results related to ultrasonic machining of titanium alloys. The application of taguchi method and F-test effect for the optimization of the process has been incorporated which was less explored by the previous researchers. By accounting for these phenomena, improved theoretical results have been obtained and consequently better correlation with experimental data is observed. From the experimental observations and with the help of basic power model, the multi-variant co-relation has been established for material removal rate, surface roughness and tool wear rate by varying the power rating, abrasive slurry concentration, grit size of abrasive particles, type of abrasive slurry, tool material and work material. The analysis of results and mathematical model has been developed with the help of statistica 7.0 software. Data related to MRR, TWR and SR for different experimental conditions has been presented. The significance of the responses also has been shown by graphical models. The degree of correlation between the analytical and experimental results is found to be quite satisfactory.

Besides the study of surface roughness by stylus method, the machined samples have been studied by scanning electron microscopy (SEM).The photomicrographs demonstrate a typical nature of machined surface, which is hardly evident from conventional stylus measurements, or transverse sections of the machined surface. These studies confirm the conclusions of the previous investigators regarding surface topography and material removal mechanism.

LIST OF TABLES

Table No.	Title	Page No.
1.1	Chemical analysis (%) of tungsten carbide	7
1.2	Chemical analysis (%) of stellite	8
1.3	Chemical analysis (%) of PCD	8
1.4	Chemical analysis (%) of TITAN 12 {UTS 240 Mpa}	8
1.5	Chemical analysis (%) of TITAN 15 {UTS 491 Mpa}	8
1.6	Chemical analysis (%) of TITAN 31 {UTS 994 Mpa}	8
2.1	Materials successfully machined by USM process	26
2.2	Properties of abrasives	26
3.1	Control variables and their levels	64
3.2	Modified L18 orthogonal array	65
3.3	Response variables	65
3.4	Taguchi design for experimentation	66
3.5	Representation of factors level	66
3.6	Test data experiment no.1	68
3.7	Test data experiment no.2	68
3.8	Test data experiment no.3	68
3.9	Test data experiment no.4	68
3.10	Test data experiment no.5	69
3.11	Test data experiment no.6	69
3.12	Test data experiment no.7	69
3.13	Test data experiment no.8	69

3.14	Test data experiment no.9	70
3.15	Test data experiment no.10	70
3.16	Test data experiment no.11	70
3.17	Test data experiment no.12	70
3.18	Test data experiment no.13	71
3.19	Test data experiment no.14	71
3.20	Test data experiment no.15	71
3.21	Test data experiment no.16	71
3.22	Test data experiment no.17	72
3.23	Test data experiment no.18	72
3.24	Observation table for experiment no. 1	77
3.25	Observation table for experiment no. 2	78
3.26	Observation table for experiment no. 3	79
3.27	Observation table for experiment no. 4	80
3.28	Observation table for experiment no. 5	81
3.29	Observation table for experiment no. 6	82
3.30	Observation table for experiment no. 7	83
3.31	Observation table for experiment no. 8	84
3.32	Observation table for experiment no. 9	85
3.33	Observation table for experiment no. 10	86
3.34	Observation table for experiment no. 11	87

3.35	Observation table for experiment no. 12	88
3.36	Observation table for experiment no. 13	89
3.37	Observation table for experiment no. 14	90
3.38	Observation table for experiment no. 15	91
3.39	Observation table for experiment no. 16	92
3.40	Observation table for experiment no. 17	93
3.41	Observation table for experiment no. 18	94
4.1	S/N ratio of MRR,SR,TWR for WC	115
4.2	Analysis of variance of MRR for WC	116
4.3	Analysis of variance of SR for WC	116
4.4	Analysis of variance of TWR for WC	117
4.5	S/N ratio of MRR,SR,TWR for stellite	118
4.6	Analysis of variance of MRR for stellite	119
4.7	Analysis of variance of SR for stellite	119
4.8	Analysis of variance of TWR for stellite	120
4.9	S/N ratio of MRR,SR,TWR for PCD	121
4.10	Analysis of variance of MRR for PCD	122
4.11	Analysis of variance of SR for PCD	122
4.12	Analysis of variance of TWR for PCD	123
4.13	Results of confirmatory experiments for tungsten carbide	124
4.14	Results of confirmatory experiments for stellite	125

4.15	Results of confirmatory experiments for PCD	125
5.1	Optimized process settings(Macro-model) for WC	129
5.2	Optimized process settings(Macro-model) for stellite	130
5.3	Optimized process settings(Macro-model) for PCD	131

LIST OF FIGURES

Figure No.	Title	Page No.
1.1	Basic features of ultrasonic machining process	4
2.1	Taguchi definition of noise	28
2.2	P-diagram for USM of tungsten carbide,stellite and diamond	31
3.1	Detailed drawing of the tool	32
3.2	Ultrasonic machine tool (Type: Sonic Mill, USA)	33
3.3	Amplitude coupling for compact 500W ultrasonic machine	33
3.4	Ultrasonic transducer for compact 500W ultrasonic machine	33
3.5	Pump for re-circulation of abrasive slurry	33
3.6	Power rating set-up for ultrasonic machine	33
3.7	Ultrasonic tool	33
3.8	Detailed drawing of the work geometry	34
3.9	MRR Vs Power rating for TITAN 12 tool while machining WC (case1)	37
3.10	TWR Vs Power rating for TITAN 12 tool while machining WC (case1)	37
3.11	MRR Vs Power rating for TITAN 15 tool while machining WC (case1)	37
3.12	TWR Vs Power rating for TITAN 15 tool while machining WC (case1)	38
3.13	MRR Vs Power rating for TITAN 31 tool while machining WC (case1)	38
3.14	TWR Vs Power rating for TITAN 31 tool while machining WC (case1)	38
3.15	MRR Vs Power rating for TITAN 12 tool while machining WC (case2)	39
3.16	TWR Vs Power rating for TITAN 12 tool while machining WC (case2)	39
3.17	MRR Vs Power rating for TITAN 15 tool while machining WC (case2)	39
3.18	TWR Vs Power rating for TITAN 15 tool while machining WC (case2)	40
3.19	MRR Vs Power rating for TITAN 31 tool while machining WC (case2)	40
3.20	TWR Vs Power rating for TITAN 31 tool while machining WC (case2)	40
3.21	MRR Vs Power rating for TITAN 12 tool while machining WC (case3)	41
3.22	TWR Vs Power rating for TITAN 12 tool while machining WC (case3)	41
3.23	MRR Vs Power rating for TITAN 15 tool while machining WC (case3)	41
3.24	TWR Vs Power rating for TITAN 15 tool while machining WC (case3)	42
3.25	MRR Vs Power rating for TITAN 31 tool while machining WC (case3)	42
3.26	TWR Vs Power rating for TITAN 31 tool while machining WC (case3)	42
3.27	MRR Vs tool material, grit size, power rating, aluminium oxide while	43

	machining WC	
3.28	TWR Vs tool material, grit size, power rating, aluminium oxide while machining WC	43
3.29	MRR Vs Power rating for TITAN 12 tool while machining WC (case4)	44
3.30	TWR Vs Power rating for TITAN 12 tool while machining WC (case4)	45
3.31	MRR Vs Power rating for TITAN 15 tool while machining WC (case4)	45
3.32	TWR Vs Power rating for TITAN 15 tool while machining WC (case4)	45
3.33	MRR Vs Power rating for TITAN 31 tool while machining WC (case4)	46
3.34	TWR Vs Power rating for TITAN 31 tool while machining WC (case4)	46
3.35	MRR Vs Power rating for TITAN 12 tool while machining WC (case5)	46
3.36	TWR Vs Power rating for TITAN 12 tool while machining WC (case5)	47
3.37	MRR Vs Power rating for TITAN 15 tool while machining WC (case5)	47
3.38	TWR Vs Power rating for TITAN 15 tool while machining WC (case5)	47
3.39	MRR Vs Power rating for TITAN 31 tool while machining WC (case5)	48
3.40	TWR Vs Power rating for TITAN 31 tool while machining WC (case5)	48
3.41	MRR Vs Power rating for TITAN 12 tool while machining WC (case6)	48
3.42	TWR Vs Power rating for TITAN 12 tool while machining WC (case6)	49
3.43	MRR Vs Power rating for TITAN 15 tool while machining WC (case6)	49
3.44	TWR Vs Power rating for TITAN 15 tool while machining WC (case6)	49
3.45	MRR Vs Power rating for TITAN 31 tool while machining WC (case6)	50
3.46	TWR Vs Power rating for TITAN 31 tool while machining WC (case6)	50
3.47	MRR Vs tool material, grit size, power rating, silicon carbide slurry while machining WC	50
3.48	TWR Vs tool material, grit size, power rating, silicon carbide slurry while machining WC	51
3.49	MRR Vs Power rating for TITAN 12 tool while machining WC (case7)	52
3.50	TWR Vs Power rating for TITAN 12 tool while machining WC (case7)	52
3.51	MRR Vs Power rating for TITAN 15 tool while machining WC (case7)	53
3.52	TWR Vs Power rating for TITAN 15 tool while machining WC (case7)	53
3.53	MRR Vs Power rating for TITAN 31 tool while machining WC (case7)	53
3.54	TWR Vs Power rating for TITAN 31 tool while machining WC (case7)	54
3.55	MRR Vs Power rating for TITAN 12 tool while machining WC (case8)	54
3.56	TWR Vs Power rating for TITAN 12 tool while machining WC (case8)	54

3.57	MRR Vs Power rating for TITAN 15 tool while machining WC (case8)	55
3.58	TWR Vs Power rating for TITAN 15 tool while machining WC (case8)	55
3.59	MRR Vs Power rating for TITAN 31 tool while machining WC (case8)	55
3.60	TWR Vs Power rating for TITAN 31 tool while machining WC (case8)	56
3.61	MRR Vs Power rating for TITAN 12 tool while machining WC (case9)	56
3.62	TWR Vs Power rating for TITAN 12 tool while machining WC (case9)	56
3.63	MRR Vs Power rating for TITAN 15 tool while machining WC (case9)	57
3.64	TWR Vs Power rating for TITAN 15 tool while machining WC (case9)	57
3.65	MRR Vs Power rating for TITAN 31 tool while machining WC (case9)	57
3.66	TWR Vs Power rating for TITAN 31 tool while machining WC (case9)	58
3.67	MRR Vs tool material, grit size, power rating, boron carbide slurry while machining WC	58
3.68	TWR Vs tool material, grit size, power rating, boron carbide slurry while machining WC	58
3.69	MRR Vs tool material, grit size, power rating, aluminium oxide slurry while machining stellite	59
3.70	TWR Vs tool material, grit size, power rating, aluminium oxide slurry while machining stellite	59
3.71	MRR Vs tool material, grit size, power rating, silicon carbide slurry while machining stellite	59
3.72	TWR Vs tool material, grit size, power rating, silicon carbide slurry while machining stellite	60
3.73	MRR Vs tool material, grit size, power rating, boron carbide slurry while machining stellite	60
3.74	TWR Vs tool material, grit size, power rating, boron carbide slurry while machining stellite	60
3.75	MRR Vs tool material, grit size, power rating, aluminium oxide slurry while machining PCD	61
3.76	TWR Vs tool material, grit size, power rating, aluminium oxide slurry while machining PCD	61
3.77	MRR Vs tool material, grit size, power rating, silicon carbide slurry while machining PCD	61
3.78	TWR Vs tool material, grit size, power rating, silicon carbide slurry	62

	while machining PCD	
3.79	MRR Vs tool material, grit size, power rating, boron carbide slurry while machining PCD	62
3.80	TWR Vs tool material, grit size, power rating, boron carbide slurry while machining PCD	62
3.81	Schematic of the ultrasonic machine tool (Type: Sonic Mill, USA)	74
3.82	Surface roughness tester, Perthometer (Mahr, M4Pi)	75
3.83	Scanning electron microscope (JSM 6100, Japan)	95
3.84	SEM Photograph for WC, Stellite and PCD (Before machining)	96
3.85	SEM Photograph for WC, Stellite and PCD (Expt. No.1)	97
3.86	SEM Photograph for WC, Stellite and PCD (Expt. No.2)	98
3.87	SEM Photograph for WC, Stellite and PCD (Expt. No.3)	99
3.88	SEM Photograph for WC, Stellite and PCD (Expt. No.4)	100
3.89	SEM Photograph for WC, Stellite and PCD (Expt. No.5)	101
3.90	SEM Photograph for WC, Stellite and PCD (Expt. No.6)	102
3.91	SEM Photograph for WC, Stellite and PCD (Expt. No.7)	103
3.92	SEM Photograph for WC, Stellite and PCD (Expt. No.8)	104
3.93	SEM Photograph for WC, Stellite and PCD (Expt. No.9)	105
3.94	SEM Photograph for WC, Stellite and PCD (Expt. No.10)	106
3.95	SEM Photograph for WC, Stellite and PCD (Expt. No.11)	107
3.96	SEM Photograph for WC, Stellite and PCD (Expt. No.12)	108
3.97	SEM Photograph for WC, Stellite and PCD (Expt. No.13)	109
3.98	SEM Photograph for WC, Stellite and PCD (Expt. No.14)	110
3.99	SEM Photograph for WC, Stellite and PCD (Expt. No.15)	111
3.100	SEM Photograph for WC, Stellite and PCD (Expt. No.16)	112
3.101	SEM Photograph for WC, Stellite and PCD (Expt. No.17)	113
3.102	SEM Photograph for WC, Stellite and PCD (Expt. No.18)	114
4.1	Effects of process parameters on S/N ratio of MRR for WC	116
4.2	Effects of process parameters on S/N ratio of SR for WC	117
4.3	Effects of process parameters on S/N ratio of TWR for WC	118
4.4	Effects of process parameters on S/N ratio of MRR for stellite	119
4.5	Effects of process parameters on S/N ratio of SR for stellite	120
4.6	Effects of process parameters on S/N ratio of TWR for stellite	120

4.7	Effects of process parameters on S/N ratio of MRR for PCD	122
4.8	Effects of process parameters on S/N ratio of SR for PCD	123
4.9	Effects of process parameters on S/N ratio of TWR for PCD	123
4.10	Comparison of initial Vs optimum conditions	126
5.1	MRR Vs Power (TITAN 12 tool, WC work material)	135
5.2	MRR Vs Power (TITAN 15 tool, WC work material)	135
5.3	MRR Vs Power (TITAN 31 tool, WC work material)	136
5.4	MRR Vs Power (TITAN 12 tool, stellite work material)	136
5.5	MRR Vs Power (TITAN 15 tool, stellite work material)	137
5.6	MRR Vs Power (TITAN 31 tool, stellite work material)	137
5.7	MRR Vs Power (TITAN 12 tool, PCD work material)	137
5.8	MRR Vs Power (TITAN 15 tool, PCD work material)	138
5.9	MRR Vs Power (TITAN 31 tool, PCD work material)	138
5.10	TWR Vs Power (TITAN 12 tool, WC work material)	139
5.11	TWR Vs Power (TITAN 15 tool, WC work material)	140
5.12	TWR Vs Power (TITAN 31 tool, WC work material)	140
5.13	TWR Vs Power (TITAN 12 tool, stellite work material)	141
5.14	TWR Vs Power (TITAN 15 tool, stellite work material)	141
5.15	TWR Vs Power (TITAN 31 tool, stellite work material)	142
5.16	TWR Vs Power (TITAN 12 tool, PCD work material)	142
5.17	TWR Vs Power (TITAN 15 tool, PCD work material)	143
5.18	TWR Vs Power (TITAN 31 tool, PCD work material)	143

LIST OF APPENDICES

Appendix No.	Description	Page No.
I	Introduction of tungsten carbide	164
II	Introduction of stellite	165
III	Introduction of Diamond	166
IV	Introduction of titanium	167

CONTENTS

	Page No.
CERTIFICATE	I
PREFACE	II-III
ACKNOWLEDGEMENT	IV-V
ABSTRACT	VI-VII
LIST OF TABLES	VIII-XI
LIST OF FIGURES	XII-XVI
LIST OF APPENDICES	XVII
CHAPTER – I	
INTRODUCTION	**1-10**
1.1 Historical background of ultrasonic machining(USM)	2
1.2 USM process	3
1.3 Objectives and issues	7
1.4 Scope of the work	7
1.5 Overall methodology of the study	8
1.6 Organization of the thesis	9
CHAPTER – II	
LITERATURE REVIEW	**11-31**
2.1 Review of literature	11
2.2 Basic elements of USM	11
2.2.1 Tool holder	11
2.2.2 Ultrasonic transducer	12
2.2.3 Ultrasonic power supply	12
2.2.4 Tools and abrasives	13
2.3 Material removal mechanisms	14
2.4 Process Parameters	16
2.4.1Work-piece properties	16
2.4.2 Tool characteristics	18
2.4.3 Abrasive slurry properties	19
2.5 Surface properties	20

2.6 Taguchi methodology 22
2.7 Combination of USM with other processes 23
2.8 Process capabilities 23
2.9 Process capabilities of conventional tool and work materials 26
2.10 Need for research and areas of study 27
2.11 Parameter design 28
2.12 Taguchi approach for design 28
2.12.1 Description of orthogonal arrays 29
2.12.2 Steps in robust design 29
2.13 Control factors, signal and noise factors for study 30

CHAPTER – III

EXPERIMENTATION 32-114

3.1 Introduction 32
3.2 Description of ultrasonic machine 32
3.3 Preliminary study to assess the existing status 35
3.4 Pilot experimentation 36
3.5 Selection of factor levels 64
3.6 Definition of S/N ratio 72
3.6.1 Lower-the-Better type problem 72
3.6.2 Higher-the-Better type problem 73
3.6.3 Nominal-the-Best type problem 73
3.7 Experimentation work 74
3.8 Analysis of microstructure 95

CHAPTER – IV

RESULTS AND DISCUSSION 115-127

4.1 Introduction 115
4.2 Analysis of results 115
4.3 Confirmatory experimentation 124
4.3.1 Performing the confirmatory experiments 124
4.3.2 Follow-up experiments 127
4.3.3 Range of applicability 127

CHAPTER – V

MODELING OF RESULTS 128-143

5.1 Introduction 128

5.2 Macro model for predicting machining characteristics of tungsten carbide,stellite and diamond 128

5.3 Micro model for predicting machining characteristics of tungsten carbide,stellite and diamond 132

5.3.1 Micro model for predicting material removal rate 132

5.3.2 Micro model for predicting tool wear rate 138

CHAPTER – VI

CONCLUSIONS AND SCOPE OF FUTURE WORK 144-148

6.1 Conclusions 144

6.2 Limitations 147

6.3 Scope of future work 148

REFERENCES 149-163

APPENDICES 164-168

CHAPTER-I

INTRODUCTION

Current techniques for mechanical working of ordinary materials like steels and cast iron are highly developed and machine tools have been greatly improved in recent years. Recent years have seen the introduction of many new materials such as tungsten and titanium carbides, diamonds, rubies, sapphire, hard steels, magnetic alloys and corrundum. Another group of materials, germanium, silicon, ferrites, ceramics, glass, quartz etc give difficulty on account of great brittleness; these materials often can not withstand the forces needed for machining. Modern materials such as high-strength steels and ceramics, which are developed to meet the needs of advanced industries like Goetze Escorts, are typically strong, hard and brittle. Whilst technologically desirable, these characteristics often render the materials difficult and sometimes impossible, to shape by machining processes into useful components and parts. The cutting action imposed by above said machining processes on brittle materials, for example, will yield components with very poor surface finish and in many cases, results in the chipping and/or fracture of the materials being machined.

The cutting process during machining is one of fracture of material at or near the tip of a cutting tool. In a ductile material, cracking (or material separation at or ahead of the tool tip) proceeds at a speed dictated by the relative velocity between the cutting tool and the work piece, as plasticity at the crack tip (i.e. crack tip blunting) prevents the crack running too far ahead of the crack or tool tip. As the same crack blunting mechanism is not available in hard and brittle materials (because of the lack of plasticity) the crack at the tool tip propagates uncontrollably ahead of the tool tip, giving rise to chipping and fracture.

The improvement of machining quality can be vitally promoted through the conversion of this machining process into one involving controllable high frequency impacts at the cutting zone. This is achieved through the generation and maintenance of ultrasonic vibrations in the cutting tool to alter the fracture process in brittle materials to one in which loading of the materials at the tool tip is incremental, repetitive and under control. Engineering ceramic materials have many attractive properties such as high hardness, high thermal resistance, chemical stability and low electrical conductivity etc. Ceramic composites are assuming increasing industrial importance in machine building

and engineering fields, mainly because of the fact that technological limitations can be overcome by the use of these non-metallic materials. It is for this reason that ceramic composites have gained acceptance in a number of applications imposing extreme demands on one or more properties of the material. Despite their outstanding properties as compared to metals, ceramic composites are only gradually gaining acceptance in mechanical and engineering applications. One reason for this is found to be in the limitations of the forming process which is done prior to sintering, which restricts the generation of complex geometries and makes it difficult to ensure adequate accuracy and surface finish.

There is also a considerable deficit in terms of the production or machining of more complex geometries in the hardened post-sintered state. With limitations on either the performance or the forming capacity of the majority of processes in current use, the machining of ceramic composites to final dimension by conventional methods is extremely difficult and time consuming. Tight tolerances and dimensions together with surfaces of good quality and acceptable sub-surface damage are something attainable at more cost during ultrasonic machining process.

The need for methods of machining these "unworkable" materials has led to the introduction of special methods e.g. electrochemical, electro erosion, electron beam and ultrasonic machining. Ultrasonic machining is a 'non-traditional' machining technique and is a part of a family of relatively modern material finishing and shaping processes described as 'chip less machining'. These processes don't use cutting tools and do not create residual stresses in the work piece. Ultrasonic machining is often used in combination with other chip less machining techniques, such as electric discharge machining, in the manufacturing of precision components.

1.1 HISTORICAL BACKGROUND OF ULTRASONIC MACHINING (USM)

The history of ultrasonic machining (USM) began with a paper by R.W. Wood and A.L Loomis in 1927 and the first patent was granted to L. Balamuth in 1945.The British patent no. 602801 (1945), issued to an American engineer, L. Balamuth, who discovered ultrasonic machining accidentally in 1942, while he was investigating the dispersion of solid in liquid by means of a magnetostrictively vibrating nickel tube. The use of ultrasonic in machining was first proposed by J.O. Farrer in 1945. The United States patent, for the process, no. 2580716 was issued in 1962.

The first report on the advanced machining equipment and technology appeared by 1954, the machine tools using the ultrasonic principle had been designed and constructed.

Originally USM used to be a finishing operation for the component processed by the electro spark machines. But then with the boom in solid state electronics, the machining of electrically non-conducting, semi conductive, and brittle material gets more and more important and, for this reason, ultrasonic machining again gained importance and prominence. In recent years, various types of ultrasonic machine tools have been developed.

1.2 USM PROCESS

The research in the field of more efficient material removal processes has been gathering momentum in recent years especially in the ways and means to reduce the occurrence of faults or cracks in the sub-surfaces of the machined ceramic composites. Ultrasonic machining process is an abrasive process, and material removal is purely mechanical. The process equipment consists of a vibrational horn (the sonotrode), a tool part, abrasive slurry and the work material as shown in figure 1.1. Ultrasonic machining is a process in which abrasive particles in slurry with water are presented to the work surface in the presence of an ultrasonically vibrating tool. It is a process which should be of considerable interest, as its potential is not limited by electrical or chemical characteristics of the work materials. This machining method can easily perform cutting, drilling and engraving, making it suitable for the processing of ceramics.

As the name implies the process operates at ultrasonic frequencies and typical frequencies used in the ultrasonic machining process range between 20 and 40 KHz. The term ultrasonic is used to describe vibration waves having a frequency above the hearing range of normal human ear i.e. beyond 15 KHz. This would include a wide range of ultrasonic is largely dependent on the generator, practical limitation imposing a maximum frequency in the region of 500 Mc/s. The wavelength in varying media is very wide. For example, when propagated in a solid medium, a wave with the frequency of 25 Kc/s will have a wavelength of about 200 mm, while one with a frequency of 500 Mc/s will have a wavelength of the order of 0.008 mm.

The acoustic range of vibration is the one which the human ear perceives i.e. in the frequency range of 30 to 15000 Hz, the ultrasonic range of vibration lies above this i.e. frequencies beyond 15000 Hz. There is no physical difference between the upper acoustic range 5000 to 15000 Hz and the ultrasonic range 15000 to 30000 Hz. Both the range of frequencies of certain intensities of sound will be heard as loud noise by the human ear and can permanently damage the auditory system. Ultrasonic frequencies of the same intensities of sound cannot be heard by human ear and they are less harmful. Ultrasonic

frequencies provide satisfactory working conditions and hence they are alone used for the material removal purposes. There are two types of waves, namely shear waves and longitudinal waves. Longitudinal waves are mostly used in ultrasonic applications since they are easily generated. They can be propagated in solids, liquids and gases and can travel at a high velocity so that their wavelength is short in most media.

The velocity of the wave can be calculated for a given material using the following expression:

Sonic velocity= $E/\rho\left[m(m-1)/(m^2-m-2)\right]^{1/2}$

E = Young's modulus

1/m= Poisson's ratio

ρ = Density of the material

The equipment used is based upon a generator energizing a magnetostrictive or piezoelectric transducer which in turn causes an attached tool to vibrate. The vibrating tool transfers energy to abrasive particles carried, within a slurry, underneath the tool tip. The interaction between these particles and the work piece results in the formation of mirror image of the tool tip in the surface of the work piece.

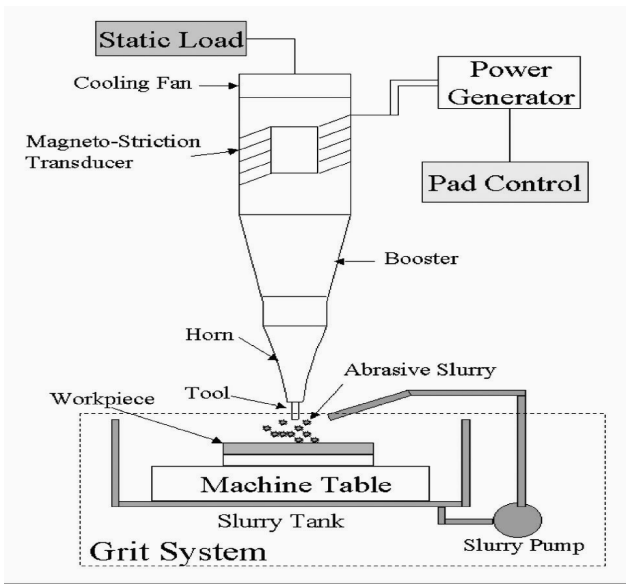

Figure 1.1 Basic features of the ultrasonic machining process

Early design used a magnetostrictive transducer attached to an exponential horn (with a nominal length of one half wavelength) with a small tool brazed to the tip of the horn. Due to the production of heat within the transducer core, this arrangement tended to have

an efficiency of about 50%. Current systems are more likely to use a piezoelectric transducer attached to a 'booster' in the form of a stepped cylinder (nominally one half wavelength long). The booster is, in turn, attached to the tool (again nominally one half wavelengths long). The change in cross-section of the booster causes amplification of the amplitude of vibration at the tool tip. A change in cross-section of the tool can be used to further amplify the vibration. The transducer/booster/tool assembly is located by a clamp around the midpoint or node of the booster.

Ultrasonic machining is a form of abrasion; the brittle material is removed by blows from grains of a harder abrasive, which is under the control of a tool, which vibrates with small amplitude. The abrasive also causes wear in the tool but this is minimized by making the tool of viscous material. The particles of abrasive are themselves cleaved in the process and so must be gradually replaced by running into the working area, a liquid carrying fresh abrasive which also serves to flush away products. The material is cut away as very small particles, but these are produced by many abrasive grains and the tool vibrates at a high frequency so the total rate of removal can be sufficient for practical purposes.

Tool may be advanced in the direction of vibration, in which case a cavity is produced whose profile corresponds precisely to that of the tool. Combinations of movements allow one to perform a variety of operations on brittle materials analogous to those of ordinary milling, shaping, profile milling, and so on. The noise resulting from this process is minimized by choosing a frequency in the low ultrasonic range (16-25 Kc/s).The valuable features of the method possibly of working super hard and very brittle materials and ease of piercing and recessing, precision working immediately attracted attention.

Ultrasonic Machining (USM) is a modern machining process with decisive advantages, as a result of which, its use is becoming more and more widespread. Last five decades have witnessed rapid developments of advanced metals and alloys, hence increasing demand for their machining and fabrication. For better performance of machining of components made from such materials, close tolerances and higher surface finish are must. Hence, for the sake of economy, the components must be machined at a fast rate in minimum number of set ups. These requirements have partly been met by the use of a number of advance machining processes as shown in table 1.1. These processes, often called as non-conventional machining methods or modern machining processes are characterized by the absence of plastic deformation and chip formation, as is normally the

case in conventional machining. For metal removal, non-conventional methods directly utilize some form of the energy viz., mechanical, electro-chemical, chemical or thermal. Some of the advance machining processes, amongst which the notable ones is USM, has found fairly widespread applications in industry. An idea of the popularity of USM may be obtained from survey conducted in USSR, here EDM accounts for 75% of total utilization of newer machining processes. In USA, a four-fold increase in the number of USM machines installed in the industry was observed between the year 1970 and 1980. Extremely high popularity enjoyed by the USM process is due to its versatility. The process is capable of machining practically all electrically conducting materials, irrespective of their strength and toughness. Even fragile jobs can conveniently be machined and complicated machining details may easily transfer from the tool onto the work piece with a high degree of accuracy and surface finish. Furthermore, the process can easily be automated and overall production rate in many cases compares favorably with the conventional processes. However, a number of problems accompanying the USM process still remain unsolved.

USM, as a production process, has influenced its existence in variety of fields and industries during the recent years. Other than tool & die making, it has occupied the area of production of component parts in aerospace, medical, optical, automotive, gauge making, templates, standards, electronics, cutting tools, ceramics, composites, and nuclear industries.Conventional Machining of Metal Matrix Composites (MMCs) posed difficulty due to abrasive nature of ceramic reinforcement. As the fraction of ceramic increased in the composite, ductility and toughness reduced while the hardness increased .USM is one such technique which can be effectively used for MMCs. To get the best out of USM, it is a must that the operators, programmers, designers and service engineers engaged in the use of the process equipment should be well aware of the inputs and outputs of the process. Unfortunately, all but a very few operating personel receive any formal training and that too perhaps only from an associate who likewise, learned by practice and became self-taught.

1.3 OBJECTIVES AND ISSUES

To carry out research on ultrasonic machining of tungsten carbide, stellite and diamond using different tool materials to know their impact on MRR and tool wear and to model these characteristics for their application in manufacturing industry. The following issues have been taken up during this research wok.

- The process capability of ultrasonic machining has been discussed for conventional tool and work materials.
- Machining of tungsten carbide, stellite and poly-crystalline diamond (PCD) have been explored by three titanium alloys as tool materials; TITAN-12, TITAN-15 and TITAN-31 in ultrasonic machining.
- Tool Wear of aforesaid tool materials have been studied in machining of tungsten carbide, stellite and poly-crystalline diamond (PCD).
- Relationship between different machining parameters (slurry type, slurry concentration, slurry grit-size, work material, tool material, power rating) and material properties (material removal rate, tool wear rate and surface roughness) have been established.
- The results achieved have been modeled for their application in manufacturing industry.

1.4 SCOPE OF THE WORK

The work has been limited to tungsten carbide, stellite and poly-crystalline diamond (PCD) as work material with three titanium alloys as tool materials ; TITAN-12,TITAN-15 and TITAN-31 for experimentation. The machining of tungsten carbide, stellite and poly-crystalline diamond (PCD) have been explored for their use in manufacturing industry. The typical composition of aforesaid work materials is as follows:

Table 1.1 Chemical analysis (%) of tungsten carbide

C	O	Co	W
27.24	3.51	4.57	64.67

Table 1.2 Chemical analysis (%) of stellite

Co	60.27	Fe	1.54	Mo	0.098
Cr	28.64	Si	1.45	B	0.001
W	4.91	C	1.24	P	0.021
Ni	1.79	Mn	0.024	S	0.010

Table 1.3: Chemical analysis (%) of PCD

C	H	N	O
85.5	1	2.5	10

Table 1.4: Chemical analysis (%) of TITAN-12, UTS 240 Mpa

C	H	N	O	Fe	Ti
0.01	0.015	0.03	0.03	0.07	99.85

Table 1.5: Chemical analysis (%) of TITAN-15, UTS 491 MPa

C	H	N	O	Fe	Ti
0.006	0.0007	0.014	0.140	0.05	99.78

Table 1.6: Chemical analysis (%) of TITAN-31, UTS 994 MPa

C	H	N	O	Al	V	Fe	Ti
0.019	0.0011	0.007	0.138	6.27	4.04	0.05	89.47

1.5 OVERALL METHODOLGY OF THE STUDY

The overall work has been divided into four phases:

1. Detailed literature survey
2. Design of experiments
3. Experimentation
4. Modeling the results

To design a methodology for carrying out analysis on machining of tungsten carbide, stellite and diamond (PCD), literature on ultrasonic machining and its constituent aspects have been reviewed extensively. The literature survey has been focused on the various

aspects of ultrasonic machining covering technical and economical viability. At the start of design of experiments (DOE) phase, pilot experiments have been performed for machining of tungsten carbide, stellite and diamond (PCD) machining with USM .The various machining conditions have been selected based upon results of pilot study. After this, considering the results of pilot study, experiments have been designed to determine the MRR of tungsten carbide, stellite and poly-crystalline diamond (PCD) with different tool materials TITAN-12, TITAN 15 and TITAN-31 under the environmental conditions. Accordingly tool wear of aforesaid tool materials have been studied. For the design of experiments (DOE), taguchi technique for robust design, using L18 orthogonal arrays has been used. The experiments have been done on USM (500 W), Sonic mill, Albuquerque, USA. The effect of MRR, TWR and SR has been established for machining of tungsten carbide, stellite and poly-crystalline diamond (PCD) with aforesaid tool materials.The following input machining parameters have been taken for the different sets of experimentation.

- Type of abrasive slurry used
- Grit size of abrasive particle
- Concentration of abrasive slurry
- Power rating of ultrasonic machine

The results showed that the response variables were strongly influenced by the control factors. So, the results obtained after experimentation have been modeled using both "MACRO" and "MICRO" modeling approach. This has been followed by taguchi, L18 orthogonal array approach for both macro modeling and Buckingham- theorem for micro modeling for implementation of various control factors in manufacturing industries to achieve the desired levels of performance.

1.6 ORGANIZATION OF THE THESIS

The thesis has been divided into six chapters. The brief description of each chapter is as following:

Chapter -I (Introduction), is concerned with general introduction of USM process and its industrial applications. The scope of present work for ultrasonic machining of tungsten carbide, stellite and diamond (PCD) has been focused. The need and importance of

ultrasonic machining with its impact on productivity and performance also has been discussed. An overview of USM and problems associated with machining of aforesaid materials for manufacturing industry has been explored. The significant issues like various control factors affecting the process have been determined. The objectives and scope of study and overall methodology applied has also been briefly explored.

Chapter-II (Literature Review), deals with the review of the published literature relevant to the present work with coverage of metal removal mechanism, tool wear rate, process parameters, surface integrity and material parameters of USM process. The literature related to control factors, signal and noise factors and response variables has also been explored.

Chapter -III (Experimentation work), presents experimental set-up for investigating the effect on MRR, TWR and surface finish. The study also includes selection of factors levels by pilot experimentation. The experimentation procedure, observational data and test data report as per taguchi designed experiments have been described.

Chapter -IV (Results and Discussion), is concerned with the detailed discussion and analysis of generated data with respect to MRR, TWR and SR.

Chapter –V (Modeling of results), is concerned with both macro and micro modeling approach. Micro model has been developed using regression analysis and macro model has been developed using taguchi approach.

Chapter -VI (Conclusions and scope of future work) is the concluding chapter which encompasses the experimental results derived and their interpretation in the light of supporting evidence generated either during the course of the present investigation or referred from the literature. Also explores the possibility for future work in the area. At the end, all the references of other researchers in the related area, consulted and utilized for the interpretations of the results, have been listed.

CHAPTER-II

LITERATURE REVIEW

2.1 REVIEW OF LITERATURE

The engineers and technologists know the process of USM for over five decades now, but accelerated developments in this area have occurred only during the last few years. Extensive research in this field has led to better understanding of the phenomenon of metal erosion, development of processes leading to higher rates of metal removal, excellent surface finish and low tool wear. Some machines with numerical and adaptive controls have also appeared in the market .Qualitative information about tool wear or the work piece erosion has been investigated. A comprehensive review of literature on diverse aspects of ultrasonic machining and machining characteristics of tungsten carbide, stellite and diamond has been investigated, which has helped to identify the areas explored in this study. In this chapter the author reviews the published literature relevant to the topic of the thesis for the following heads:

2.2 BASIC ELEMENTS OF USM

The machines for USM range from small table-top sized units to large capacity machine tools. In addition to the part size capacity of a USM machine, suitability for a particular application is also determined by power rating. The material removal rate is directly related to power capacity of the machine. All USM machines share common subsystems regardless of the physical size or power. The most important of these subsystems are the power supply, transducer, tool holder, tool and abrasives [118,123].

2.2.1 Tool holder

The purpose of tool holder is to attach and hold the tool to the transducer. It transfers the ultrasonic vibration from the converter to the tool. Material for horn should have good acoustical properties. Titanium is considered for the fabrication of horns. Horns are also made of brass, steel and monel [94-96]. These horns are generally used for tools that are over 25.4mm in diameter. Tool holders are attached to the transducer by means of a large, loose-fitting screw. Half hard copper washers are used between the transducer and tool holder to dampen and cushion the interface, which further reduces the chances of unwanted ultrasonic welding. The horn is variously referred to as an acoustic coupler, velocity/mechanical transformer, tool holder, concentrator, stub or sonotrode [152,159].The oscillation amplitude

at the face of a transducer is too small (0.001-0.1 μm) in order to achieve any reasonable cutting rate, therefore, the horn is used as an amplification device.

The tool holders are available in two configurations: amplifying and non-ammplifying.Non-amplifying tool holders are cylindrical and results in the same stroke amplitude at the output end as at the input end [151]. Amplifying tool holders have a modified cross-section and are designed to increase the amplitude of the tool stroke. The material used should have high wear resistance, good elastic and fatigue strength properties, and have optimum values of toughness and hardness for the application. Tungsten carbide, silver steel and Monel are commonly used tool materials. Diamond (PCD) has been recently used for the machining of very hard work piece such as hot iso-statically pressed silicon nitride. Tool can be attached to tool horn by either soldering, brazing or screw fitting [134-136]. Also, the actual tool configuration can be machined on to the end of the horn. Threaded joints are conventionally used because of the quick and easy tool changing, however problems can occur such as self-loosening, loss of acoustic power, fatigue failure etc.

2.2.2 Ultrasonic transducer

The 20,000Hz electrical energy from the power supply is applied to the transducer element, herein after referred to as the converter, which transforms the high frequency electrical oscillation into high frequency mechanical vibration. Two types of transducers used for USM are based on two different principle of operation, piezoelectric and magnetostrictive.The heart of the converter is a lead zirconate titanate electrostrictive element which when subjected to an alternating voltage, expand and contract at the frequency of the voltage[122]. This electrostrictive converter is highly efficient and the degree of energy conversion is 96%. Magnetostrictive transducers are usually constructed from a laminated stack of nickel or nickel alloy sheets [121]. These types of transducers are rugged but have electromechanical conversion efficiencies ranging from only 20 to 35%.

2.2.3 Ultrasonic power supply

This solid state variable output power supply with internal or external power control, converts (50-60) Hz electrical power into 20,000 Hz electrical power [124,125]. The power supply for USM is more accurately characterized as a high power sine-wave generator that offers the user control over both the frequency and power of the generated signal. The power supply is designed for continuous duty industrial operation. For optimum efficiency, it is equipped with automatic frequency control and automatic load compensation, providing constant output amplitude at desired setting to meet the different

energy requirement encountered during the operation cycle [20, 29, 32]. The power supply incorporates an overload monitor to protect the system from the conditions that could normally result in failure if an overload condition occurs [127,129]. The monitor shut off the ultrasonic for the balance of the cycle and activates the front panel overload indicator lamp. Although the monitor will automatically reset itself for subsequent operation until the fault condition is eliminated. The monitor will reactivate on each operating cycle preventing damage to the transistors.

2.2.4 Tools and abrasives

For minimum tool wear, tools should be constructed from relatively ductile materials such as stainless steel, brass and mild steel [131,132]. The harder the tool material, the faster its wear rate will be. Depending on the abrasive used, work piece / tool wear ratios can range from 1:1 to 100:1. Whenever possible, USM tools to be used for hole drilling are constructed from easily obtained materials such as music wire, stainless steel tubing or hypodermic needles. The tool is normally held against the work piece by a static load exerted via a counter weight/static weight, spring pneumatic/hydraulic or solenoid feed system [119,120]. Sahu and Sagar [49] developed the abrasive cut-off wheel having side grooves. For the optimum results, the system should maintain a uniform working force while machining and be sufficiently sensitive to overcome the resistance due to the cutting action. Static load values of 0.1-30 N are typically used. The force is particularly critical when drilling small holes less than 0.5mm diameter as bending of the tool can occur under too high a load. Solid tools used to produce cavities can be fabricated by machining, casting or coining; however finishing or polishing operations are sometimes necessary because the tool holders should be free from scratches, nicks and heavy machining marks, because these produce risers and lead to early fatigue failure[126]. Because of the over cut that occurs with this process, allowances must be made to use tool smaller than the desired hole or cavity e.g. to allow for the diameter of tubing to drill holes equal to the desired hole diameter minus twice the abrasive particle size. The most desirable method of attaching the tool to the holder is silver brazing. This eliminates the fatigue problems associated with mechanical screw attachment method. Amin et.al [39] established a computer-aided design procedure for the horn profile and material, based on finite-element analysis. The optimization procedure was followed for the profile to obtain maximum magnification, for higher rates of material removal and safe working stresses

for the horn material.Azarhoushang and Akbari [82] presented the design of an ultrasonically vibrated tool holder and the experimental investigation of ultrasonically assisted drilling of Inconel 738-LC. The circularity, cylindricity, surface roughness and hole oversize of the ultrasonically and conventionally drilled workpieces were measured and compared. The obtained results showed that the application of ultrasonic vibration can improve the hole quality considerably. Zeng et.al [58] presented the results on tool wear and cutting forces in RUM of SiC. Skelton [94] studied a magnetostrictive transducer used to vibrate a carbide-tipped cutting tool during turning. It was found that cutting force components to be less than with a static tool, particularly at low cutting speeds.Wang et al. [19] investigated the use of ultrasonic vibration lapping to enhance the precision of micro holes drilled by micro electro-discharge machining. It was concluded from the experimental results that the machining method, compounded the MEDM and MUVL process had a good ability to produce precision micro holes with high aspect ratio. A slurry concentration of 20% was more suitable for the circular tool processes, while a concentration of 10% was effective in the stepped circular tool processes. If circular tools were used in the MUVL processes, the variations between entrances and exits would decrease with increasing ultrasonic vibration amplitudes. Furthermore, if stepped circular tools were used, the differences between the diameters of the entrances and exits were smallest at the vibration amplitudes of 5.4 μm. Tool rotating speed significantly affected the grinding effect of abrasive particles for the MUVL method. Wong et.al [37] presented an approach to approximate the exponential curve required for CNC machining of the exponential tool holder.The fast algorithms were developed to approximate the exponential curve as a composite curve of linear or circular segments for a given tolerance.It was concluded that the tool holders having tapering cross sections to increase the amplitude of the tool stroke, resulted in higher material removal rate.

2.3. MATERIAL REMOVAL MECHANISMS

Shaw [162] investigated the machining mechanisms of hard and brittle materials. These mechanisms comprised of: Material abrasion by direct hammering of the abrasive particles against the work piece surface; Micro chipping by impact of the free moving abrasive particles;Cavitation effect from the abrasive slurry; Chemical action associated with the fluid used. The individual or combined effect of the above mechanisms resulted in work piece material removed by shear, by fracture (for hard and work hardened

material) and displacement of material at the surface, without removal, by plastic deformation, which realized simultaneously at the transient surface [140,145,146].Miller [112] assumed that the abrasive particles are of cubical shape developed an expression for material removal rate that included plastic deformation, work hardening and chipping. Rozenberg [27] reviewed the theories and on the basis of high speed photography and concluded that material removal was primarily due to hammer blows by the tool on the abrasive in contact with the work surface. It was investigated the effect of cavitation and concluded that it affects the ultrasonic machining process in two ways: one by erosion of the tool and second by reducing the amount of abrasive in the gap. Davim [102] detemined the design of optimization of cutting conditions for turning metal matrix composites based on the orthogonal arrays. Zhao et.al [103] determined that bending vibration cutter bar played very important role in the ultrasonic vibration cutting systems. The new ultrasonic vibrating cutting system included symmetrical, side clamping structure, and it possessed two stage amplification function.Wei et.al (2007) studied ultrasonic-assisted lapping of gears and compared with conventional lapping in material removal process and mechanism. The results of this set of experiments revealed that the optimum conditions for a high removal rate in the ultrasonic lapping experiments of spiral-bevel gears were of brake torque, 0.12 Nm; pinion rotational speed, 600 rpm; and slurry concentration of 20%. The contributions by percentage of torque, speed and concentration to the removal rate were 8.13, 19.26 and 68.11, respectively.Lee et.al [30] concluded that any increase in the amount of work/energy imparted to the machined ceramics in terms of the amplitude of the tool tip, the static load applied and the grit size of the abrasive, resulted in an increase in the material removal rate and a roughening of the machined surface.This conclusion was also verified by various researchers [141-144].Rajurkar et.al [104] presented experimental simulation of the process mechanics in an attempt to analyze the material removal mechanism in machining of ceramic (Al_2O_3). The results showed that low-impact force caused only structural disintegration and particle dislocation and the high-impact force contributed to cone cracks and subsequent crater damage. Fang et.al [44] presented various experimental techniques to study this transition and discussed the mechanism of the surface generation.

Wang et.al [50] discussed on fundamental principles of ultrasonic machining, the material removal mechanism and the calculation of critical factors. Ductile machining of brittle materials, even at a high criticaldepth-of-cut, was realized by applying ultrasonic vibration to a diamond tool tip. A surface roughness Ra of 100 μm at a 2 μm depth of cut

was achieved. Liu et.al [14] studied ductile mode chip formation in conventional cutting and ultrasonic vibration assisted cutting of tungsten carbide work piece material.It was investigated through experimental grooving tests using CBN tools on a CNC lathe. The experimental results showed that as the depth of cut was increased, there was a transition from ductile mode to brittle mode chip formation in grooving both with and without ultrasonic vibration assistance. Soundararajan and Radhakrishnan [85] studied a simple but effective approach using a profile relocation technique to study the relative role of the two processes. Kainth et.al [35] presented an analysis of material removal in ultrasonic machining considering direct impact of abrasive grains on the workpiece. Non-uniformity of abrasive grains was considered by using a probability distribution for the diameter of the abrasive particles. Pei et.al [70] presented the experimental evidence to show that plastic flow can also be one of the material removal modes in RUM in addition to brittle fracture. Majeed et.al [16] studied $Al_2O_3/LaPO_4$ composites of varying compositions in order to evaluate the response to machining. They illustrated the significance of $LaPO_4$ addition on machinability of $Al_2O_3/LaPO_4$ composites in terms of MRR, AE response and whole geometry and associated defects. Pei and Ferreira [17] worked on the modeling of ductile-mode material removal in rotary ultrasonic machining and concluded that as the vibration amplitude, static force increased and the tool rotational speed increased, MRR increased.

2.4 PROCESS PARAMETERS

2.4.1 Work piece properties

Goetze [42] suggested that the work-piece of tungsten carbide be mounted rigidly on a heavy, movable anvil, and that this whole anvil assembly be forced at a given pressure against a tool tip which was made to vibrate by the ultrasonic transducer. Lia et.al [109] developed a three-dimensional finite element analysis (FEA) model to study the effects of three parameters (cutting depth, support length, and pretightening load) on the maximum normal stress and von Mises stress in the region where the edge chipping initiates. Guzzo et.al [113] investigated the ultrasonic abrasion of different work piece materials like alumina, zirconia, quartz, glass, ferrite by using a stationary ultrasonic machine. They concluded that in the case of alumina, zirconia and quartz, the rates of material removal decreased with the depth of machining. Hocheng et.al [26] studied an ultrasonic polish of mild steel and conducted an experiment on typical mold steel with emphasis on the effect of the abrasive size and the static load on the surface finish.Ramakrishnan and

Brahmankar[15] studied the fatigue characteristics of electrodischarge machined alumina particulate reinforced aluminium matrix composites.

Singh and Khamba [106] investigated the ultrasonic machining of tough materials like titanium and its alloys. The results of study highlighted that higher hardness of work piece was not the criteria for higher material removal rate in machining of titanium and its alloys. Kim and choi [75] studied ultrasonic vibration cutting as a substitute for such processes in the precision machining of optical plastics (CR-39) which was used for optical lenses was suggested and experimented upon. As a result, in micro cutting by ultrasonic vibration, it was confirmed that surfaces of ductile cutting were obtained, for depths of cut of less than 2.7 μm. Wang and Li [59] studied the effects of alloying yttrium on the wear behavior of a commercial wear-resistant alloy, stellite 6, at elevated temperatures. The wear behaviors of the samples at various temperatures from the room temperature up to 650 °C were evaluated using a high temperature pin-on-disc tribometer. Thoe et.al[7] reviewed the fundamental principles of ultrasonic machining, the material removal mechanisms involved and the effect of operating parameters on material removal rate, tool wear rate and work piece accuracy with particular emphasis on the machining of engineering ceramics. Liaoa et. al[8] discussed the ultrasonic vibration assisted drilling of Inconel 718 super alloy and concluded that the chip size was reduced, and the variation of torque in drilling becomes smaller. George et.al [9] determined that electrode wear rate reduced substantially, within the region of experimentation, if the parameters were set at their lowest values, while the parameters set at their highest values increased the MRR drastically for the electric discharge machining of carbon composites. Moriwaki et.al [86] studied the ultraprecision ductile cutting of glass.It was realized by applying ultrasonic vibration to a single crystal diamond tool in the cutting direction. The transparent surface of soda-lime glass with surface roughness of 0.03 μm R_{max} was obtained by face turning.

Zhou et.a [87] investigated the ultrasonic vibration diamond cutting of glasses to determine the effect of tool vibration on the brittle–ductile transition mechanism. The effect of cutting speed on the critical depth of cut was studied by groove cutting experiments. Hsu et.al [60] discussed the machining characteristics of Inconel 718 by combining ultrasonic vibration with high-temperature-aided cutting. It was investigated that cutting was increasingly difficult owing to precipitating the hard secondary phase of

γ″(Ni_3Nb), thus the cutting force was higher than that at room temperature. Formation of built-up-edge (BUE) when using a NX2525 cermet cutter was far less than that of a TN35 tungsten carbide cutter, the surface roughness and the cutting force were lower than those for a TN35 tungsten carbide cutter. Singh and Khamba [61] reviewed machining of titanium and its alloys with three different slurries (namely silicon carbide, boron carbide and alumina) and detailed background work on machinability of the same in ultrasonic drilling. Dam et.al [38] investigated that tough materials gave a low production rate, a high tool wear, and a low surface roughness and for brittle materials the relationships were reversed; high production rate, low tool wear and high surface roughness.

2.4.2 Tool characteristics

Lia et.al [47] investigated the feasibility to machine CMC using RUM. A three-variable two-level full factorial design was employed to reveal main effects as well as interaction effects of three RUM process parameters (spindle speed, feed rate, and ultrasonic power). Adithan and Venkatesh [31] presented different aspects of tool wear. Tool wear in ultrasonic drilling was affected by a number of factors such as work material, tool material, work material thickness, tool size and cross sectional area, heat treatment of the tool, static load, cutting time and type of abrasives used. Komaraiah and Narasimha [40] investigated that the harder the tool material, the larger the material removal rates. The results showed of the various tool materials used, Nimonic-80A proved to be the best. Khairy [53] studied the mechanisms underlying the micro chipping action in ultrasonic machining that was mainly localized hammering and free impact by abrasive grains in the slurry. These effects were characterized to occur in random fashion with respect to their strength and location on the work surface. Chiang [114] outlined the modeling and analysis of the effects of machining parameters on the performance characteristics in the EDM process of Al_2O_3+TiC mixed ceramic. Xiao et. al [163] investigated to effect of tool nose radius in ultrasonic vibration cutting of hard material and developed a vibration cutting method. They outlined that in the case of nickel base alloy incone 1600, the allowable tool nose radius in vibration cutting was 0.2 mm, while one in conventional cutting was 0.02 mm. The nearest value (Ry = 4.7 um) of the predicted surface as a suitable nose radius.The vibration cutting's experiment using the suitable nose radius of 0.2 mm showed that the tool fracture was prevented and the machining accuracy was

improved in comparison with an initial nose radius of 0.02 mm. Lin [18] studied the ultrasonic exponential horns in longitudinal and torsional composite vibration modes.

2.4.3 Abrasive slurry properties

Several abrasives are available in various sizes for ultrasonic machining (grit). The criteria for selection of an abrasive for a particular application include hardness, usable life, cost and particle size [130,137]. In order of hardness, boron carbide, silicon carbide and aluminum oxide are the most commonly used abrasives. The abrasive used for an application should be harder than the material being machined; otherwise the usable life time of the abrasive will be substantially shortened. Boron carbide is selected when machining the hardest work piece materials or when the highest material removal rates are desired [133,138]. Although the cost is five to ten times greater than the next hardest abrasive, silicon carbide, the usable life of boron carbide is 200 machine operating hours before cutting effectiveness is lost and disposal is necessary. This compares with a usable life time of approximately 60 hours for silicon carbide. The combination of high removal rates and extended life time justify the higher cost of boron carbide. The size of abrasive particles influences the removal rate and surface finish obtained. Abrasive for USM are generally available in grit sizes ranging from 240 to 800 while the coarser grit exhibit the highest removal rates, they also result in the roughest surface finish and are therefore, used only for roughing operation, conversely, 800 grit abrasives will result in fine surface finishes but at a drastic reduction in metal removal rate. The most popular general purpose abrasive used, based on the above considerations, is 320 grit boron carbide. The abrasive material is mixed with water to from the slurry. The abrasive material is mixed with water to form the slurry. The most common abrasive concentration is 50% by weight; however, this can vary from 30 to 60 percent. The thinner mixtures are used to promote efficient flow when drilling deep holes or when forming complex cavities. Once the abrasive has been selected and mixed with water, it is stored in a reservoir at the USM machine and pumped to the tool work piece interface by recirculating pumps at rates up to 26.5 lit/min. Higher power ultrasonic machine require the addition of a light-duty cooling system to remove waste heat from the abrasive slurry[147-149]. Hocheng et.al [51] discussed the effects of various parameters of ultrasonic drilling of two-dimensional carbon fiber-reinforced silicon carbide(C/SiC) composites including abrasives, volume ratio, electric current and down-force, on the material removal rate, hole clearance, edge

quality and tool wear. Komaraiah et.al [54] studied the influences of the type and size of the abrasive grains used and the amplitude of ultrasonic oscillations. An attempt was made to study the influence of the rotation of the work piece, in addition to an ultrasonically oscillated tool, on the material removal rate and surface roughness of the work pieces produced.Hocheng and Hsu [36] highlighted the influence of the concentration of abrasives, the size of abrasive grains, the energy of ultrasonic oscillation and the feed rate of tool on the machinability in respect of material removal rate, surface roughness and hole clearance on the ultrasonic drilling of Carbon/Epoxy and Carbon/PEEK. The examination of surfaces and abrasives after machining illustrated the hammering and impact of the abrasive particles on the workpiece. Klopfstei et.al [84] studied the Micro-ultrasonic machining of single crystal silicon using 0.1 and 0.25µm diamond abrasives and a 200µmdiameter cemented carbide cylindrical tool. Anantha Ramu et.al [115] discussed the behavior of certain tool material and work material combinations with respect to penetration rate and tool wear under the influence of different parameters in ultrasonic drilling. Singh and Khamba [116] investigated that ultrasonic power rating significantly improved the material removal rate with contribution of 28%, followed by type of tool with contribution of 24.6%. The third significant factor was type of slurry with contribution of 13.3%. Singh and Khamba [56] proposed and applied approach to macromodelling of the material removal rate, the tool wear rate, and surface roughness during ultrasonic machining of titanium and its alloys. Jadoun et.al [57] studied the effect of process parameters work piece material, tool material, grit size of the abrasive, power rating and slurry concentration on tool Wear Rate (TWR) of ultrasonic drilling on alumina-based ceramics using silicon carbide abrasive. Ghahramani and Wang [80] analyzed the mechanism, dynamics, and trends of USM process and also discussed applications on the ceramic (Al_2O_3). Chunxiang et.al [97] presented the cutting speeds of the tool, the rake angle and clearance angle through the cycles of elliptical vibration cutting for separating type ultrasonic elliptical vibration cutting.

2.5 SURFACE PROPERTIES

Margaret et. al [21] worked on ultrasonic grating spectroscopy and characterization of fluid and slurries.The ultrasonic diffraction grating was formed by machining triangular grooves, 300 microns apart, on a stainless steel surface. It was investigated that the signal

of reflected yielded the velocity of sound in the liquid and particle size.Makarov et.al [22] investigated the plastic deformation of mild steel subjected to ultrasonic treatment. The stress-time history and the tool displacement in addition to the accumulation of plastic deformation was determined that reflected the material damage evolution process at the different scale levels. Jones and Hull [23] developed a better polishing method called as ultrasonic flow polishing and the surface finish was improved by factor of up to 10.1. it was investigated that the process had the capacity to produce a high quality finish on the surface of the cavity and caused minimal deterioration to its profile or dimensional accuracy. Dhar et.al[24] evaluated the effect of current (c), pulse-on time (p) and air gap voltage (v) on metal removal rate (MRR), tool wear rate (TWR), radial over cut (ROC) on electric discharge machining of Al–4Cu–6Si alloy–10 wt.% SiC_P composites.Skiedraitė et.al [45] investigated that metal cutting by using ultrasonic frequencies vibrations was more rational in comparison with traditional cutting method and resulted in improvement of machined surface. Guzzo et.al [46] investigated the potential of ultrasonic machining as a tool to produce seed crystals for hydrothermal growth of synthetic quartz with required surface finish and unconventional geometries.They observed that the density of dislocations, nucleated at the early stage of the growth period, increased with increasing roughness of the seed-crystal surface based on X-ray topographic images. Adithan and Venkatesh [52] investigated the influences of certain important parameters such as static load, machining time, type of abrasives, grit size and work material on dimensional and form accuracy .Guzzo et.al [48] investigated the wear mechanisms associated with the ultrasonic abrasion of quartz. Ultrasonic abrasion was carried out in *X*-, *Y*-, *Z*- and AT-cut plates of natural quartz and *Z*-cut plates of synthetic quartz.They concluded that the wear rate was affected by the crystallographic orientation of quartz specimens and was inversely proportional to the product $K_{1c}^{3/2}H^{1/2}$.

Palanikumar [55] discussed the use of taguchi and response surface methodologies for minimizing the surface roughness in machining glass fiber reinforced (GFRP) plastics with a diamond (PCD) tool. It was concluded that the most significant machining parameter for surface roughness was feed followed by cutting speed. Spur et.al [33] investigated on ultrasonic assisted creep feed grinding of sintered silicon nitride and alumina. It was concluded that in order to improve the machining process of advanced ceramics, grinding could be combined with ultrasonic vibrations at high frequencies of about 22 kHz and low amplitudes between 4 and 15 μm. Aspinwall, et.al [11] investigated

the use of ultrasonic machining for the production of holes in γ-trial. Scott and Yung [1] presented in-process monitoring and control of surface roughness during machining processes via ultrasonic sensing. It was outlined that it was possible to maintain surface roughness within 10% of the target value for tool wear up to 0.3mm. Chang and Chun [12] evaluated laser-assisted machining (LAM) as an economically viable process for manufacturing precision aluminum oxide ceramic parts. They concluded that rotational speed, with a contribution percentage as high as 42.68%, had the most dominant effect on LAM system performance, followed by feed, depth of cut, and pulsed frequency. Jain et.al [13] investigated the mechanism of material removal in electrical discharge diamond grinding. Simon et.al [10] presented the design of an ultrasonically vibrated work piece holder, and a two-stage experimental investigation of ultrasonically assisted drilling of aluminum work pieces. Pei and Ferreira [25] investigated an experiment of the newly-developed rotary ultrasonic face milling machine (RUFM) process and studied the main effects as well as the interaction effects of the process parameters on the process outputs such as material Removal Rate (MRR), cutting force, material removal mode and surface roughness.Babitsky et.al[66] presented the results of the research in ultrasonically assisted machining and outlined that the application of ultrasonic vibration could improve the surface quality considerably and improvements of up to 25–50% was achieved**.** Jain et.al [91] intended to fulfil this need in the area of advanced machining. Various analytical and some semi-empirical/empirical material removal models (approximately 40) for different mechanical type advanced machining processes were comprehensively and exhaustively reviewed, and were presented in a format suitable for quick reference.The performance of any machining process was evaluated in terms of machining rate and surface finish produced.

2.6 TAGUCHI METHODOLOGY

Leung [3] discussed the potential problems of taguchi's modeling approach. The objective of taguchi' s robust design method was to reduce the output variation from the target (the desired output) by making the performance insensitive to noise, such as manufacturing imperfections, environmental variations and deterioration. Singh and Kumar [2] optimized the feed force for turned parts through taguchi. Younes et.al[4] introduced a new look at the taguchi method to obtain high quality products at low cost and in a short time is an economical and technological challenge to today's engineering

community that made it possible, by choosing the proper levels, to evaluate the ratio of two factors as a new factor in the same orthogonal array[139,153-154]. Akbari et.al[35] studied the effect of ultrasonic vibration for increasing the performance of grinding process of fine ceramic. Mohammadi et.al [110] applied taguchi's quality engineering for the separation of copper ions from a solution using a laboratory electro dialysis set-up to evaluate the optimal experimental conditions and hence to achieve the highest removal percentage and the best robustness of the quantization from the least number of experimental runs. It was concluded that four influential factors were: concentration 1000 ppm, temperature 60°C, flow rate 0.07 ml/s and voltage 30 V.

2.7 COMBINATION OF USM WITH OTHER PROCESSES

Taichiu and Jianxin[28] explained two mechanical surface treatments, i.e. ultrasonic machining (USM) and abrasive blasting, to restore and improve these properties for the electro-discharge machined (EDMed) surfaces of the toughened and electro conductive Al_2O_3/TiC/Mo/Ni ceramic composite. It was outlined from the comparison of the flexural strength of EDMed and modified specimens that the modified specimens yielded an apparent strengthening with a concurrent increase in Weibull modulus. Lin et.al [78] presented an experimental investigation of the machining characteristics of titanium alloy (Ti–6Al–4V) using a combination process of electro-discharge machining (EDM) with ultrasonic machining (USM). It was investigated that this combination EDM/USM process could increase the MRR and decrease the thickness of the recast layer. Guzzo et.al [34] investigated the ultrasonic machining of natural quartz in relation to crystal orientation and the rate of cutting was measured along directions perpendicular to X-, Y-, Z- and AT-cut planes. They concluded from scanning electron microscopy analysis brittle micro cracking was the main wear mechanism involved with material. Lee[108] proposed a control system to improve the efficiency of machining a workpiece with varying thickness in the wire electrical discharge machining (WEDM) process. The results showed that the cutting speed can be obviously improved by proposed control strategy.

2.8 PROCESS CAPABILITIES

Kremer [107] determined that ultrasonic machining was recently gained recognition as an influential process in the technology of cutting and shaping produce for which non-mechanical processes prove inadequate. Hahn and Schulze [41] described a new

technique sonoerosively shaping glass, ceramic or composite components .The process used an oscillating tool at medium frequency and abrasive slurry, which acted to transmit the mechanical vibrations of the tool against the machined surfaces. Gan et.al [43] applied ultrasonic vibration to a single-crystal diamond tool-tip, ductile machining of fused silica could be achieved even for 2 cm depth of cut. It was concluded that the increase in the critical depth of cut was significant and was a function of the ratio of vibration speed to cutting speed. Also the surface roughness Ra of 100 nm was obtained for up to 2 cm depth of cut. Kremer et.al [100] studied the EDM assisted with ultrasonic vibrations of the electrode. It was outlined the beneficial effect of ultrasonic vibrations: increased feed rate by a better flushing, particularly for difficult conditions such as finishing with narrow gap: lower damage due to heating ,thinner recast layer, increased fatigue life. Balamuth [101] studied the applications of ultrasonic vibrations to machine tools such as grinders and lathes and concluded smoother cutting and smaller power requirements. Onikura et.al [99] studied the fabrication of micro cylindrical tools and micro flat drills of ultra-fine grain cemented carbides by grinding with ultrasonic vibration and investigated that grinding under compressive force was possible to grind to a diameter of 11 μm with a length of 160 μm.

Nath et.al [98] investigated the effects of UVC in cutting of DF2 material, on abrasive wear and on the transition of low to high tool wear rate in the machining of the same material.The UVC process resulted in better surface finishes as compared to CT, and UVC required lower cutting forces than in the CT process. Also they outlined that UVC had lower tool flank wear rate compared to CT under all cutting conditions. Moriwaki and Shamot [92] proposed a new cutting method named ultrasonic elliptical vibration cutting and applied to cutting of metals by utilizing a new vibrator to vibrate the cutting tool elliptically at ultrasonic frequency. It was concluded that the cutting performance, in terms of the cutting force and the chip thickness, was improved significantly by applying the elliptical vibration to the cutting tool. Kumabe et.al [93] proposed that adding high frequency vibration stress to ceramics, which had a tensile stress weakness was the basis for the precise and efficient cutting of ceramics. It was concluded that by using this new cutting process, a cutting volume of 25 $mm^2 \times 0.02$ mm per 6 was obtained, and a cutting surface roughness of 1–6 μm R_{max} was achieved.Egash et.al[90] studied the microholes with a diameter of 10 μm drilled in glass by ultrasonic vibration cutting using a microtool fabricated by wire electrodischarge grinding. The application of ultrasonic vibrations

resulted in a decrease in the required cutting force, an extension of the tool life, an increase in the permissible penetration and tool length and smoother machined surfaces. Zhixin et.al [72] developed an ultrasonic vibration pulse electro-discharge machining (UVPEDM) technique to produce holes in engineering ceramics. It was investigated that this new technique was effective in the obtaining of a high material removal rate.Mult et.al [73] investigated on ultrasonic assisted creep feed grinding of sintered silicon nitride and alumina and concluded that in order to improve the machining process of advanced ceramics, grinding could be combined with ultrasonic vibrations at high frequencies of about 22 kHz and low amplitudes between 4 and 15 μm. Guo et.al [74] investigated the combined technology of ultrasonic and wire electrical discharge machining (WEDM), in which the design of the vibrating device was described. They concluded that there exist an optimum relationship between the vibration amplitude of the wire and the discharge energy, by which the highest cutting rate and the best machined surface quality was obtained. Zhang et.al [76] proposed spark erosion with ultrasonic frequency using a D.C. power supply instead of the usual pulse power supply, the pulse discharge being produced by the relative motion between the tool and the workpiece. Guo et.al [77] established that by means of experiments employing single pulse discharge that the high frequency vibration of the wire electrode was able to bring about multiple channel discharges so that better surface quality and a high cutting rate could be obtained simultaneously. Seah et.al [67] investigated the design of efficient tool holders or horns for the ultrasonic machining process by employing the finite-element method (FEM) to analyse the pertinent design characteristics of the horn.Reza et.al[62]studied the effects of ultrasonic vibration of the tool electrode on the surface integrity of tungsten carbide (WC-10%Co) in the electro-discharge machining (EDM) process.Choi et.al [63] studied the chemical-assisted ultrasonic machining (CUSM) method in order to improve the material removal rate and the integrity of the machined surface. Neugebauer and Stoll [65] studied the application of ultrasonic drilling in the manufacture of deep holes and the problems occurred in terms of chip formation and chip removal, burr formation at the cutter exit, tool stress, as well as process reliability**.**Tsutsumi et.al[68] investigated the machining performance in the drilling and grinding of ceramics to obtain high-quality ground components . The relationships between the voltage and the machining rate of electrical discharge machining in electrolyte were investigated for the drilling of holes of small diameter (0.5 mm) in non-conducting ceramics. It was concluded from the X-ray diffraction measurement that the surface compressive residual stresses increased with increase in

feed-rate or with decrease in wheel speed and the residual stresses decreased with decrease in chip cross-sectional area. Tuersley et.al [69] reported the trade-off between the material removal rate and the level of near-surface damage that the ultrasonic process involved.Tosun et.al [71] presented an investigation on the effect and optimization of machining parameters on the kerf (cutting width) and material removal rate (MRR) in wire electrical discharge machining (WEDM) operations. The experimental studies were conducted under varying pulse duration, open circuit voltage, wire speed and dielectric flushing pressure.

2.9 PROCESS CAPABILITIES OF CONVENTIONAL TOOL AND WORK MATERIALS

Table 2.1 Materials successfully machined by USM process

Agate	Alabaster	Barium carbide (sintered)
Ceramics	Corrundum	Diamond
Earthenware	Felspar	Ferrites
Fluorites	Germanium	Glass
Glass-Micanite	Granite	Graphite
Gypsum	Hard alloy (tungsten and titanium carbide)	Marble
Jadeite	Jasper	Mother-of-pearl
Nephrite	Onyx	Porcelain
Quartz (crystalline and fused)	Rock crystal	Ruby
Sapphire	Silicon	Stealite
Thermo corrundum	Tourmaline	Zirconium boride

Table 2.2 Properties of abrasives

Abrasive	**Knoop hardness**	**Relative cutting power**
Boron Carbide	2800	0.50-0.60
Aluminium oxide	2000-2100	0.14-0.16
Diamond	6500-7000	1.0
Silicon Carbide	2480-2500	0.25-0.45
Cubic Boron Nitride	4700	0.95

2.10 NEED FOR RESEARCH AND AREAS OF STUDY

Statistical experimentation is one of the main tool development in manufacturing industry.This is concerned with the application of modern off-line quality control techniques (pre-production or independent of production experimentation and analysis) to product and process engineering. In other words, it eliminates the need for mass inspection by building quality into the product and process at the design stage. Professor Genichi Taguchi was the founder of this methodology. He devised a quality improvement technique that uses experimental design methods for efficient characterization of a product or process, combined wit a statistical analysis of its variability. This approach allows quality considerations to be at an early stage of any new venture: in the design and prototype phase for a product; during routine maintenance; or during installation and commissioning of a manufacturing process.

Taguchi designs are balanced, that is, no factor is weighted more or less in an experiment, thus allowing factors to be analyzed independently of each other. Minitab provides both static and dynamic response experiments.

- In a static response experiment, the quality characteristic of interest has a fixed level.
- In a dynamic response experiment, the quality characteristic operates over a range of values and the goal is to improve the relationship between an input signal and an output response. An example of a dynamic response experiment is an automotive acceleration experiment where the input signal is the amount of pressure on the gas pedal and the output response is vehicle speed. You can create a dynamic response experiment by adding a signal factor to a design. The goal of robust experimentation is to find an optimal combination of control factor settings that achieve robustness.Against (insensitivity to) noise factors, statistica 7.0 software calculates response tables, linear model results, and generates main effects and interaction plots for:

- Signal-to-noise ratios (S/N ratios, which provide a measure of robustness) Vs the control factors.
- Means (static design) or slopes (dynamic design) Vs the control factors
- Standard deviations Vs the control factors
- Natural log of the standard deviations vs. the control factors

Use the results and plots to determine what factors and interactions are important and evaluate how they affect responses. To get a complete understanding of factor effects it is advisable to evaluate S/N ratios, means (static design), slopes (dynamic design), and standard deviations. Make sure that you choose an S/N ratio that is appropriate for the type of data you have and your goal for optimizing the response.

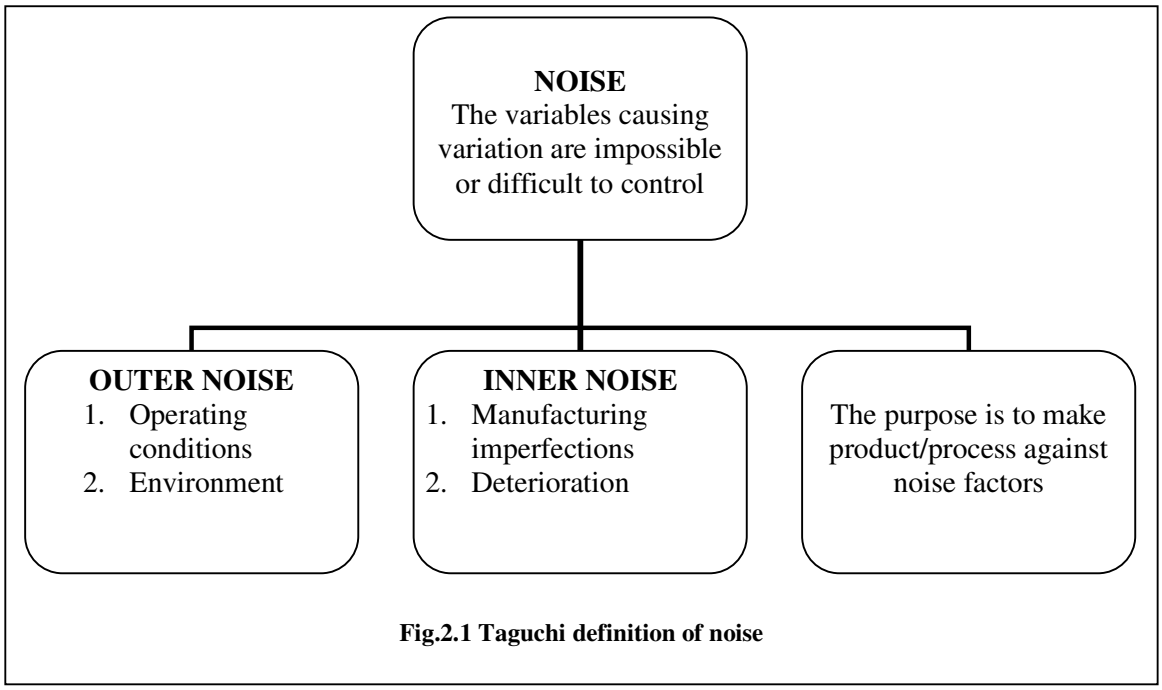

Fig.2.1 Taguchi definition of noise

2.11 PARAMETER DESIGN

This is the part of technique that identifies those settings of the controllable factors that reduce performance variation caused by the noise factors while keeping the response of interest on target. At this stage once attempt to reduce or remove the effect of noise factors rather than the noise factors themselves. This variation is simulated during the experiment, by systematically varying the noise factors at each of the various settings of the controllable factors under study.The controllable factor settings studied are those suggested by the rows of an experiment design (inner array), usually a fractional orthogonal array; in such a design, every level of a factor occurs wit every level of all other factors the same number of times.

At every level-combination of the controllable factors, some observations should be obtained while changing the settings of the noise factors, assuming of course that the noise factors can be controlled and changed, at least for the purposes of the experiment. A fractional orthogonal array can then be utilized to determine the level combinations of the noise factors. In such a case, the experimenter can simulate the variability of the noise factors on each controllable factor setting and determine the setting which minimizes the variability.

2.12 TAGUCHI APPROACH FOR DESIGN

The following steps are involved for the taguchi design approach:

Phase 1: Planning

- Define the problem and the objective
- Identification of control factor and levels
- Design the matrix experiments

Phase 2: Conducting

- Conducting the experiments

Phase 3: Analysis

- Data analysis
- Optimum levels determination for factors

Phase 4: Validation

- Validation of experiment

2.12.1 Description of orthogonal arrays

Orthogonal arrays are special experimental designs that require only a small number of experimental trials to discover main factor effects.Oas are "fractional factorial designs" and symmetrical subsets of all combinations of treatments in the corresponding full factorial designs. Before one attempts to select an OA to guide the design optimization experiments, one must answer the following critical questions.

1. How many factors are to be studied?
2. How many treatment levels are possible for each factor?
3. What specific 2-factor interactions are to be investigated?
4. Would one encounter any particular difficulty during the runs i.e. some factors may not permit frequent treatment changes?

The first step in selecting the correct standard OA involves counting the total degree of freedom (DOF) present in the study. This count fixes the minimum number of experiments that must be run to study the factors involved. Except in unusual circumstances, the investigator will be able to locate a standard OA fitting he needs. Taguchi identified several basic OA which he called "standard OA". These OA usually suffice the needs of most design optimization study. After finding the DOF, the selection of the appropriate standard OA becomes reasonably straightforward.

2.12.2 Steps in robust design

1. Experiment planning and problem formulation: Experiment planning guidelines are consistent with modern work disciplines of working as teams. Consensus decisions about experimental objectives and factors make the projects more successful.

2. Experiment layout: High emphasis is put on cost and size of experiments. Size of the experiment for a given number of factors and levels is standardized. Approach and priority for column assignments are established. Clear guidelines are available to deal with factors and interactions (interaction tables). Uncontrollable factors are formally treated to reduce variation. Discrete prescriptions for setting up test conditions under uncontrollable factors are described. Guidelines for carrying out the experiments and number of samples to be tested are defined.

3. Data analysis: Steps for analysis are standardized (main effect, ANOVA and Optimum). Standard practice for determination of the optimum is recommended. Guidelines for test of significance and pooling are defined.

4. Interpretation of results: Clear guidelines about meaning of error term. Discrete indicator about confirmation of results. Ability to quantify improvements in terms of dollars (loss function).

2.13 CONTROL FACTORS, SIGNAL AND NOISE FACTORS FOR STUDY

The study presented in this research work is based on machining problems associated with tungsten carbide, stellite and diamond. The concern is primarily with obtaining the optimum system configuration with minimum expenditure of experimental resources. The P-diagram (Process diagram) for the process has been shown in figure 2.2.The parameters that influence the output are identified and divided into two classes: Noise factors and Control factors. The best setting of control factors is determined through experiments. For the analysis, statistica 7.0 software has been used. The robust design method lends itself well for optimization through the macro-modeling approach.

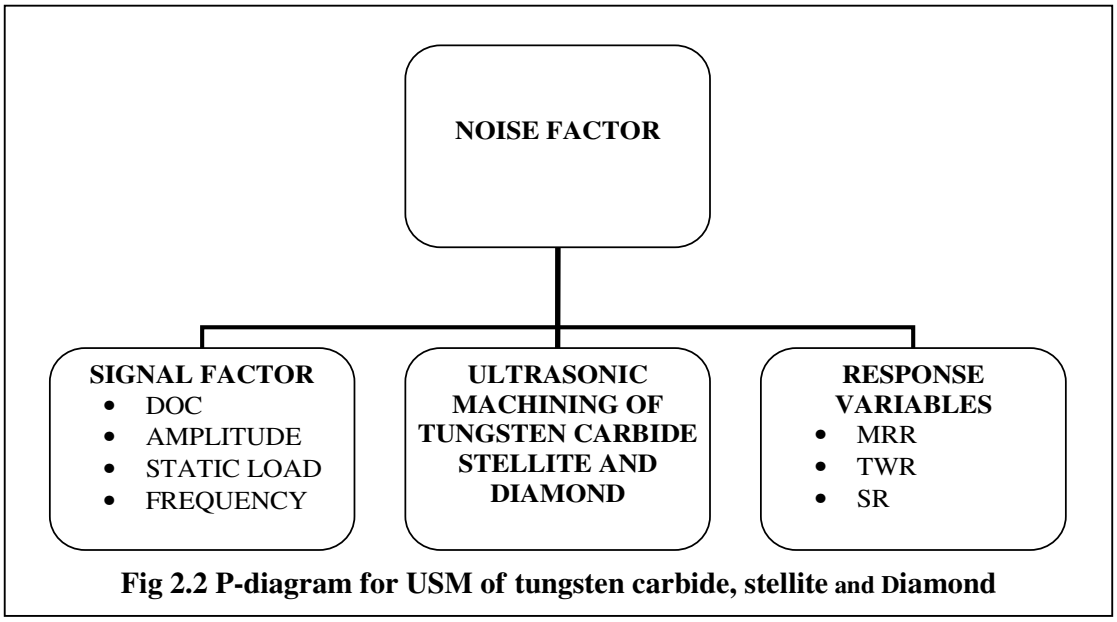

Fig 2.2 P-diagram for USM of tungsten carbide, stellite and Diamond

There appears to be no simple relationship between the MRR and physical characteristics of work material, such as tensile strength, percentage elongation and micro-hardness or impact strength [81, 164]. Some practical work has been evidenced for machining brittle materials using USM. For tough materials, very little effort has been put in to explore the machining capacity of USM. In the present work, it is proposed to model machining capacity of tough materials using USM for their applications in manufacturing industry. This research work is intended to establish the benefits accrued in terms of higher material removal rate and longer tool life with better surface finish, for the manufacturing industry as a result of the improvement of machining characteristics of tungsten carbide, stellite and diamond with USM.

CHAPTER III

EXPERIMENTATION

3.1 INTRODUCTION

An experimental set-up having a provision for variation in process parameters was designed and fabricated. The dimensions of the tool were decided keeping in view the limitations of the horn shape to economize the machining operation.The figure 3.1 represents the detailed drawing of the tool. An electronic balance (Metler, Least count: 0.1 mg); and stop watch (Least count: 0.01 min) were used to determine MRR and TWR. For measuring surface roughness (Perthometer M4Pi, Least count: 0.01 microns) was used. Four repetitions were made for the entire experimentation and corresponding MRR, TWR and SR were recorded.

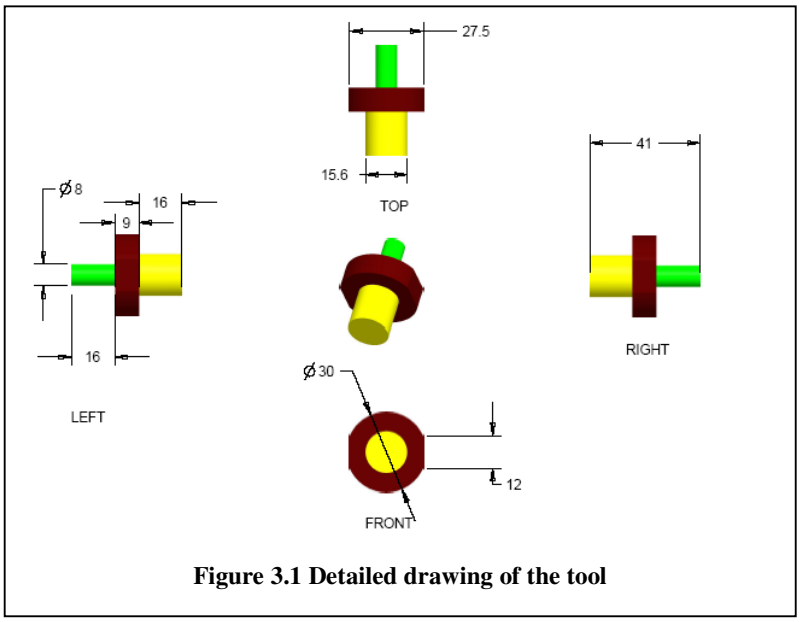

Figure 3.1 Detailed drawing of the tool

3.2 DESCRIPTION OF ULTRASONIC MACHINE

The USM machine tool used for the study is of 500 W capacity, which consists of an ultrasonic spindle kit; a constant pressure feed system and slurry flow system. The ultrasonic spindle kit comprises an ultrasonic spindle, mounted with cylindrical horn of 25.4mm diameter, a power supply unit.The figure 3.2 represents the ultrasonic machine tool (Type: Sonic Mill, USA) used in the experimentation work.

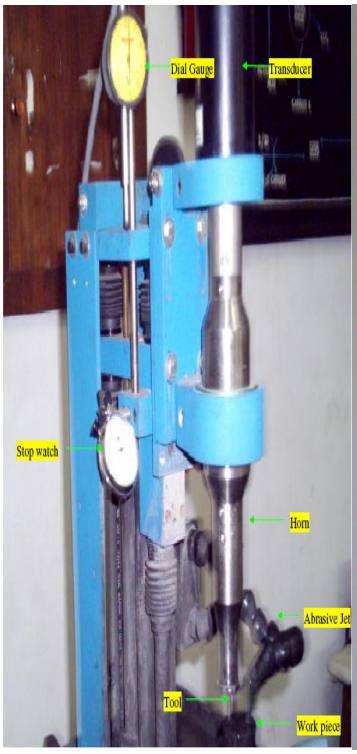

Figure 3.2

Figure 3.3

Figure3.4

Figure3.5

Figure3.6

Figure 3.7

Figure 3.2Ultrasonic machine tool (Type: Sonic Mill, USA)
Figure 3.3 Amplitude coupling for compact 500W ultrasonic machine
Fgure 3.4 Ultrasonic transducer for compact 500W ultrasonic machine
Figure 3.5 Pump for re-circulation of abrasive slurry
Figure 3.6 Power rating set-up for ultrasonic machine
Figure 3.7 Ultrasonic tool

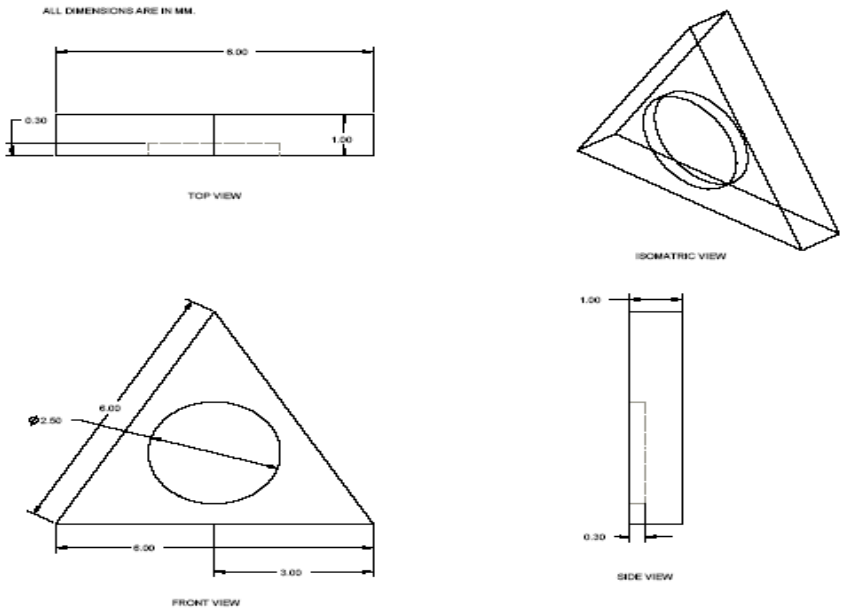

Triangular work-piece

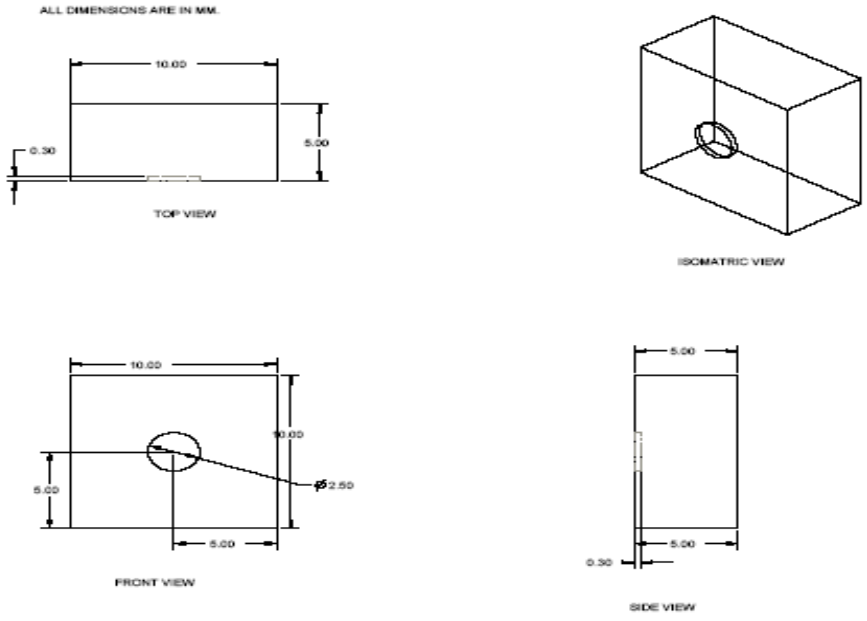

Rectangular work-piece

Figure 3.8: Detailed drawing of the work geometry

The power supply converts 50 Hz electric supply to high frequency 20 kHz AC output. This is fed to piezoelectric transducer located in the spindle. The transducer converts the electrical input in to mechanical vibrations. The amplitude of vibrations is made fixed in range of 0.0253-0.0258 mm with a frequency of 20 kHz +/- 200 Hz. The static load for feed rate was fixed at 1.724 kg and slurry flow rate at 30.6 l/min. The replaceable tools used for machining were solid tools having same area of cross-section. The other parts of the experimental set up, amplitude coupling (figure 3.3), ultrasonic transducer (figure 3.4), Pump for re-circulation of abrasive slurry (figure 3.5), Power rating set-up (figure 3.6) and the ultrasonic tool (figure 3.7) are shown.

3.3 PRELIMINARY STUDY TO ASSESS THE EXISTING STATUS

In order to identify the process parameters that affect the quality of components processed by USM can be classified as follows:

1. Machine based parameters: Ultrasonic power, amplitude and frequency of vibrations, medium flow rate, temperature of medium, type of tool material, shape of tool horn

2. Media based parameters: Viscosity, grain size (type and shape), concentration of abrasives in medium

3. Work-piece based parameters: Geometry of work-piece (circular, rectangular, or irregular shape etc.), length to diameter ratio, chemical composition of the work material.

The following six independent parameters have been chosen for this study:

1. Tool materials

2. Work materials

3 Abrasive slurry concentrations

4 Different types of abrasives

5. Abrasive grit sizes

6. Power ratings of ultrasonic machine

The range of these parameters will be selected on the basis of preliminary experiments conducted by using one variable at a time approach. The work pieces selected are tungsten carbide, stellite and diamond as it has been reported that chemical composition of work piece material significantly affect the machining properties.

3.4 PILOT EXPERIMENTATION

The large numbers of experiments were conducted with different input conditions by using one variable at a time approach. The stage of pilot experimentation has been divided into nine cases.The response parameters in the present study are material removal rate (MRR), tool wear rate (TWR), and surface roughness (SR). MRR is defined as the loss of weight (work material) per unit time after processing with USM. Similarly, TWR is defined as loss of weight (tool material) per unit time after machining with USM.

Mathematically,

$MRR= (W_1-W_2)/t$

'W_1' is initial weight of the work-piece in gram (before machining)

'W_2' is final weight of the work-piece in gram (after machining)

't' is the machining time in min

Similarly

$TWR= (W_1-W_2)/t$

'W_1' is initial weight of the tool in gram (before machining)

'W_2' is final weight of the tool in gram (after machining)

't' is the machining time in min

As the tool materials used for the experimentation possess different values of densities, the tool wear rate in terms of 'change in volume' per unit time could be a better measure of the rate at which the different tool materials are eroded while machining takes place. Hence, the tool wear rate as well as material removal rate was calculated as reduction in volume per unit time (mm^3/min) so as to facilitate more accurate comparison of the TWR for different tool materials under varying process conditions.

$MRR = (W_1-W_2)/t. \rho$

ρ = density of the work material in g/mm^3

$TWR= (W_1-W_2)/t. \rho$

ρ = density of the corresponding tool material in g/mm^3

Case 1: Aluminium oxide slurry, Grit size 220, Slurry Concentration 25%

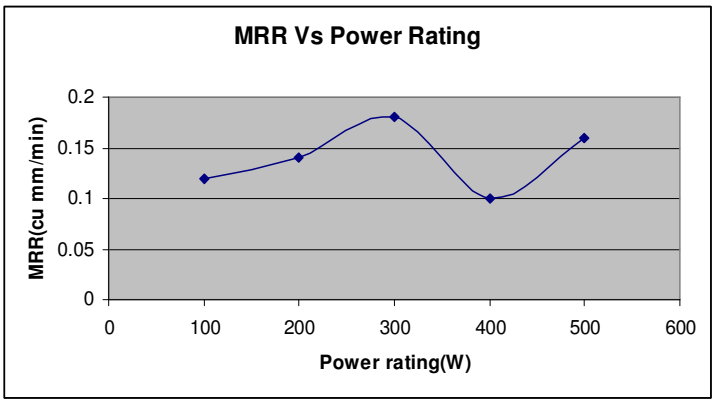

Figure 3.9 MRR Vs Power rating for TITAN12 tool while machining WC

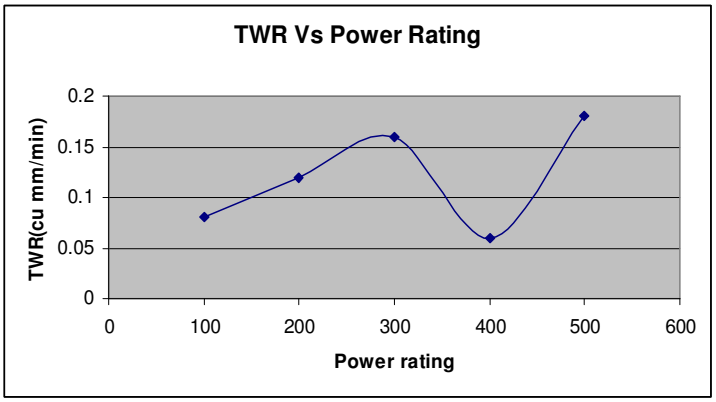

Figure 3.10TWR Vs Power rating for TITAN12 tool while machining WC

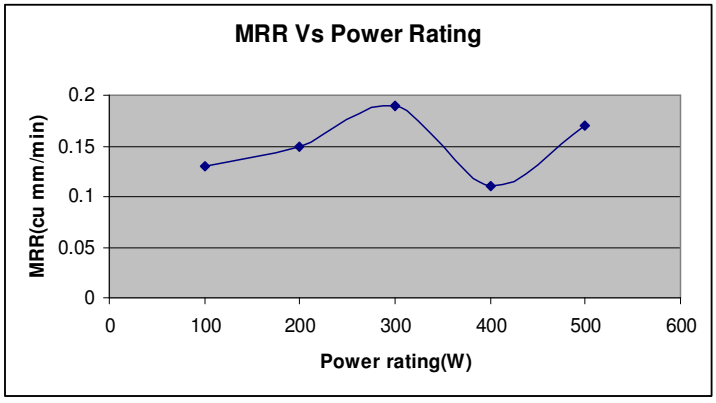

Figure 3.11 MRR Vs Power rating for TITAN15 tool while machining WC

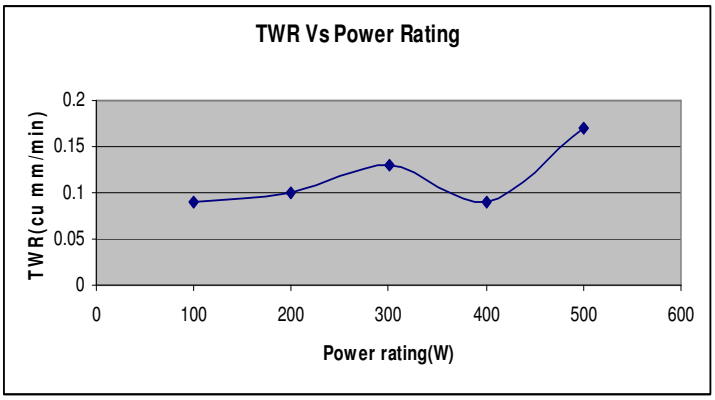

Figure 3.12 TWR Vs Power rating for TITAN15 tool while machining WC

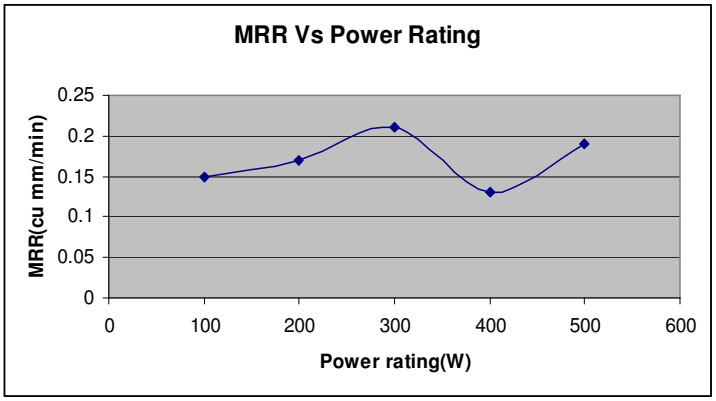

Figure 3.13 MRR Vs Power rating for TITAN 31 tool while machining WC

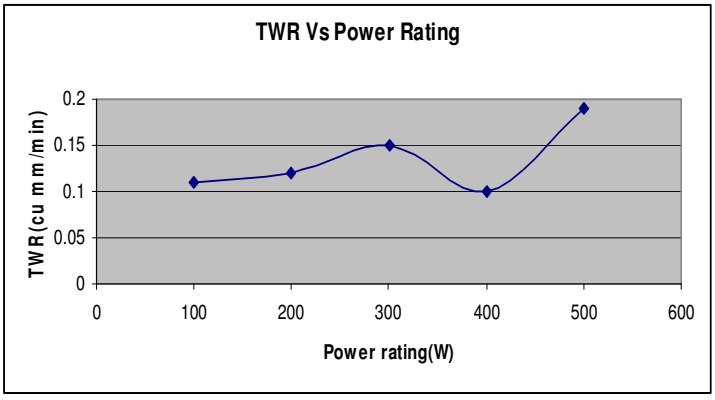

Figure 3.14 TWR Vs Power rating for TITAN 31 tool while machining WC

Case 2: Aluminium oxide slurry, Grit size 320, Slurry Concentration 25%

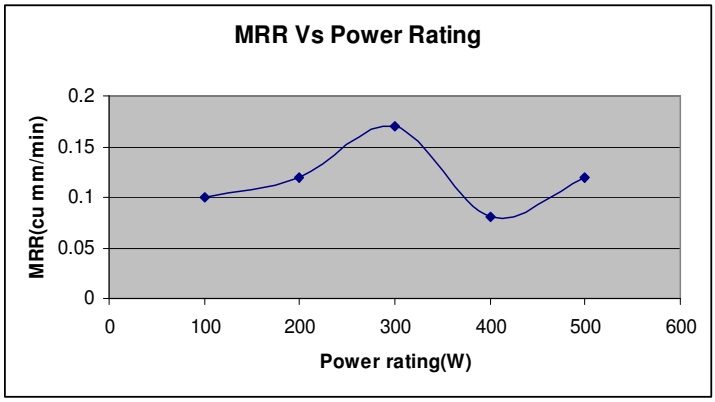

Figure 3.15 MRR Vs Power rating for TITAN 12 tool while machining WC

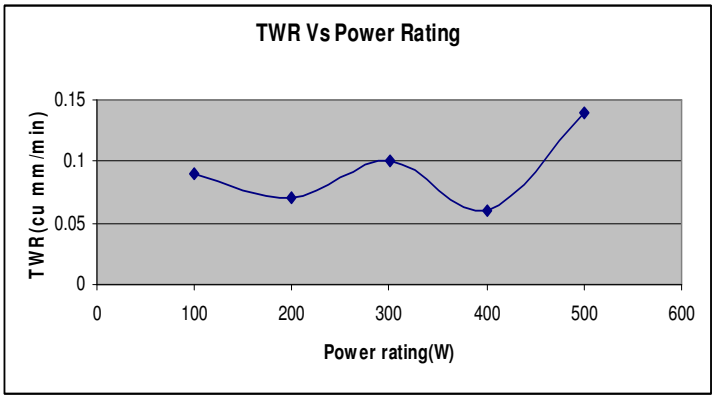

Figure 3.16 TWR Vs Power rating for TITAN 12 tool while machining WC

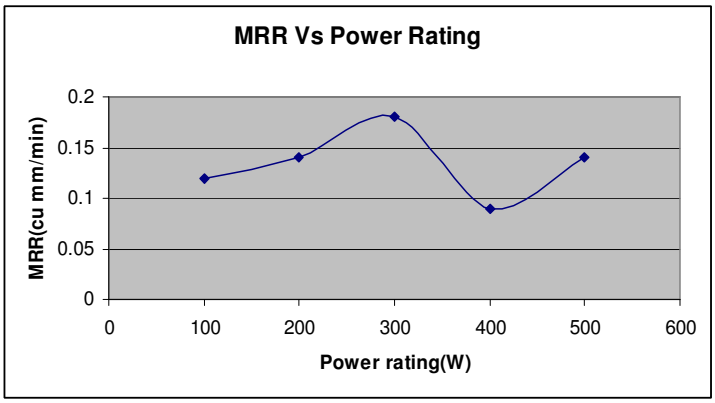

Figure 3.17 MRR Vs Power rating for TITAN 15 tool while machining WC

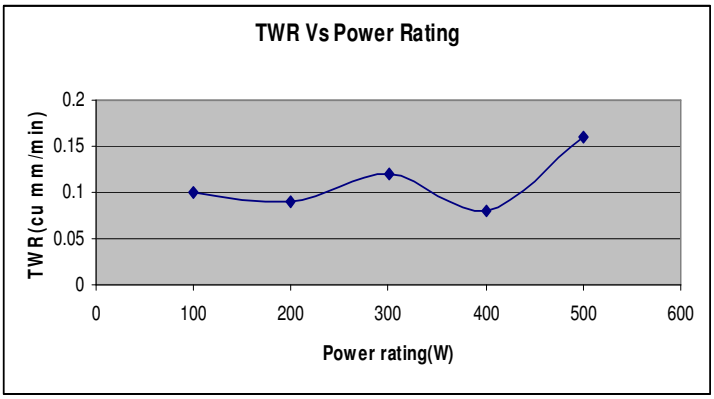

Figure 3.18 TWR Vs Power rating for TITAN 15 tool while machining WC

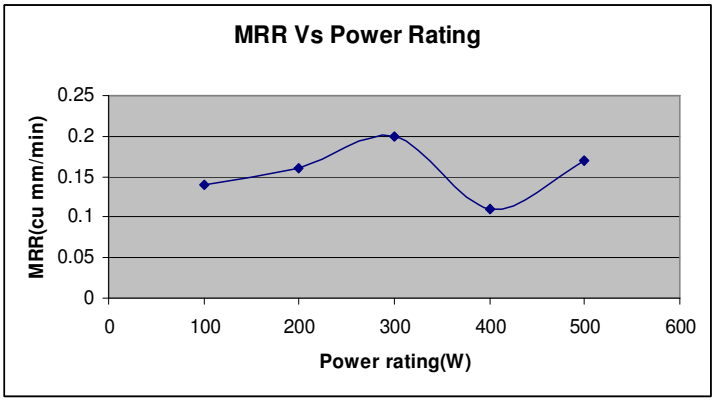

Figure 3.19 MRR Vs Power rating for TITAN 31 tool while machining WC

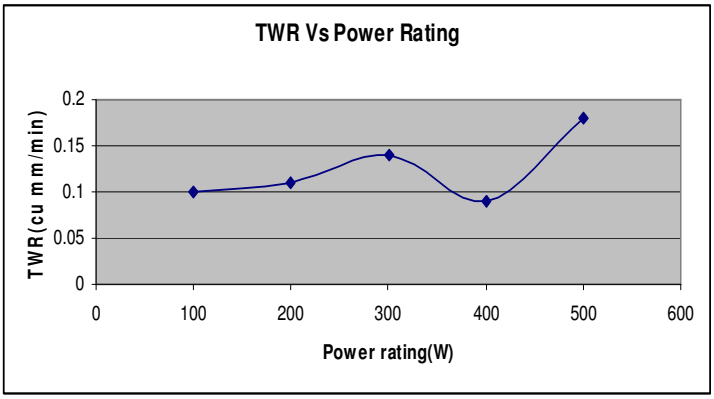

Figure 3.20 TWR Vs Power rating for TITAN 31 tool while machining WC

Case 3: Aluminum oxide slurry, Grit size 500, Slurry Concentration 25%

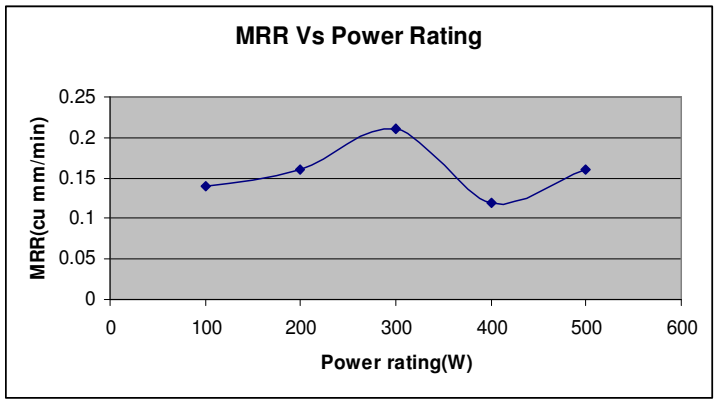

Figure 3.21 MRR Vs Power rating for TITAN 12 tool while machining WC

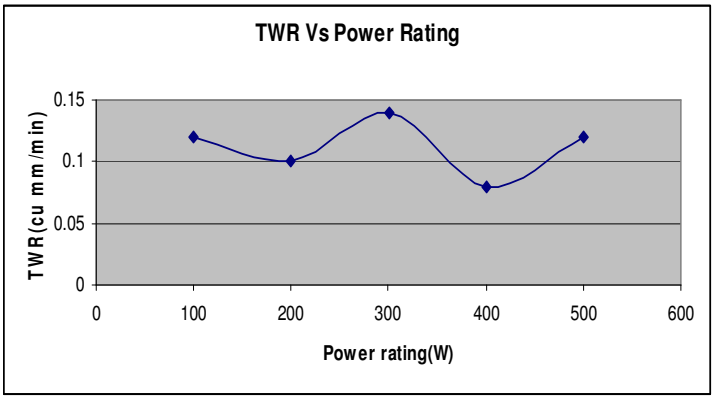

Figure 3.22 TWR Vs Power rating for TITAN 12 tool while machining WC

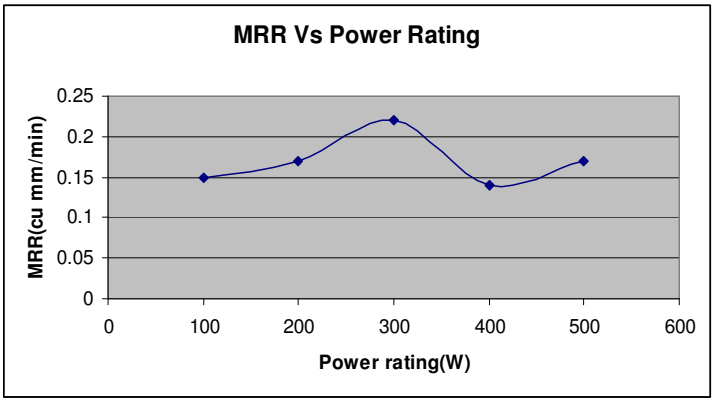

Figure 3.23 MRR Vs Power rating for TITAN 15 tool while machining WC

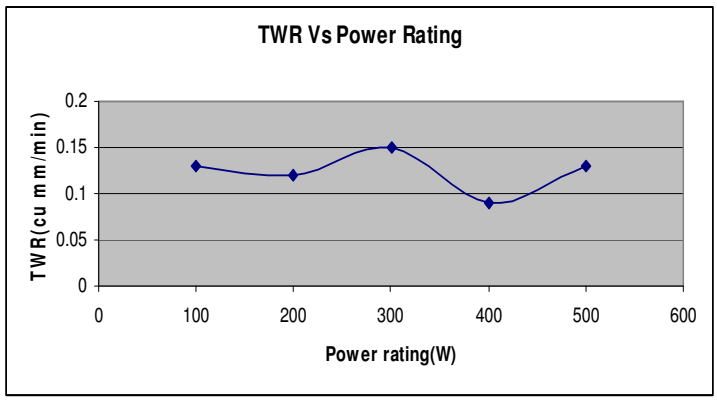

Figure 3.24 TWR Vs Power rating for TITAN 15 tool while machining WC

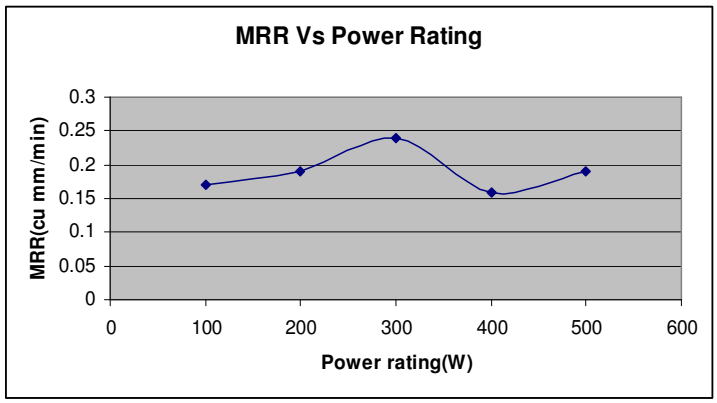

Figure 3.25 MRR Vs Power rating for TITAN 31 tool while machining WC

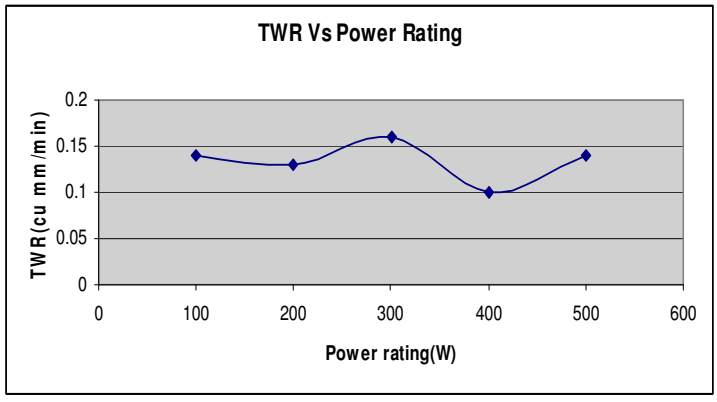

Figure 3.26 TWR Vs Power rating for TITAN 31 tool while machining WC

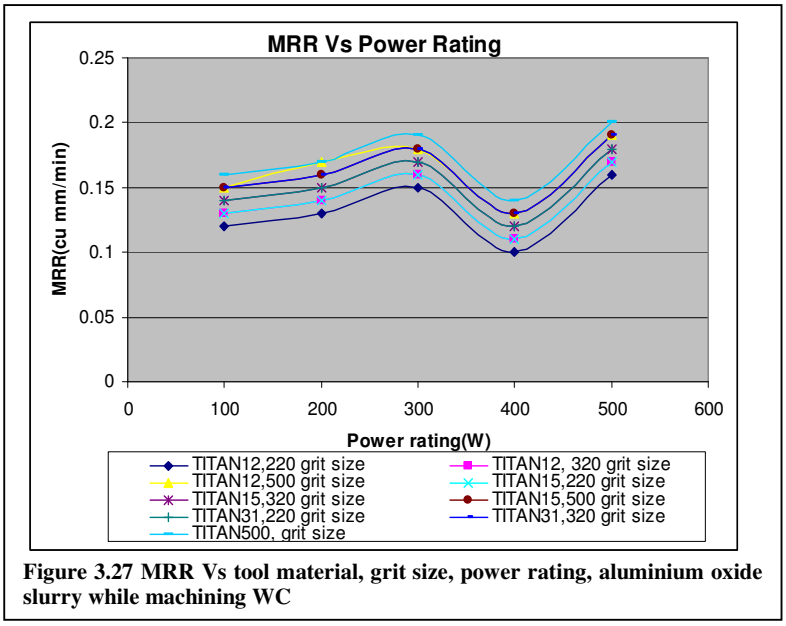

Figure 3.27 MRR Vs tool material, grit size, power rating, aluminium oxide slurry while machining WC

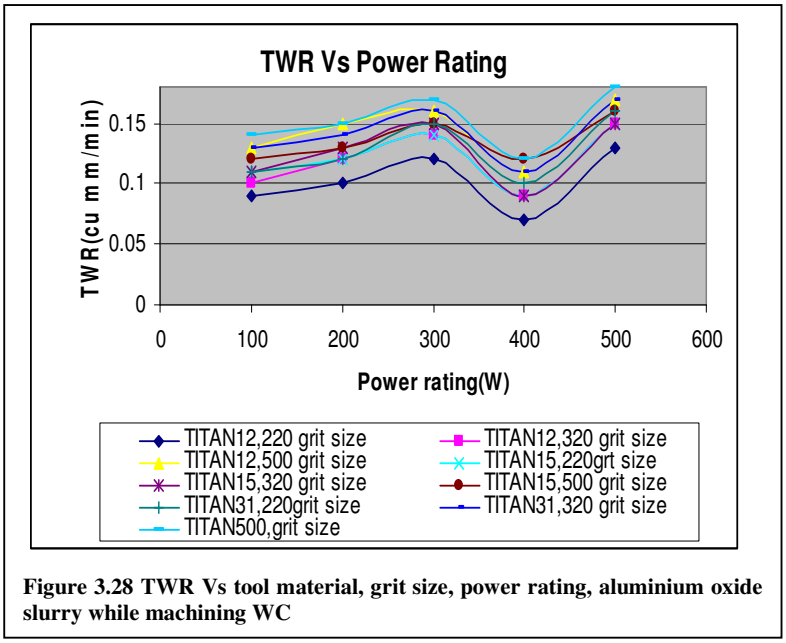

Figure 3.28 TWR Vs tool material, grit size, power rating, aluminium oxide slurry while machining WC

From the pilot experimentation conducted in cases (1-3), the following conclusions have been drawn:

1. It is not always necessary that if work piece of higher hardness is machined, it will result in more MRR; but it is combined effect of material composition relative to tool, resulting in work hardening of work piece or tool. It can be predicted that selection of operating parameter levels is critical in order to achieve acceptable productivity.

2. The variation of MRR & TWR with respect to power rating for aluminium oxide slurry with grit size of 220 and slurry concentration of 25% has been presented in the figures (3.9- 3.14) respectively. Similarly the variation using the abrasive grit sizes of 320 and 500 has been shown in figures (3.15-3.20 & 3.21-3.26) respectively. From these variations, it has been concluded that the machining characteristics (MRR, TWR) in ultrasonic machining of tungsten carbide have been found to be correlated and dependent upon the input parameters such as abrasive slurry grit size, type of tool material and power rating of the ultrasonic machine used.
3. It can be observed that for the tungsten carbide, both MRR as well as TWR tend to increase with a corresponding increase in the coarseness of the slurry used irrespective of the abrasive used for preparation of the slurry from figures (3.27-3.28) respectively. Also, the MRR and TWR obtained with different tool materials (TITAN12, TITAN15 and TITAN31) are significantly different when all other input parameters are controlled and remain fixed. Thus, the tool material properties such as hardness and toughness have been found to control the machining characteristics in USM of tungsten carbide.
4. The material removal rate and the tool wear rate have been affected by using the different types of abrasive slurries. It could be concluded that use of boron carbide slurry results in better material removal rate for same process conditions in comparison to silicon carbide and aluminum oxide. This can be attributed to the higher hardness and cutting ability of boron carbide in comparison to silicon carbide abrasive and aluminum oxide.

Case 4 : Silicon carbide slurry, Grit size 220, Slurry Concentration 25%

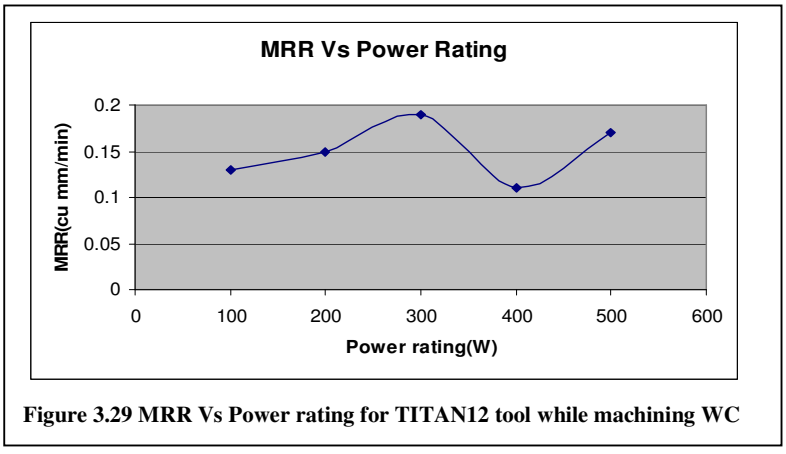

Figure 3.29 MRR Vs Power rating for TITAN12 tool while machining WC

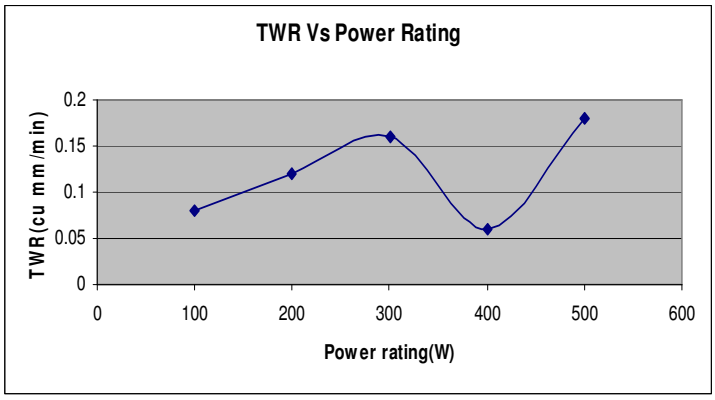

Figure 3.30 TWR Vs Power rating for TITAN12 tool while machining WC

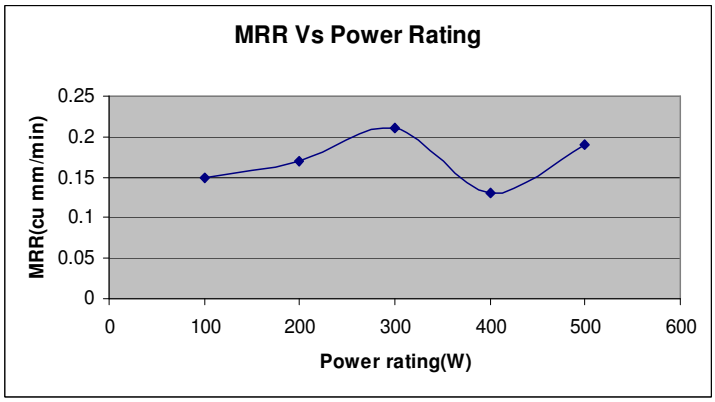

Figure 3.31 MRR Vs Power rating for TITAN15 tool while machining WC

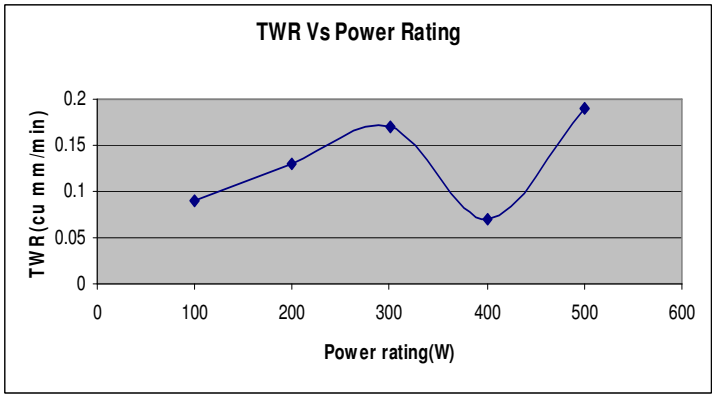

Figure 3.32 TWR Vs Power rating for TITAN15 tool while machining WC

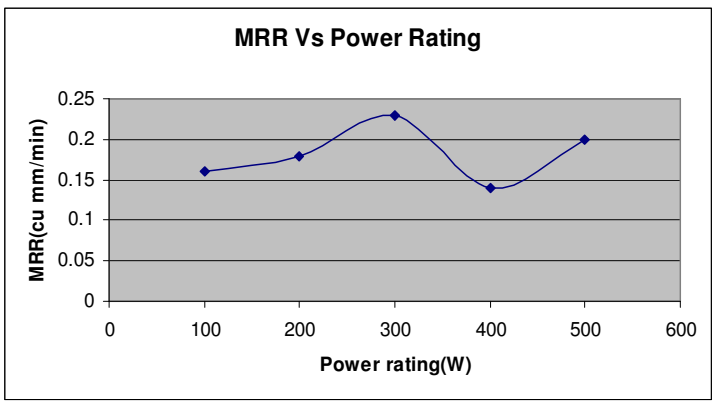

Figure 3.33 MRR Vs Power rating for TITAN31 tool while machining WC

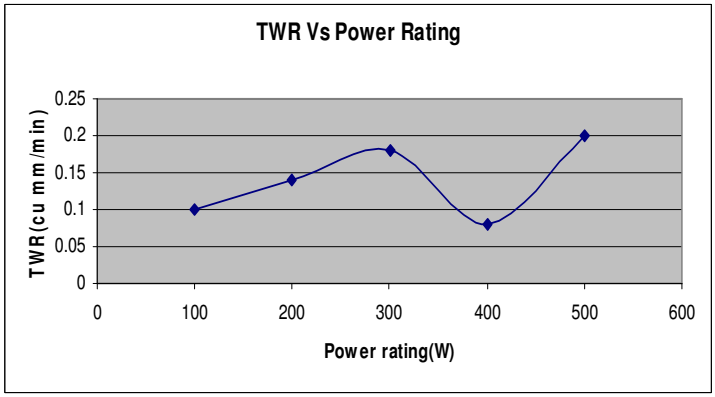

Figure 3.34 TWR Vs Power rating for TITAN31 tool while machining WC

Case 5: Silicon carbide slurry, Grit size 320, Slurry Concentration 25%

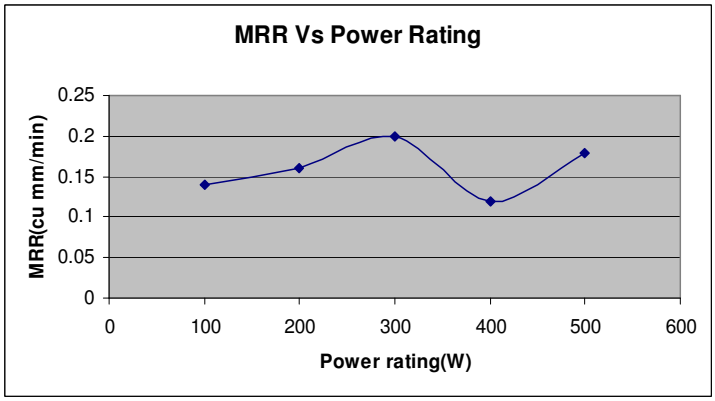

Figure 3.35 MRR Vs Power rating for TITAN12 tool while machining WC

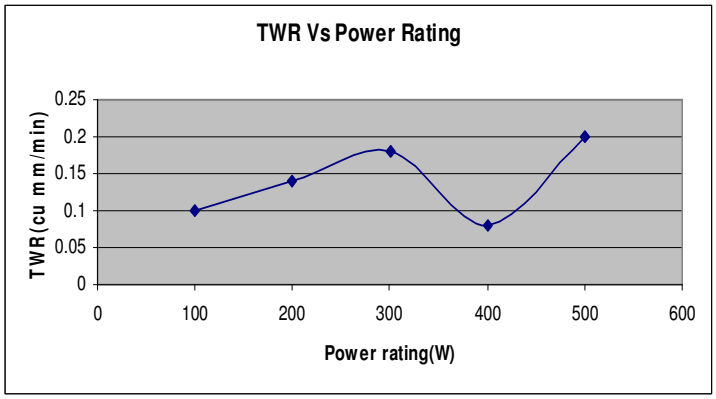

Figure 3.36 TWR Vs Power rating for TITAN12 tool while machining WC

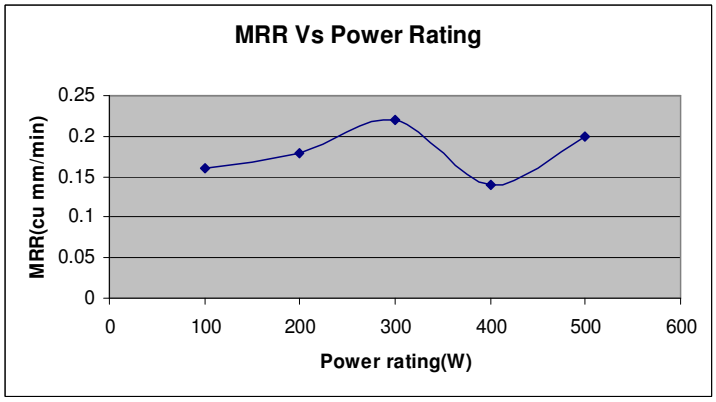

Figure 3.37 MRR Vs Power rating for TITAN15 tool while machining WC

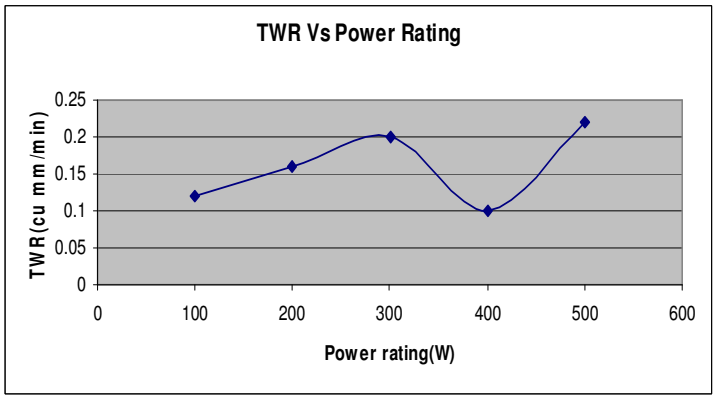

Figure 3.38 TWR Vs Power rating for TITAN15 tool while machining WC

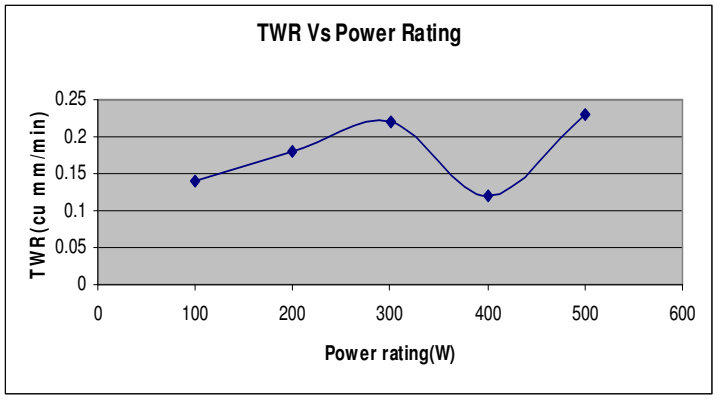

Figure 3.39 MRR Vs Power rating for TITAN31 tool while machining WC

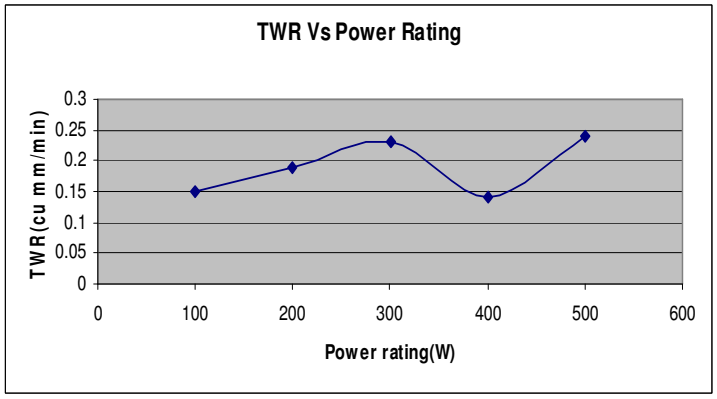

Figure 3.40 TWR Vs Power rating for TITAN31 tool while machining WC

Case 6 : Silicon carbide slurry, Grit size 500, Slurry Concentration 25%

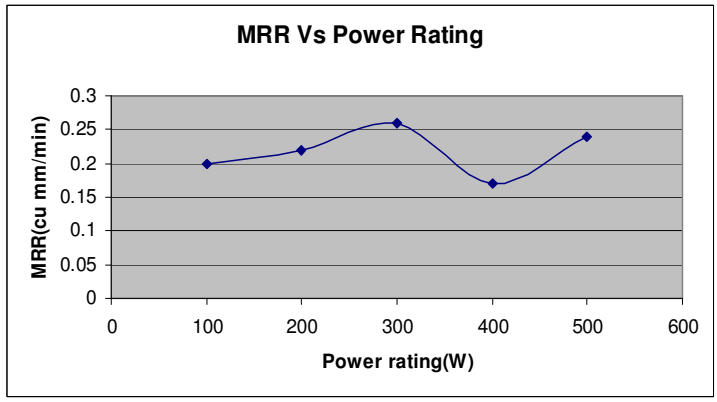

Figure 3.41 MRR Vs Power rating for TITAN12 tool while machining WC

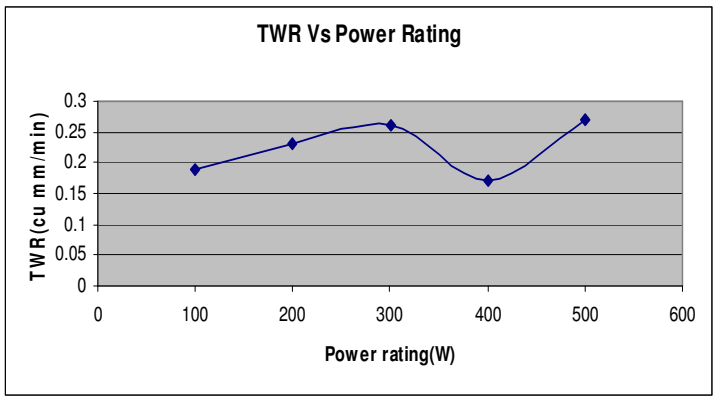

Figure 3.42 TWR Vs Power rating for TITAN12 tool while machining WC

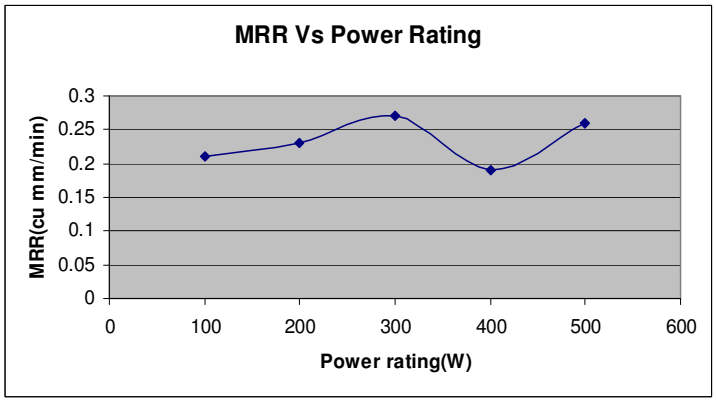

Figure 3.43 MRR Vs Power rating for TITAN15 tool while machining WC

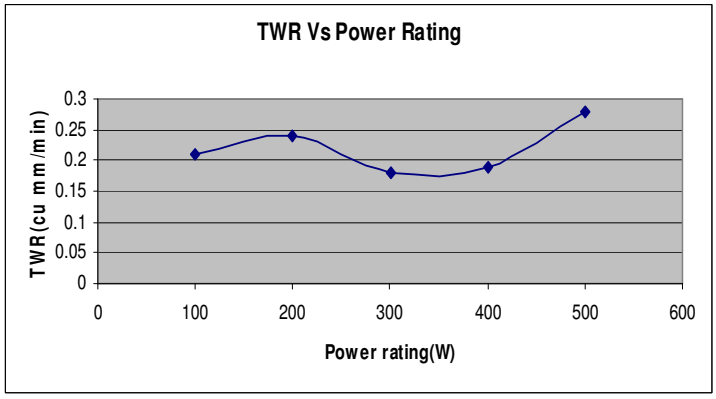

Figure 3.44 TWR Vs Power rating for TITAN15 tool while machining WC

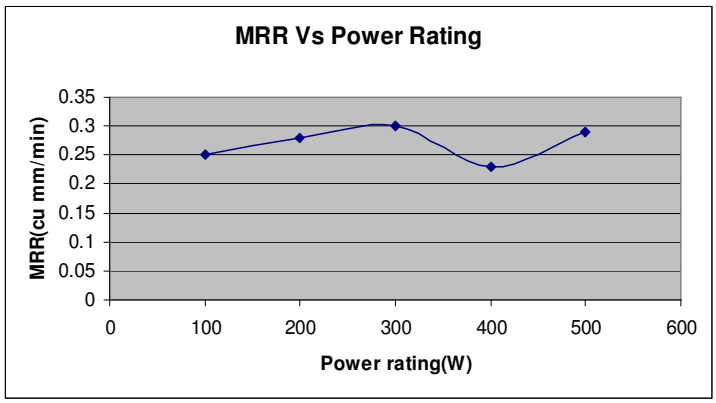

Figure 3.45 MRR Vs Power rating for TITAN31 tool while machining WC

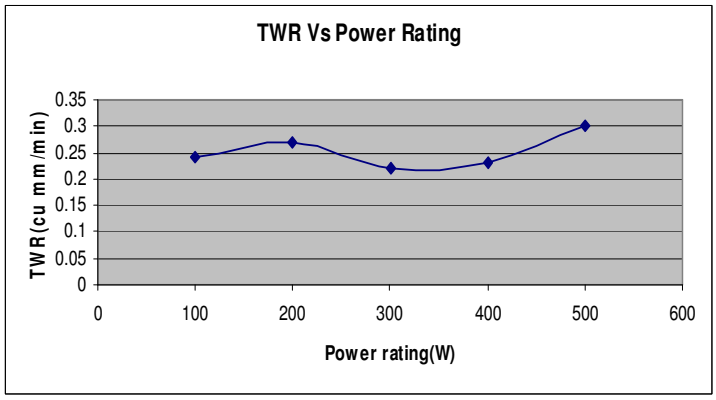

Figure 3.46 TWR Vs Power rating for TITAN31 tool while machining WC

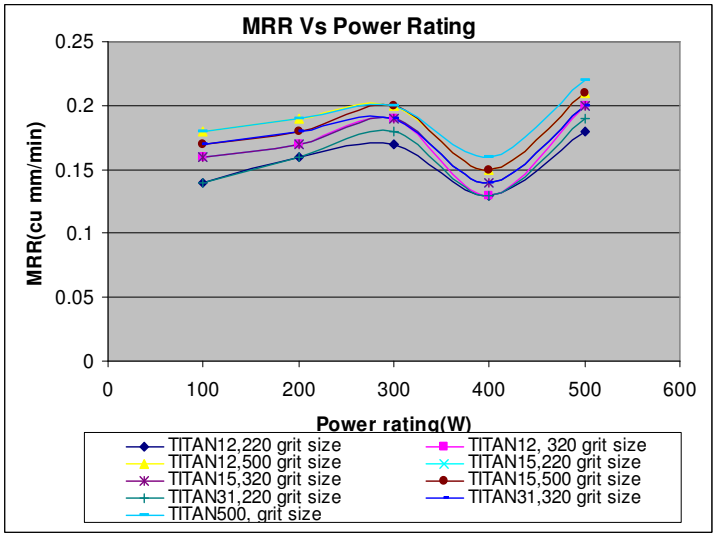

Figure 3.47 MRR Vs tool material, grit size, power rating, silicon carbide slurry while machining WC

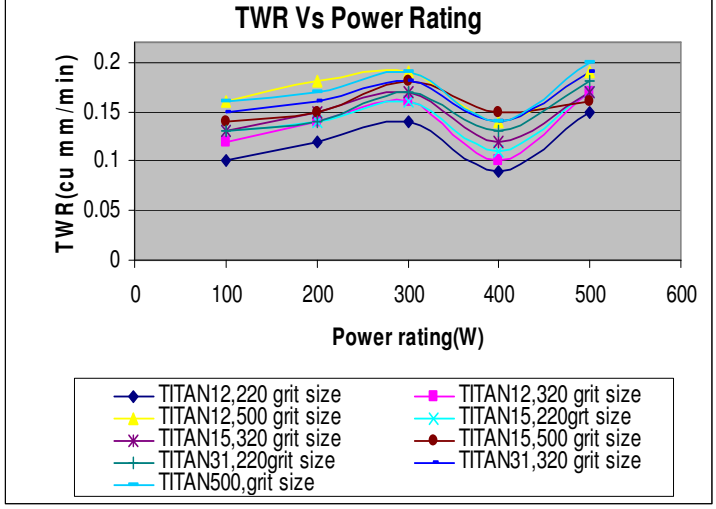

Figure 3.48 TWR Vs tool material, grit size, power rating, silicon carbide slurry while machining WC

The following conclusions have been drawn from the pilot experimentation conducted in cases (4-6).

1. The variation of MRR & TWR with respect to power rating for silicon carbide slurry with grit size of 220 and slurry concentration of 25% has been presented in the figures (3.29- 3.34) respectively. Similarly the variation using the abrasive grit sizes of 320 and 500 has been shown in figures (3.35-3.40 & 3.41-3.46) respectively. From these variations, it has been concluded that the machining characteristics (MRR, TWR) in ultrasonic machining of tungsten carbide have been found to be correlated and dependent upon the input parameters such as abrasive slurry grit size, type of tool material and power rating of the ultrasonic machine used.

2. It is not always necessary that if work piece of higher hardness is machined, it will result in more MRR; but it is combined effect of material composition relative to tool, resulting in work hardening of work piece or tool. It can be predicted that selection of operating parameter levels is critical in order to achieve acceptable productivity.
3. It can be observed that for the tungsten carbide, both MRR as well as TWR tend to increase with a corresponding increase in the coarseness of the slurry used irrespective of the abrasive used for preparation of the slurry from figures (3.47-3.48) respectively. Also, the MRR and TWR obtained with different tool materials

(TITAN12, TITAN15 and TITAN31) are significantly different when all other input parameters are controlled and remain fixed. Thus, the tool material properties such as hardness and toughness have been found to control the machining characteristics in USM of tungsten carbide.

4. The material removal rate and the tool wear rate have been affected by using the different types of abrasive slurries. It could be concluded that use of boron carbide slurry results in better material removal rate for same process conditions in comparison to silicon carbide and aluminum oxide. This can be attributed to the higher hardness and cutting ability of boron carbide in comparison to silicon carbide abrasive and aluminum oxide.

Case 7: Boron carbide slurry, Grit size 220, Slurry Concentration 25%

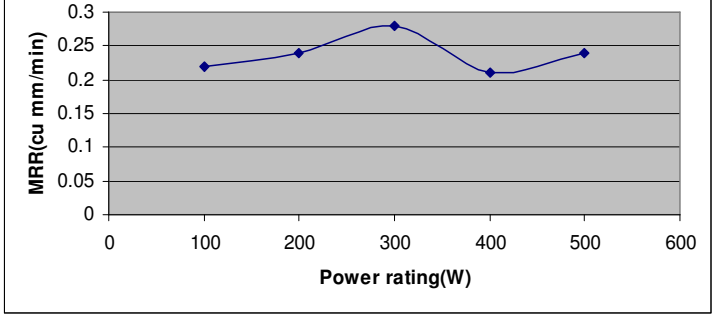

Figure 3.49 MRR Vs Power rating for TITAN12 tool while machining WC

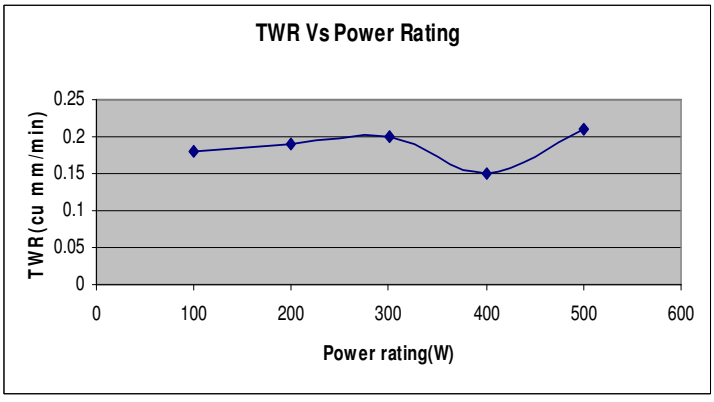

Figure 3.50 TWR Vs Power rating for TITAN12 tool while machining WC

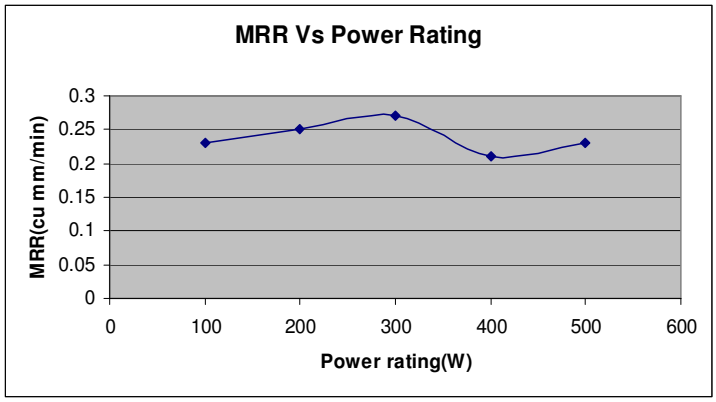

Figure 3.51 MRR Vs Power rating for TITAN15 tool while machining WC

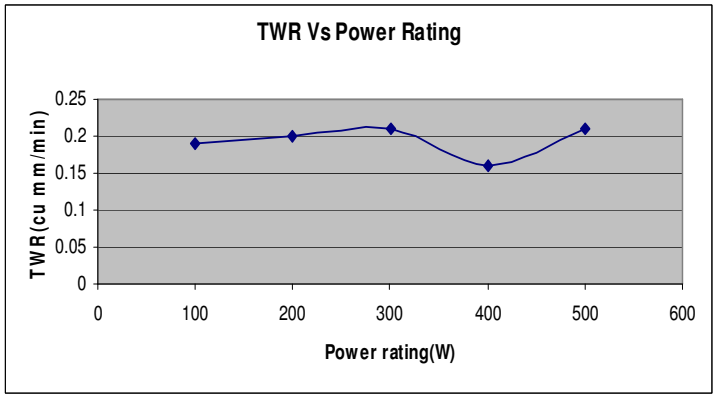

Figure 3.52 TWR Vs Power rating for TITAN15 tool while machining WC

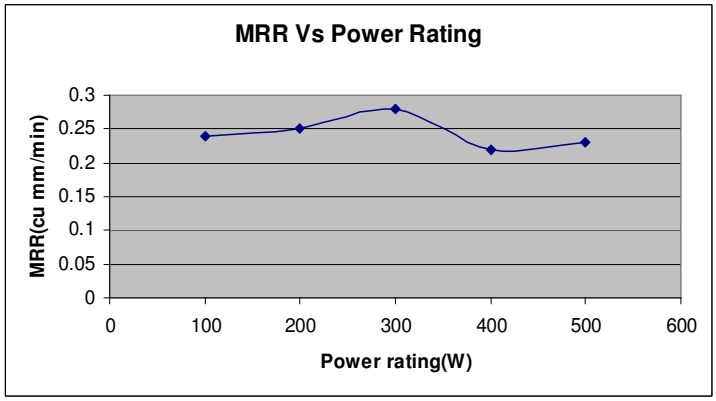

Figure 3.53 MRR Vs Power rating for TITAN31 tool while machining WC

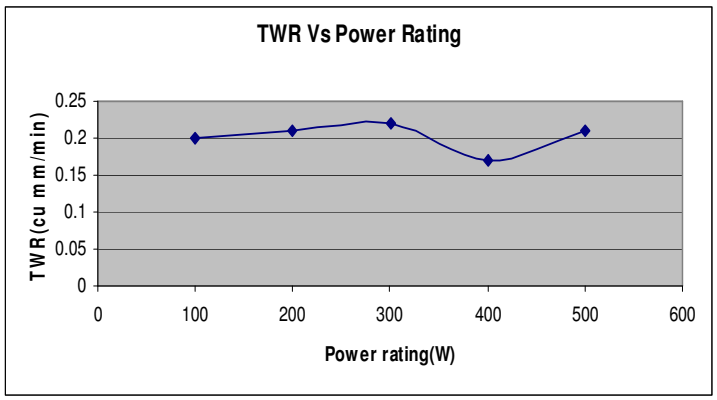

Figure 3.54 TWR Vs Power rating for TITAN31 tool while machining WC

Case 8: Boron carbide slurry, Grit size 320, Slurry Concentration 25%

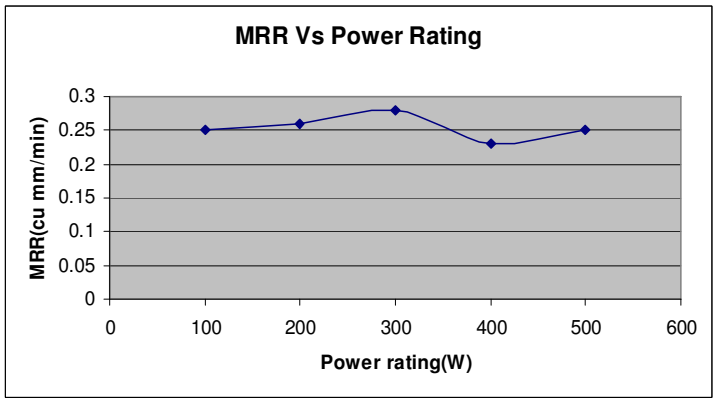

Figure 3.55 MRR Vs Power rating for TITAN12 tool while machining WC

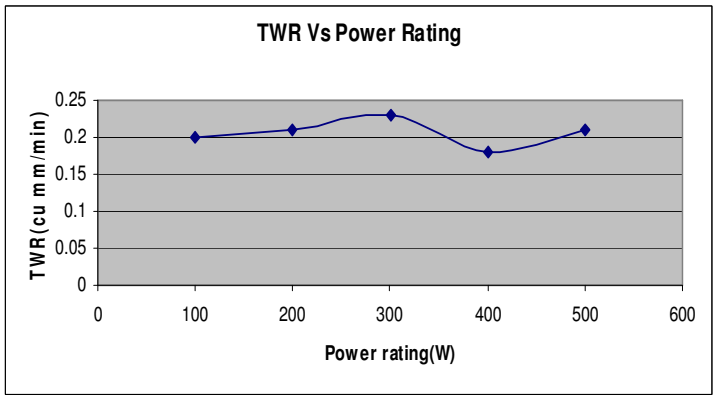

Figure 3.56 TWR Vs Power rating for TITAN12 tool while machining WC

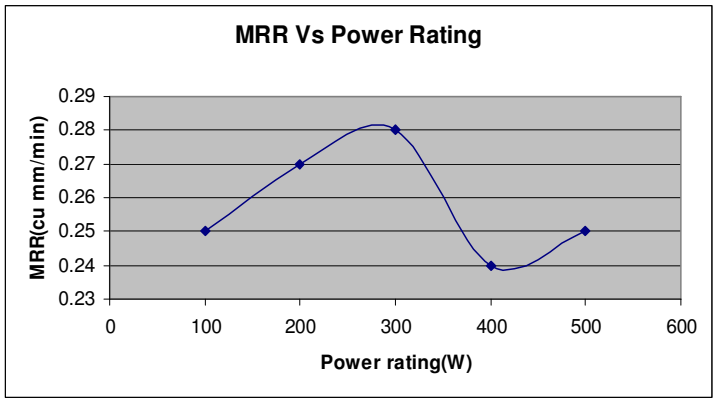

Figure 3.57 MRR Vs Power rating for TITAN15 tool while machining WC

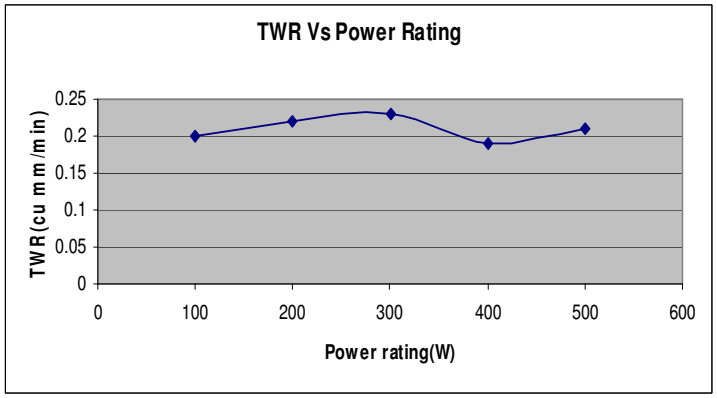

Figure 3.58 TWR Vs Power rating for TITAN15 tool while machining WC

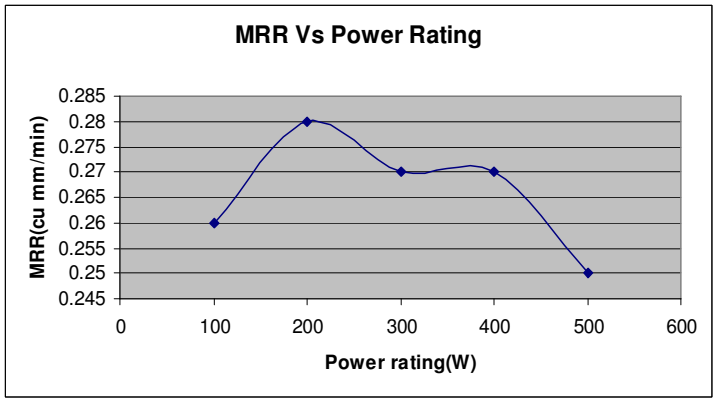

Figure 3.59 MRR Vs Power rating for TITAN31 tool while machining WC

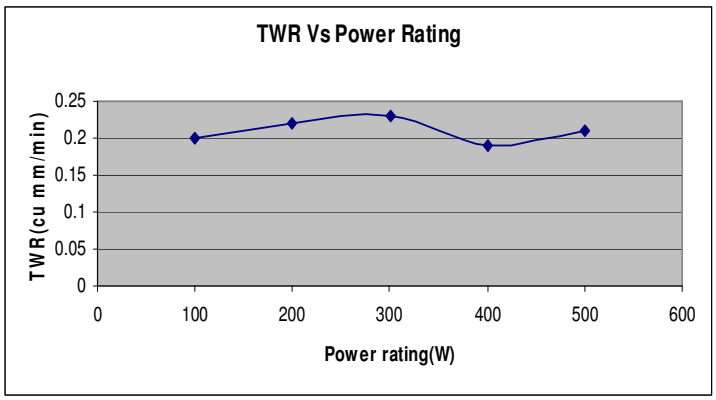

Figure 3.60 TWR Vs Power rating for TITAN31 tool while machining WC

Case 9: Boron carbide slurry, Grit size 500, Slurry Concentration 25%

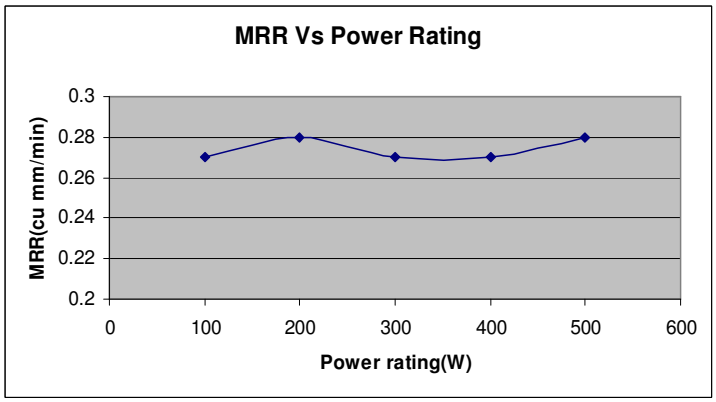

Figure 3.61 MRR Vs Power rating for TITAN12 tool while machining WC

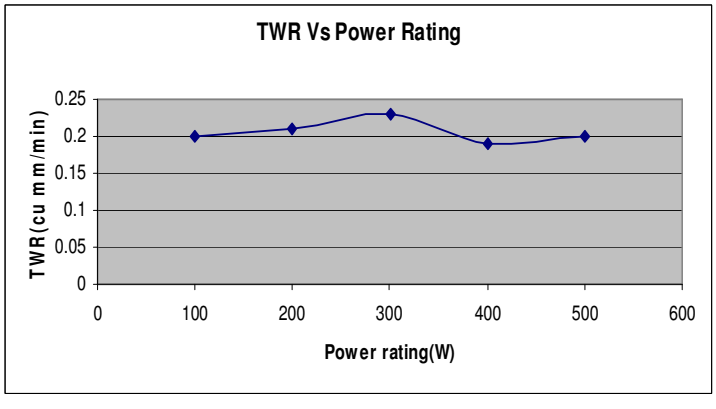

Figure 3.62 TWR Vs Power rating for TITAN12 tool while machining WC

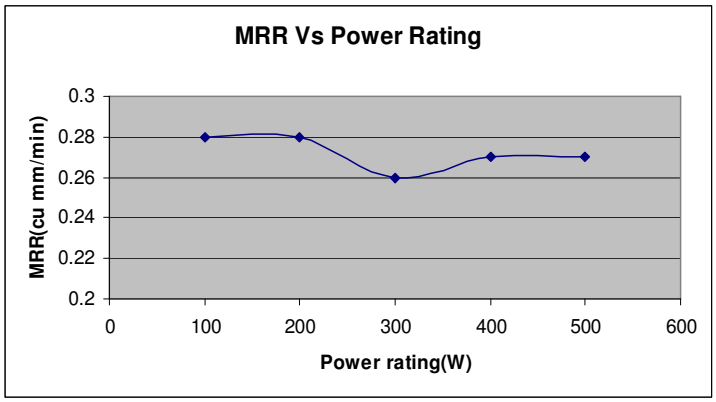

Figure 3.63 MRR Vs Power rating for TITAN15 tool while machining WC

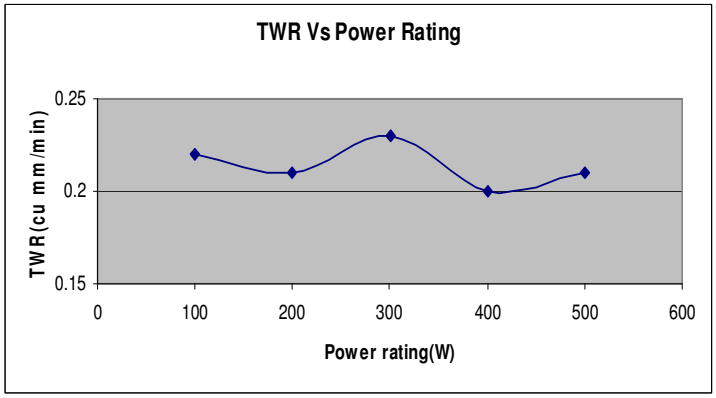

Figure 3.64 TWR Vs Power rating for TITAN15 tool while machining WC

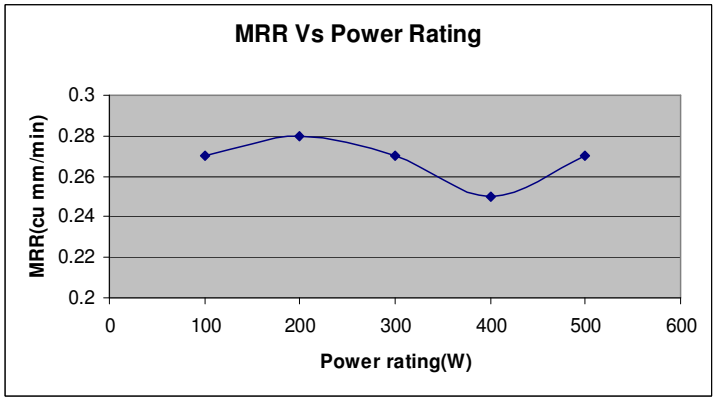

Figure 3.65 MRR Vs Power rating for TITAN31 tool while machining WC

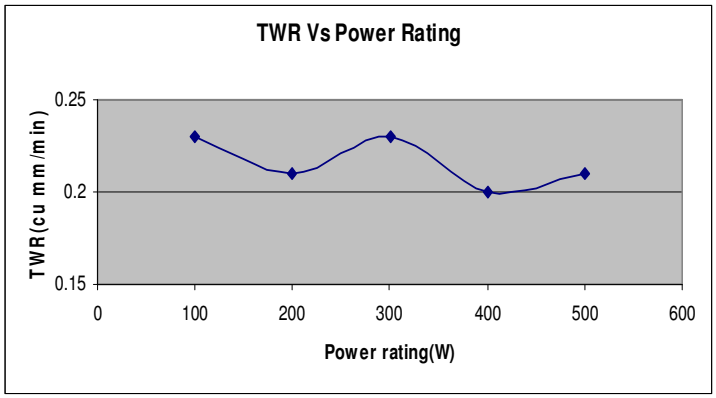

Figure 3.66 TWR Vs Power Rating for TITAN31 tool while machining WC

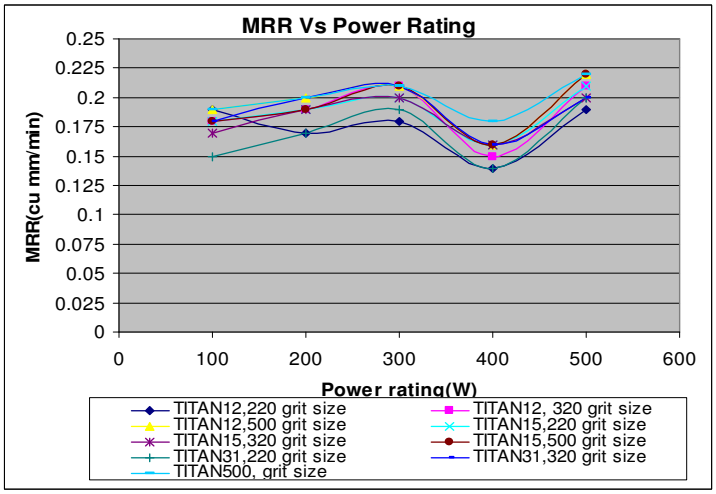

Figure 3.67 MRR Vs tool material, grit size, power rating, Boron carbide slurry while machining WC

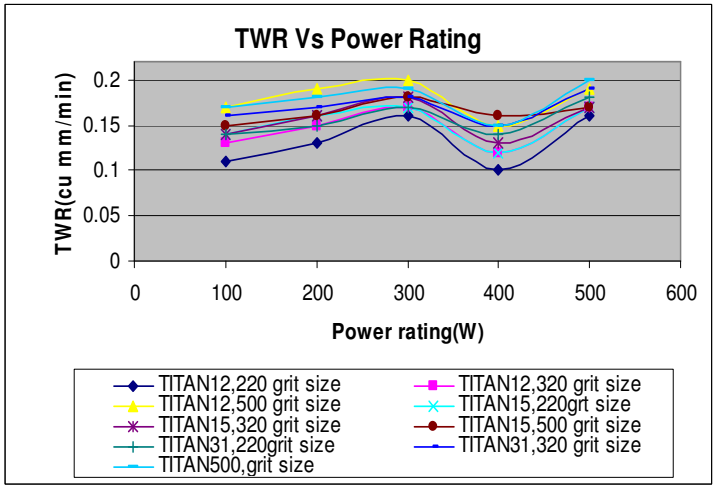

Figure 3.68 TWR Vs tool material, grit size, power rating, Boron carbide slurry while machining WC

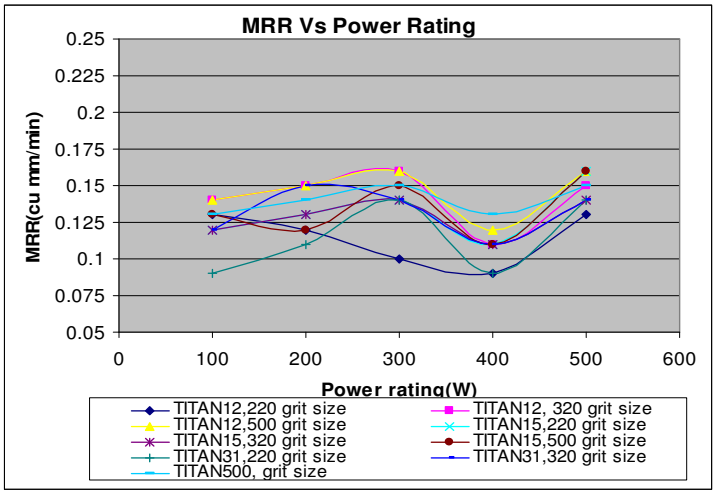

Figure 3.69 MRR Vs tool material, grit size, power rating, aluminium oxide slurry while machining stellite

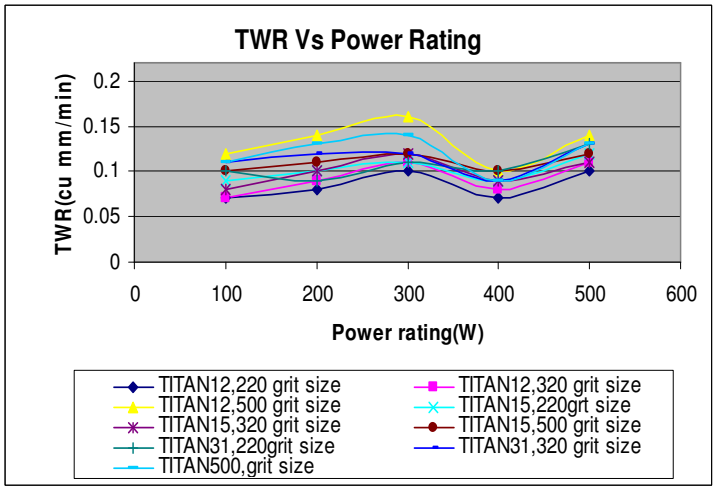

Figure 3.70 TWR Vs tool material, grit size, power rating, aluminium oxide slurry while machining stellite

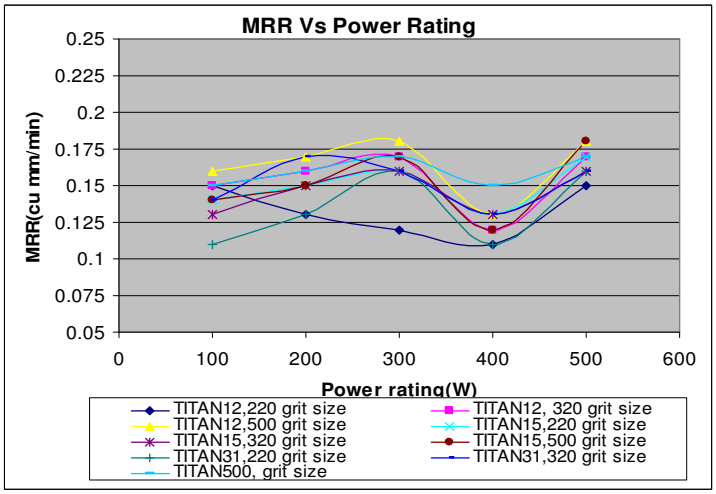

Figure 3.71 MRR Vs tool material, grit size, power rating, silicon carbide slurry while machining stellite

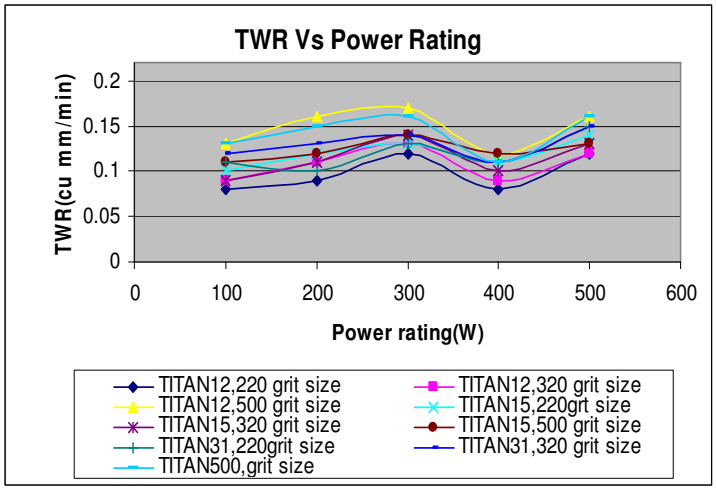

Figure 3.72 TWR Vs tool material, grit size, power rating, silicon carbide slurry while machining stellite

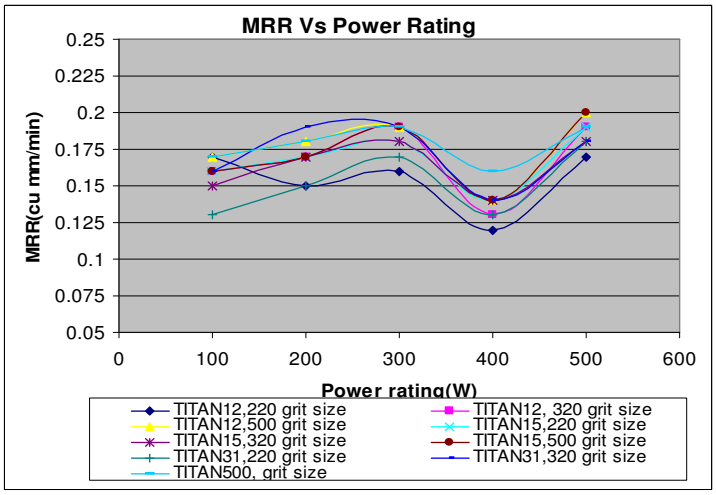

Figure 3.73 MRR Vs tool material, grit size, power rating, Boron carbide slurry while machining stellite

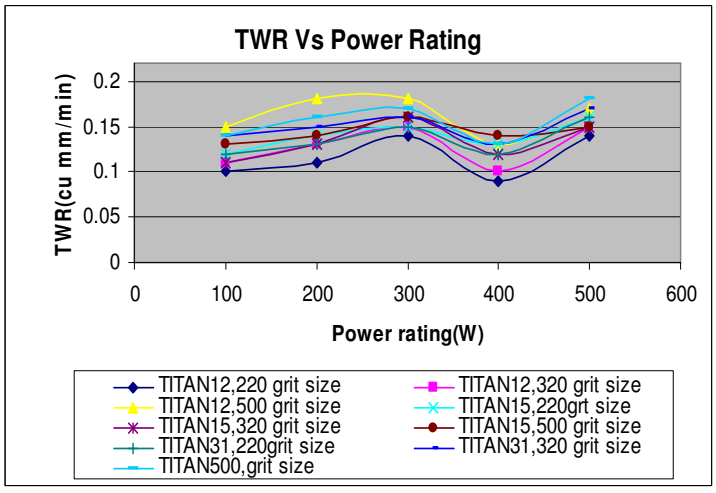

Figure 3.74 TWR Vs tool material, grit size, power rating, Boron carbide slurry while machining stellite

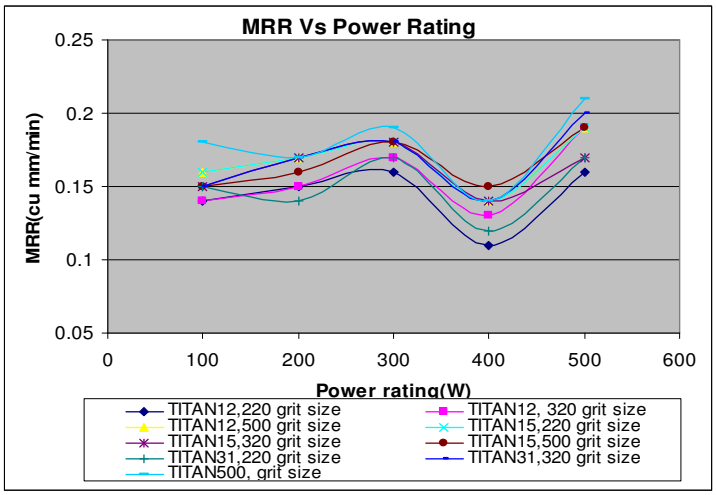

Figure 3.75 MRR Vs tool material, grit size, power rating, aluminium oxide slurry while machining PCD

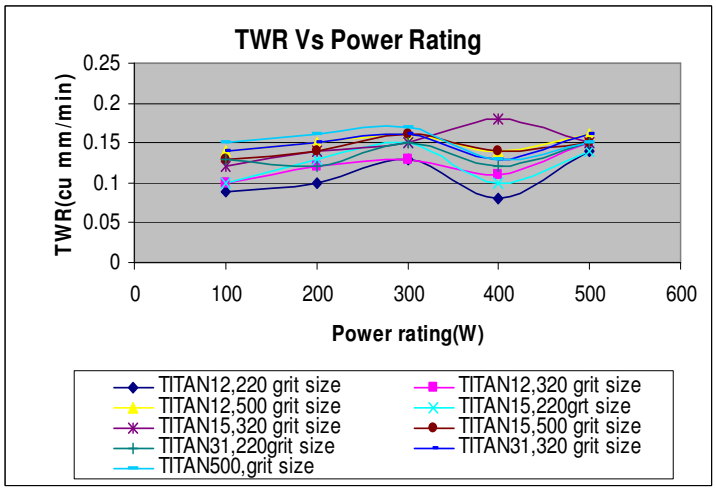

Figure 3.76 TWR Vs tool material, grit size, power rating, aluminium oxide slurry while machining PCD

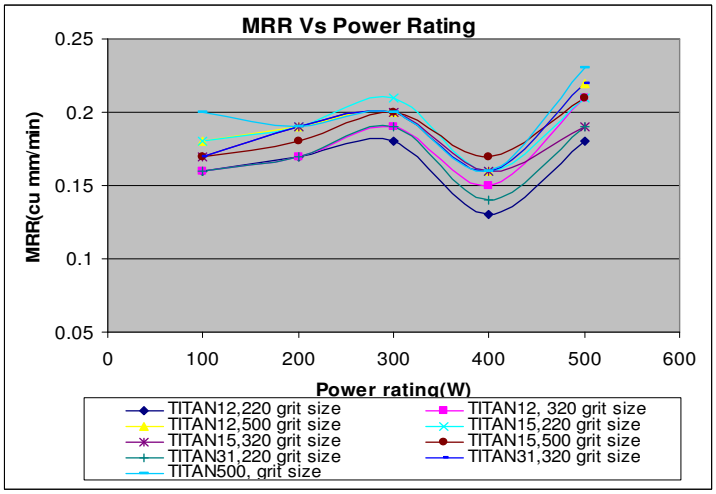

Figure 3.77 MRR Vs tool material, grit size, power rating, silicon carbide slurry while machining PCD

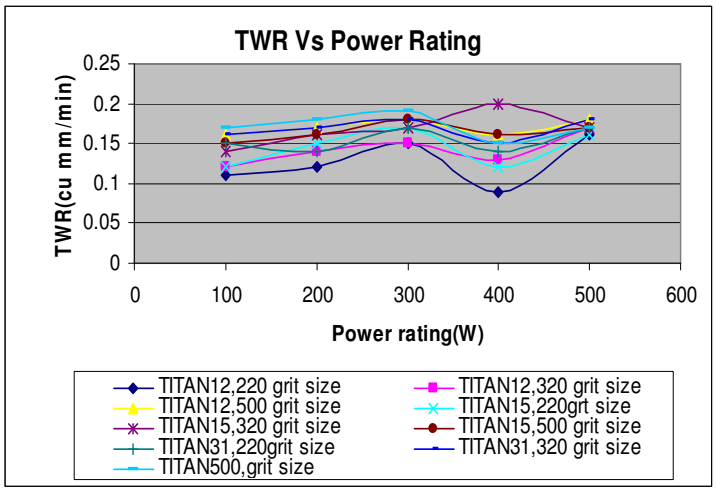

Figure 3.78 TWR Vs tool material, grit size, power rating, silicon carbide slurry while machining PCD

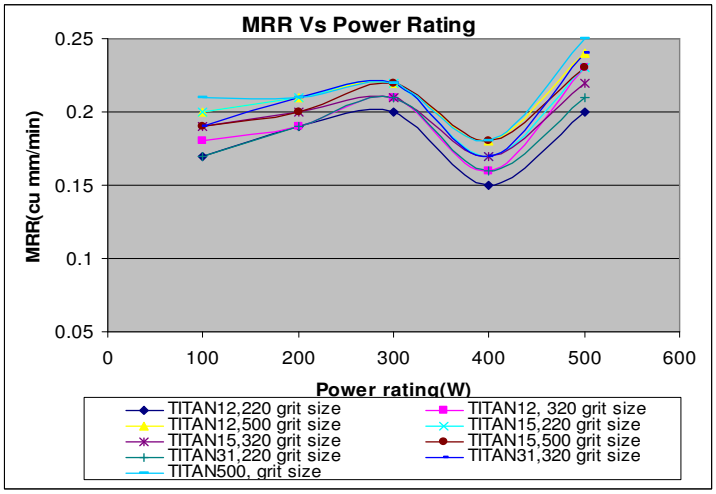

Figure 3.79 MRR Vs tool material, grit size, power rating, Boron carbide slurry while machining PCD

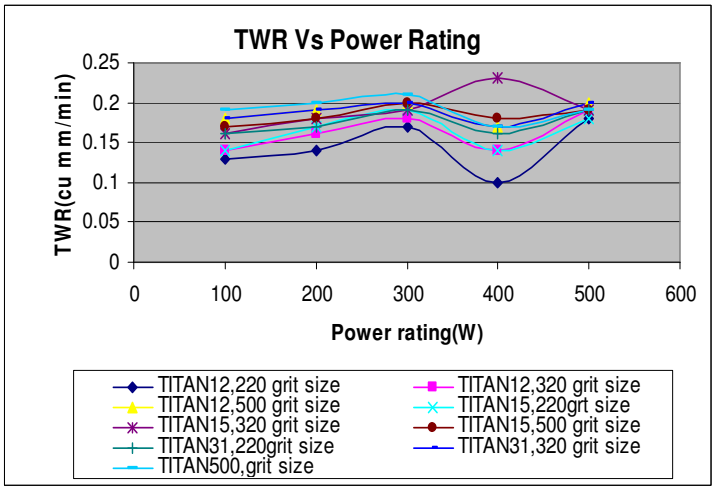

Figure 3.80 TWR Vs tool material, grit size, power rating, Boron carbide slurry while machining PCD

The following conclusions have been drawn from the pilot experimentation conducted in cases (7-9).

1. The variation of MRR & TWR with respect to power rating for boron carbide slurry with grit size of 220 and slurry concentration of 25% has been presented in the figures (3.49- 3.54) respectively. Similarly the variation using the abrasive grit sizes of 320 and 500 has been shown in figures (3.55-3.60 & 3.61-3.66) respectively. From these variations, it has been concluded that the machining characteristics (MRR, TWR) in ultrasonic machining of tungsten carbide have been found to be correlated and dependent upon the input parameters such as abrasive slurry grit size, type of tool material and power rating of the ultrasonic machine used.

2. It is not always necessary that if work piece of higher hardness is machined, it will result in more MRR; but it is combined effect of material composition relative to tool, resulting in work hardening of work piece or tool. It can be predicted that selection of operating parameter levels is critical in order to achieve acceptable productivity.
3. It can be observed that for the tungsten carbide, both MRR as well as TWR tend to increase with a corresponding increase in the coarseness of the slurry used irrespective of the abrasive used for preparation of the slurry from figures (3.67-3.68) respectively. Also, the MRR and TWR obtained with different tool materials (TITAN12, TITAN15 and TITAN31) are significantly different when all other input parameters are controlled and remain fixed. Thus, the tool material properties such as hardness and toughness have been found to control the machining characteristics in USM of tungsten carbide.
4. Also the variation of MRR & TWR with respect to power rating for stellite using different abrasive slurries of aluminium oxide, silicon carbide and boron carbide of different grit sizes 220,320 and 500 has been presented in figures (3.69-3.74). Similarly, the variation has been determined for PCD as presented in figures (3.75-3.80) respectively.

3.5 SELECTION OF FACTORS LEVELS

As the objective of study is aimed to carry out research on ultrasonic machining of tungsten carbide, stellite and Diamond (as work material) using different tool materials to know their impact on material removal rate (MRR), tool wear rate (TWR), and to model these characteristics for their application in manufacturing industry.In light of above objective, the factors levels have been decided depending upon commercial availability, experimental constraints and machine tool capacity. This information is available from pilot experiments conducted. For example, three levels of tool were selected because these three commercially available tools resulted in different behaviors of MRR and TWR. So, each tool material has been designated as a level. Similarly three levels of slurry concentration, slurry type, power rating and slurry grit size were designated. These levels represent threshold points from where change in trend has been observed in pilot tests. Table 3.1 shows different control variables and their levels.

Table 3.1 CONTROL VARIABLES AND THEIR LEVELS

S.No	Factors	Levels	Level 1	Level 2	Level 3
A	Tool material	3	TITAN12	TITAN15	TITAN31
B	Abrasive slurry	3	Al_2O_3	SiC	B_4C
C	Slurry concentration (%)	3	20	25	30
D	Abrasive Grit size	3	220	320	500
E	Power rating (%)	3	25	50	75

For the selection of a particular OA, the number of parameters, the number of levels, and their possible interactions must be taken into consideration. The case under study involves five parameters, each is of three levels. Now as per requirements of the study L18 OA comes out as one of the solution. The modified L18 OA is shown in table 3.2. Interaction between column 1 and 2 can be estimated without sacrificing any column. Column 1 and 2 can be combined to form a 6-level column. Interactions between any other pair of columns are confounded partially with the remaining columns. Based upon the standard L18 OA, response variables and control log for experimentation has been shown in tables 3.3 & 3.4 respectively.

Table 3.2 MODIFIED L18 ORTHOGONAL ARRAY

Experiment number	Columns				
1	1	1	1	1	1
2	2	2	2	2	2
3	3	3	3	3	3
4	1	1	2	2	3
5	2	2	3	3	1
6	3	3	1	1	2
7	1	2	1	3	2
8	2	3	2	1	3
9	3	1	3	2	1
10	1	3	3	2	2
11	2	1	1	3	3
12	3	2	2	1	1
13	1	2	3	1	3
14	2	3	1	2	1
15	3	1	2	3	2
16	1	3	2	3	1
17	2	1	3	1	2
18	3	2	1	2	3

Table 3.3 RESPONSE VARIABLES

Response number	Response 1	Response 2	Response 3
Response name	MRR	TWR	SR
Response units	mm^3/min	mm^3/min	Microns
Response type	continuous	continuous	Continuous

The 18 rows of the L18 array represent the 18 experiments to be conducted. Thus, experiment 1 is to be conducted at level 1 for each six control factors. These levels can be read from table 3.4.

Table 3.4 TAGUCHI DESIGN FOR EXPERIMENTATION

Experiment No.	A: Tool Material	B:Abrasive slurry	C:Slurry Concentration	D: Grit size	E: Power Rating
1	Titan 12	Al_2O_3	20	220	25
2	Titan 15	SiC	25	320	50
3	Titan 31	B_4C	30	500	75
4	Titan 12	Al_2O_3	25	320	75
5	Titan 15	SiC	30	500	25
6	Titan 31	B_4C	20	220	50
7	Titan 12	SiC	20	500	50
8	Titan 15	B_4C	25	220	75
9	Titan 31	Al_2O_3	30	320	25
10	Titan 12	B_4C	30	320	50
11	Titan 15	Al_2O_3	20	500	75
12	Titan 31	SiC	25	220	25
13	Titan 12	SiC	30	220	75
14	Titan 15	B_4C	20	320	25
15	Titan 31	Al_2O_3	25	500	50
16	Titan 12	B_4C	25	500	75
17	Titan 15	Al_2O_3	30	220	50
18	Titan 31	SiC	20	320	75

For conducting final run of experiments all five factors have been denoted by specific letter with suffix representing specific parameter and its level as shown in table 3.5.

Table 3.5 REPRESENTATION OF FACTORS LEVEL

Factor type	Level 1	Level 2	Level 3
Tool material	A1	A2	A3
Abrasive slurry	B1	B2	B3
Slurry concentration	C1	C2	C3
Aabrasive grit size	D1	D2	D3
Power rating	E1	E2	E3

The notations used are having following full meanings.

A-Tool material

A1- TITAN12

A2- TIAN15

A3- TITAN31

B-Abrasive slurry

B1- Alumina

B2- Silicon carbide

B3- Boron carbide

C – Slurry concentration by weight

C1- 20%

C2- 25%

C3- 30%

D- Abrasive grit size

D1- 220

D2- 320

D3- 500

E –Power rating

E1- 25 %(of 500 W) =125 W

E2- 50 %(of 500W) = 250W

E3- 75% (of 500 W) =375W

The 18 sets of experiments were performed in order to accommodate all the factors shown in table 3.4. These 18 sets of experiments have been repeated four times and final conclusions have been made by taking averages of results of four sets of observations. The test data for 18 sets of experiments is shown in tables (3.6-3.23) respectively.

3.6 Test data experiment no.1

Control factors design

A1-Tool material	B1-Slurry type
C1-Slurry concentration	D1- Slurry grit size
E1- Power rating	

3.7 Test data experiment no.2

Control factors design

A2-Tool material	B2-Slurry type
C2-Slurry concentration	D2- Slurry grit size
E2- Power rating	

3.8 Test data experiment no.3

Control factors design

A3-Tool material	B3-Slurry type
C3-Slurry concentration	D3- Slurry grit size
E3- Power rating	

3.9 Test data experiment no.4

Control factors design

A1-Tool material	B1-Slurry type
C2-Slurry concentration	D2- Slurry grit size
E3- Power rating	

3.10 Test data experiment no.5

Control factors design

A2-Tool material	B2-Slurry type
C3-Slurry concentration	D3- Slurry grit size
E1- Power rating	

3.11 Test data experiment no.6

Control factors design

A3-Tool material	B3-Slurry type
C1-Slurry concentration	D1- Slurry grit size
E2- Power rating	

3.12 Test data experiment no.7

Control factors design

A1-Tool material	B2-Slurry type
C1-Slurry concentration	D3- Slurry grit size
E2- Power rating	

3.13 Test data experiment no.8

Control factors design

A2-Tool material	B3-Slurry type
C2-Slurry concentration	D1- Slurry grit size
E3- Power rating	

3.14 Test data experiment no.9

Control factors design

A3-Tool material	B1-Slurry type
C3-Slurry concentration	D2- Slurry grit size
E1- Power rating	

3.15 Test data experiment no.10

Control factors design

A1-Tool material	B3-Slurry type
C3-Slurry concentration	D2- Slurry grit size
E2- Power rating	

3.16 Test data experiment no.11

Control factors design

A2-Tool material	B1-Slurry type
C1-Slurry concentration	D3- Slurry grit size
E3- Power rating	

3.17 Test data experiment no.12

Control factors design

A3-Tool material	B2-Slurry type
C2-Slurry concentration	D1- Slurry grit size
E1- Power rating	

3.18 Test data experiment no.13

Control factors design

A1-Tool material	B2-Slurry type
C3-Slurry concentration	D1- Slurry grit size
E3- Power rating	

3.19 Test data experiment no.14

Control factors design

A2-Tool material	B3-Slurry type
C1-Slurry concentration	D2- Slurry grit size
E1- Power rating	

3.20 Test data experiment no.15

Control factors design

A3-Tool material	B1-Slurry type
C2-Slurry concentration	D3- Slurry grit size
E2- Power rating	

3.21 Test data experiment no.16

Control factors design

A1-Tool material	B3-Slurry type
C2-Slurry concentration	D3- Slurry grit size
E1- Power rating	

3.22 Test data experiment no.17

Control factors design

A2-Tool material	B1-Slurry type
C3-Slurry concentration	D1- Slurry grit size
E2- Power rating	

3.23 Test data experiment no.18

Control factors design

A3-Tool material	B2-Slurry type
C1-Slurry concentration	D2- Slurry grit size
E3- Power rating	

3.6 DEFINITION OF SIGNAL TO NOISE RATIO (S/N)

In the taguchi method, a loss function has been defined to gauge the deviation between the experimental and desired value of a performance characteristics. The loss function is further transformed into a signal-to-noise ratio. Finding a correct objective function to maximize in an engineering design problem is very important. Failure to do, can lead to great inefficiencies in experimentation and even wrong conclusions about the optimum levels. The task of finding what adjustments are meaningful in a particular problem and determine the correct S/N ratio is not always easy. Three categories of performance characteristics are usually used in the analysis of the S/N ratio, i.e lower-the-better, Higher-the-better and nominal-the-best. These are explained as follows:

3.6.1 Lower-the-Better type problem

For lower the better type problem, the quality characteristics is continuous and non negative i.e. it can take any value from 0 to α. Its most desired value is zero. Such problems are characterized by the absence of a scaling factor or any other adjustment factor. Because there is no adjustment factor in these problems, one should simply minimize the quality loss without adjustment i.e. we should minimize:

Q=k (mean square quality characteristics)

$$Q = k\left(1/n\sum_{i=1}^{n} y_i^2\right)$$

Minimizing Q is equivalent to maximizing η, defined by the following equation

$$\eta = -10\log_{10}\left(1/n\sum_{i=1}^{n} y_i^2\right)$$

where η is the inspection index, defined as the signal-to-noise ratio (unit: dB), n is the number of repetitions for each trial independently of the values assigned to noise factors, and y_i is the value of the response obtained in the i^{th} repetition of the trial.In this case the signal is constant, to make quality characteristics equal to zero.Therefore, the S/N ratio measures merely the effect of noise.

3.6.2 Higher–the-Better type problem

Here, the quality characteristic is continous and non-negative and one would like to be as large as possible.Also, there was no adjustment factor. The objective function to be maximized in this case is given by:

$\eta = -10\log_{10}$ (mean square reciprocal quality characteristics)

$$\eta = -10\log_{10}\left(1/n\sum_{i=1}^{n} 1/y_i^2\right)$$

3.6.3 Nominal-the-Best type problem

Here, as in lower-the-better type problem, the quality characteristic is continous and non-negative i.e. it can take any value from 0 to α. Its target value is non zero and finite. For these problems when the mean becomes zero, the variance also becomes zero. Also, for these problems we can find a scaling factor that can serve as adjustment factor to move the mean on target.This type of problem occurs frequently in engineering design. The objective function to be maximized for such problem is:

$$\eta = 10\log_{10}\left(\mu^2/\sigma^2\right)$$

$$\sigma^2 = 1/(n-1)\sum_{i=1}^{n}(y_i - \mu)^2$$

where μ is mean and σ^2 is variance.

The optimization of the nominal-type-best problems can be accomplished in two steps:

1. Maximize or minimize sensitivity to noise. During this step we select the levels of control factors to maximize while we ignore the mean.

2. Adjust the mean on target. During this step we use the adjustment factor to bring the mean on target without changing.

For the case under study Nominal-the-Best type situation is selected as objective function, as because there were three response parameters namely MRR, TWR and SR and all three output responses are interrelated and have interdependence among each other.

3.7 EXPRIMENTATION WORK

The experiments were conducted in eighteen set-ups. In the first set-up, experiment was performed to determine the effect of TITAN-12 tool on tungsten carbide work using alumina slurry of 220 grit size with 20% concentration by weight in distilled water as suspension media. The experiment was started by setting power rating of the machine at 25 %(of 500W) i.e.125W of ultrasonic drilling machine. Figure 3.81 shows the schematic of the ultrasonic machine tool used for experimentation for eighteen set-ups.

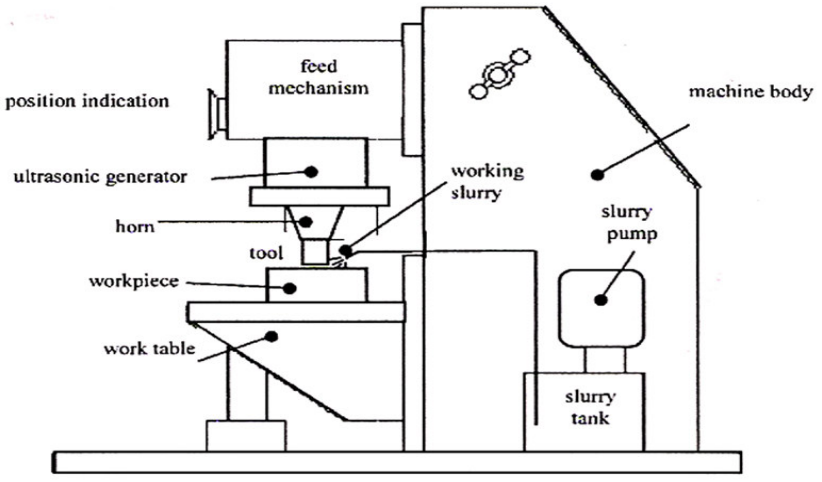

Figure 3.81 Schematic of the Ultrasonic Machine Tool (Type: Sonic Mill, USA)

The initial masses of tungsten carbide and tool (TITAN-12) were measured.Then machine was allowed to machine with constant slurry flow rate .The depth was closely observed using dial gauge and correspondingly, time taken for machining was measured using stop watch.The tool used was of solid cylindrical cross section. After machining was completed, again job (work-piece) and tool masses were measured for finding difference in weight loss by using the electronic balance. The material removal rate (MRR) was calculated by taking the ratio of weight loss of work to the product of machining time and density of work material. The tool wear rate (TWR) was calculated by taking the ratio of weight loss of tool to the product of machining time and density of tool. After this, tungsten carbide work piece was observed for surface roughness using perthometer.The perthometer set up is shown as in figure 3.82. The same process was repeated in eighteen set-ups.

Figure 3.82 Surface roughness tester, Perthometer (Mahr, M4Pi)

The following are the specifications of surface roughness, perthometer.

- Principle of measurement : Stylus method
- Measurement ranges : 100 – 150 µm
- Cut-off wavelengths: 0.08 – 0.25 – 0.8 – 2.5 mm
- Tracing lengths : 1.5 – 4.8 – 15 mm

- Number of sampling lengths : 1……5 selectable
- Parameters : R_a, R_q, R_z, R_{max}, R_p, R_t, M_r (material ratio)
- Tolerance monitoring: Maximum/minimum for all parameters selected.
- Measuring unit : µm, µin selectable
- Dimensions (W x D x H) :175 x 85 x 70 mm
- Weight : Approx. 600g

Table 3.24 Observation table for experiment no.1

Control factors design

A1- TITAN12 B1-Alumina

C1-20% D1- 220

E1- 25%

S.No	Work material	MRR (mm^3/min)	TWR (mm^3/min)	SR (microns)
1	WC	0.164	0.102	0.68
2	WC	0.176	0.104	0.54
3	WC	0.182	0.082	0.48
4	WC	0.185	0.112	0.56
5	St	0.162	0.102	0.64
6	St	0.165	0.104	0.58
7	St	0.176	0.082	0.64
8	St	0.178	0.112	0.60
9	PCD	0.184	0.098	0.8
10	PCD	0.190	0.120	0.64
11	PCD	0.180	0.104	0.96
12	PCD	0.190	0.020	0.78

Table 3.25 Observation table for experiment no.2

Control factors design

A2- TITAN15 B2-SiC

C2-25% D2- 320

E2- 50%

S.No	Work material	MRR (mm^3/min)	TWR (mm^3/min)	SR (microns)
1	WC	0.168	0.106	0.62
2	WC	0.164	0.114	0.58
3	WC	0.172	0.064	0.60
4	WC	0.182	0.082	0.74
5	St	0.164	0.106	0.60
6	St	0.152	0.114	0.54
7	St	0.168	0.064	0.60
8	St	0.178	0.082	0.76
9	PCD	0.190	0.100	0.84
10	PCD	0.210	0.086	0.92
11	PCD	0.190	0.040	1.14
12	PCD	0.210	0.032	1.40

Table 3.26 Observation table for experiment no.3

Control factors design

A3- TITAN31 B3-B_4C

C3-30% D3- 500

E3- 75%

S.No	Work material	MRR (mm^3/min)	TWR (mm^3/min)	SR (microns)
1	WC	0.184	0.112	0.80
2	WC	0.204	0.126	0.84
3	WC	0.224	0.102	0.86
4	WC	0.198	0.064	0.92
5	St	0.174	0.112	0.70
6	St	0.182	0.126	0.78
7	St	0.204	0.102	0.84
8	St	0.184	0.064	0.86
9	PCD	0.204	0.048	0.90
10	PCD	0.220	0.150	0.84
11	PCD	0.210	0.024	0.90
12	PCD	0.240	0.060	1.34

Table 3.27 Observation table for experiment no.4

Control factors design

A1- TITAN12 B1-Alumina

C2-25% D2- 320

E3- 75%

S.No	Work material	MRR (mm^3/min)	TWR (mm^3/min)	SR (microns)
1	WC	0.168	0.104	0.70
2	WC	0.172	0.102	0.68
3	WC	0.178	0.048	0.72
4	WC	0.180	0.082	0.76
5	St	0.164	0.104	0.64
6	St	0.164	0.102	0.68
7	St	0.168	0.048	0.76
8	St	0.176	0.082	0.74
9	PCD	0.180	0.160	0.64
10	PCD	0.224	0.160	0.68
11	PCD	0.230	0.014	0.86
12	PCD	0.282	0.102	0.84

Table 3.28 Observation table for experiment no.5

Control factors design

A2- TITAN15 B2-SiC

C3-30% D3- 500

E1- 25%

S.No	Work material	MRR (mm^3/min)	TWR (mm^3/min)	SR (microns)
1	WC	0.158	0.112	0.54
2	WC	0.142	0.108	0.60
3	WC	0.160	0.092	0.75
4	WC	0.166	0.082	0.62
5	St	0.148	0.112	0.58
6	St	0.136	0.108	0.70
7	St	0.140	0.092	0.78
8	St	0.162	0.082	0.64
9	PCD	0.178	0.180	0.78
10	PCD	0.228	0.180	0.78
11	PCD	0.242	0.062	0.92
12	PCD	0.268	0.082	1.56

Table 3.29 Observation table for experiment no.6

Control factors design

A3- TITAN31 B3-B_4C

C1-20% D1- 220

E2- 50%

S.No	Work material	MRR (mm^3/min)	TWR (mm^3/min)	SR (microns)
1	WC	0.184	0.124	0.74
2	WC	0.178	0.120	0.68
3	WC	0.186	0.098	0.70
4	WC	0.170	0.058	0.82
5	St	0.174	0.124	0.68
6	St	0.176	0.12	0.76
7	St	0.169	0.098	0.64
8	St	0168	0.058	0.80
9	PCD	0.22	0.082	0.62
10	PCD	0.232	0.086	0.84
11	PCD	0.260	0.048	0.88
12	PCD	0.160	0.072	1.64

Table 3.30 Observation table for experiment no.7

Control factors design

A1- TITAN12 B2-SiC

C1-20% D3- 500

E2- 50%

S.No	Work material	MRR (mm^3/min)	TWR (mm^3/min)	SR (microns)
1	WC	0.125	0.108	0.40
2	WC	0.102	0.106	0.44
3	WC	0.115	0.042	0.32
4	WC	0.098	0.082	0.48
5	St	0.120	0.108	0.60
6	St	0.110	0.106	0.54
7	St	0.105	0.042	0.48
8	St	0.140	0.082	0.84
9	PCD	0.21	0.19	0.52
10	PCD	0.24	0.092	0.90
11	PCD	0.282	0.082	1.04
12	PCD	0.248	0.104	0.92

Table 3.31 Observation table for experiment no.8

Control factors design

A2- TITAN15 B3-B_4C

C2-25% D1- 220

E3- 75%

S.No	Work material	MRR (mm^3/min)	TWR (mm^3/min)	SR (microns)
1	WC	0.142	0.104	0.42
2	WC	0.138	0.100	0.54
3	WC	0.128	0.062	0.66
4	WC	0.162	0.064	0.58
5	St	0.137	0.104	0.48
6	St	0.127	0.100	0.58
7	St	0.118	0.062	0.62
8	St	0.160	0.064	0.58
9	PCD	0.230	0.14	0.98
10	PCD	0.242	0.084	0.68
11	PCD	0.288	0.046	1.24
12	PCD	0.310	0.084	1.80

Table 3.32 Observation table for experiment no.9

Control factors design

A3- TITAN31 B1-Alumina

C3-30% D2- 320

E1- 25%

S.No	Work material	MRR (mm^3/min)	TWR (mm^3/min)	SR (microns)
1	WC	0.126	0.062	0.48
2	WC	0.115	0.114	0.54
3	WC	0.118	0.082	0.38
4	WC	0.102	0.074	0.18
5	St	0.120	0.062	0.50
6	St	0.116	0.114	0.60
7	St	0.114	0.082	0.68
8	St	0.102	0.074	0.48
9	PCD	0.224	0.068	0.92
10	PCD	0.260	0.160	0.86
11	PCD	0.210	0.104	1.54
12	PCD	0.260	0.082	1.42

Table 3.33 Observation table for experiment no.10

Control factors design

A1- TITAN12 B3-B_4C

C3-30% D2- 320

E2- 50%

S.No	Work material	MRR (mm^3/min)	TWR (mm^3/min)	SR (microns)
1	WC	0.194	0.082	0.78
2	WC	0.218	0.112	0.84
3	WC	0.262	0.078	0.80
4	WC	0.245	0.112	0.70
5	St	0.184	0.082	0.80
6	St	0.214	0.112	0.60
7	St	0.240	0.078	0.78
8	St	0.240	0.112	0.68
9	PCD	0.228	0.042	0.88
10	PCD	0.262	0.064	1.04
11	PCD	0.190	0.072	0.92
12	PCD	0.250	0.146	1.80

Table 3.34 Observation table for experiment no.11

Control factors design

A2- TITAN15 B1-Alumina

C1-20% D3- 500

E3- 75%

S.No	Work material	MRR (mm^3/min)	TWR (mm^3/min)	SR (microns)
1	WC	0.162	0.084	0.78
2	WC	0.164	0.104	0.64
3	WC	0.176	0.102	0.62
4	WC	0.172	0.114	0.60
5	St	0.158	0.084	0.78
6	St	0.162	0.104	0.68
7	St	0.168	0.102	0.68
8	St	0.170	0.114	0.58
9	PCD	0.230	0.146	0.74
10	PCD	0.252	0.058	1.08
11	PCD	0.182	0.014	0.84
12	PCD	0.254	0.040	0.92

Table 3.35 Observation table for experiment no.12

Control factors design

A3- TITAN31 B2-SiC

C2-25% D1- 220

E1- 25%

S.No	Work material	MRR (mm^3/min)	TWR (mm^3/min)	SR (microns)
1	WC	0.180	0.104	0.54
2	WC	0.172	0.106	0.68
3	WC	0.182	0.106	0.62
4	WC	0.190	0.092	0.58
5	St	0.165	0.104	0.64
6	St	0.165	0.106	0.72
7	St	0.178	0.106	0.64
8	St	0.180	0.092	0.64
9	PCD	0.242	0.074	0.98
10	PCD	0.190	0.072	1.10
11	PCD	0.292	0.018	1.64
12	PCD	0.294	0.062	1.80

Table 3.36 Observation table for experiment no.13

Control factors design

A1- TITAN12 B2-SiC

C3-30% D1- 220

E3- 75%

S.No	Work material	MRR (mm^3/min)	TWR (mm^3/min)	SR (microns)
1	WC	0.162	0.108	0.62
2	WC	0.182	0.112	0.75
3	WC	0.168	0.108	0.80
4	WC	0.172	0.086	0.68
5	St	.158	0.108	0.68
6	St	0.176	0.112	0.78
7	St	0.158	0.108	0.72
8	St	0.170	0.086	0.72
9	PCD	0.262	0.058	0.86
10	PCD	0.264	0.082	0.96
11	PCD	0.310	0.01	1.42
12	PCD	0.202	0.07	1.46

Table 3.37 Observation table for experiment no.14

Control factors design

A2- TITAN15 B3-B_4C

C1-20% D2- 320

E1- 25%

S.No	Work material	MRR (mm^3/min)	TWR (mm^3/min)	SR (microns)
1	WC	0.168	0.106	0.68
2	WC	0.175	0.108	0.70
3	WC	0.180	0.120	0.72
4	WC	0.178	0.112	0.80
5	St	0.162	0.106	0.70
6	St	0.170	0.108	0.80
7	St	0.160	0.120	0.76
8	St	0.172	0.112	0.78
9	PCD	0.246	0.140	0.78
10	PCD	0.280	0.120	0.11
11	PCD	0.190	0.220	0.64
12	PCD	0.304	0.084	0.78

Table 3.38 Observation table for experiment no.15

Control factors design

A3- TITAN31 B1-Alumina

C2-25% D3- 500

E2- 50%

S.No	Work material	MRR (mm^3/min)	TWR (mm^3/min)	SR (microns)
1	WC	0.158	0.116	0.64
2	WC	0.152	0.116	0.48
3	WC	0.164	0.128	0.52
4	WC	0.170	0.118	0.58
5	St	0.154	0.116	0.78
6	St	0.148	0.116	0.60
7	St	0.154	0.128	0.70
8	St	0.168	0.118	0.68
9	PCD	0.192	0.074	0.94
10	PCD	0.282	0.074	1.20
11	PCD	0.246	0.034	0.68
12	PCD	0.282	0.102	1.52

Table 3.39 Observation table for experiment no.16

Control factors design

A1- TITAN12 B3-B_4C

C2-25% D3- 500

E3- 75%

S.No	Work material	MRR (mm^3/min)	TWR (mm^3/min)	SR (microns)
1	WC	0.120	0.104	0.38
2	WC	0.132	0.114	0.42
3	WC	0.140	0.116	0.46
4	WC	0.124	0.058	0.54
5	St	0.130	0.104	0.44
6	St	0.124	0.114	0.78
7	St	0.130	0.116	0.68
8	St	0.120	0.058	0.58
9	PCD	0.188	0.024	1.04
10	PCD	0.274	0.082	0.94
11	PCD	0.272	0.068	1.74
12	PCD	0.286	0.05	1.42

Table 3.40 Observation table for experiment no.17

Control factors design

A2- TITAN 15 B1-Alumina

C3-30% D1- 220

E2- 50%

S.No	Work material	MRR (mm^3/min)	TWR (mm^3/min)	SR (microns)
1	WC	0.132	0.108	0.42
2	WC	0.128	0.116	0.40
3	WC	0.120	0.118	0.52
4	WC	0.118	0.058	0.38
5	St	0.124	0.108	0.48
6	St	0.120	0.116	0.68
7	St	0.132	0.118	0.58
8	St	0.116	0.058	0.48
9	PCD	0.124	0.108	0.48
10	PCD	0.120	0.116	0.68
11	PCD	0.132	0.118	0.58
12	PCD	0.116	0.058	0.48

Table 3.41 Observation table for experiment no.18

Control factors design

A3- TITAN31 B2- SiC

C1-20% D2- 320

E3- 75%

S.No	Work material	MRR (mm^3/min)	TWR (mm^3/min)	SR (microns)
1	WC	0.138	0.114	0.48
2	WC	0.140	0.118	0.52
3	WC	0.128	0.048	0.42
4	WC	0.145	0.114	0.38
5	St	0.128	0.114	0.46
6	St	0.135	0.118	0.80
7	St	0.125	0.048	0.46
8	St	0.140	0.114	0.50
9	PCD	0.128	0.114	0.46
10	PCD	0.135	0.118	0.80
11	PCD	0.125	0.048	0.46
12	PCD	0.140	0.114	0.50

3.8 ANALYSIS OF MICROSTRUCTURE

The microstructure has been analyzed by using digital scanning electron microscope as shown in fig.3.83.

Figure 3.83 Scanning electron microscope(JSM 6100,Japan)

3.8.1 Analysis of microstructure of WC, stellite and PCD (Before machining)

Figure 3.84(a,b&c) shows the microstructure of tungsten carbide, stellite and diamond before machining with USM. It can be observed that the grain size is almost uniform with equiaxed grain shape. The equiaxed grains are free from stresses, therefore the possibility of irregular fracture or cracking during machining is very low. Moreover, these grains are soft. Hence, the material is having fair machinability, while ultrasonic machining of these

materials was done.The scanning electron microscopy (SEM) was performed on the ultrasonically machined samples to study the microstructure of these materials.

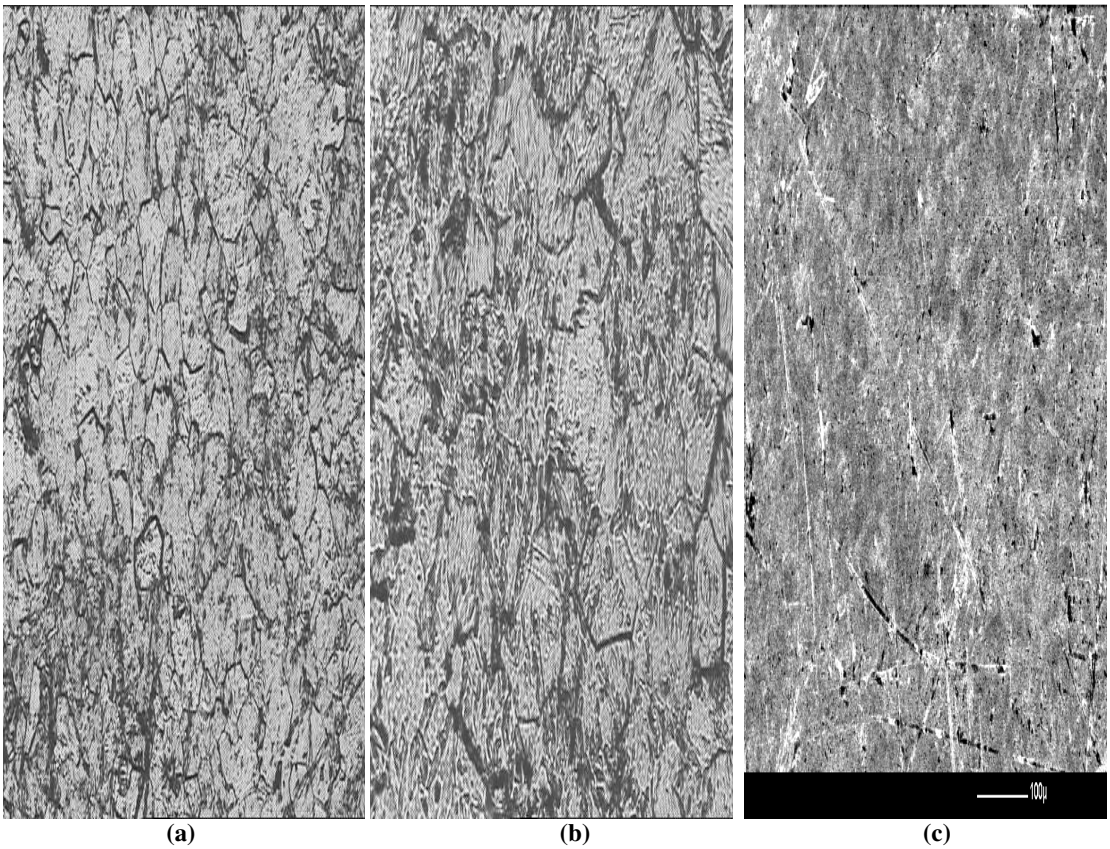

(a) **(b)** **(c)**

Figure 3.84 SEM Photograph for WC, Stellite and PCD (Before machining)

Material removal in USM process is believed to occur by brittle fracture mode. In mechanical shaping processes for brittle materials, material has been found to be removed by the propagation and intersection of cracks [83,105]. While the cutting of brittle materials is performed, in general, by brittle fracture, the chip can be removed plastically at an extremely small depth of cut [88-89]. In other words, the mechanism of material removal may change from brittle fracture to plastic deformation at extremely small material removal rates while machining with USM.

3.8.2 Analysis of microstructure of WC, stellite and PCD (Expt. No.1)

Figure 3.85 presents the microstructure of tungsten carbide, stellite and diamond after ultrasonic machining, considering the experimental conditions as designed in experiment no. 1. It was observed that the material possessed significant amount of plastic deformation before failure and there is no evidence of brittle fracture. Hence, the material

was machined by ductile failure of the work material. This could be attributed to the extremely low energy input into the abrasive as the experimental conditions involved use of a very low power rating (25%) and softer abrasive slurry (alumina).Neither any pinhole nor crack was observed.

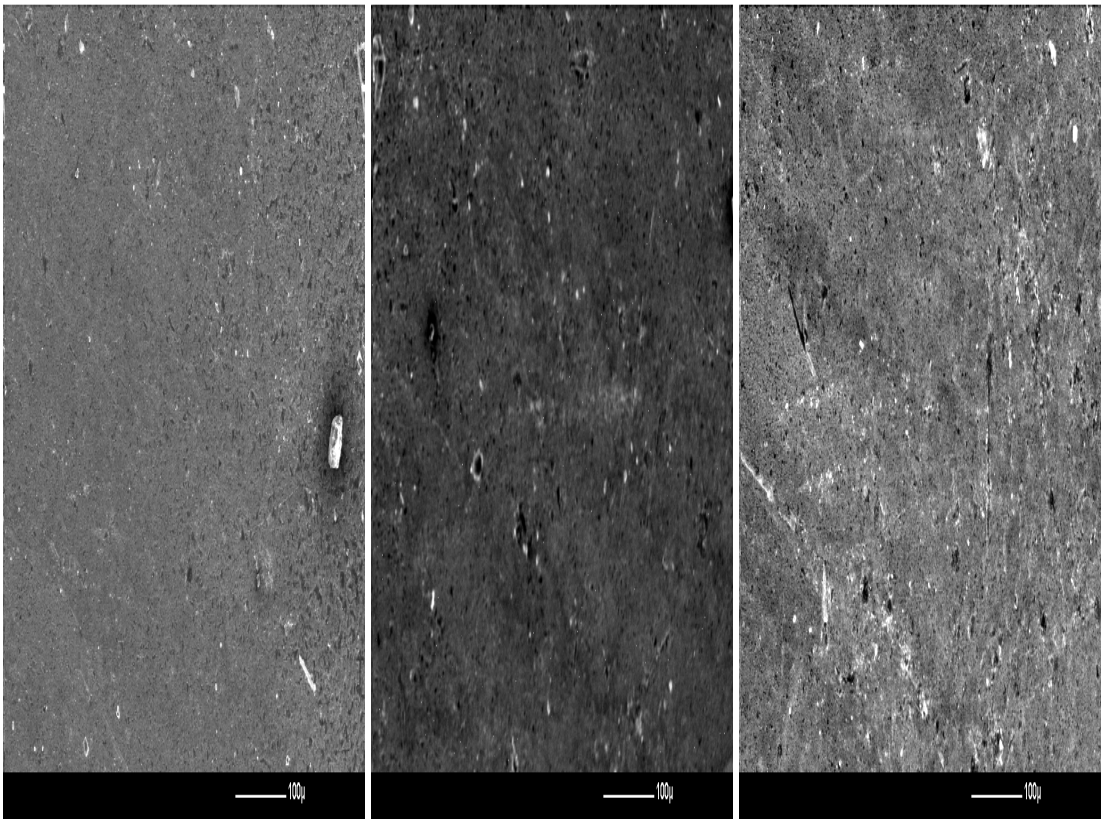

(a) **(b)** **(c)**

Figure 3.85 SEM Photograph for WC, Stellite and PCD (Expt No. 1)

3.8.3 Analysis of microstructure of WC, stellite and PCD (Expt. No.2)

Figure 3.86 presents the microstructure of tungsten carbide, stellite and diamond after ultrasonic machining, considering the experimental conditions as designed in experiment no. 2. It was observed that the majority of failure was of brittle fracture type, but very fine pinholes were also recognized as shown in figure 3.86(a) which evidences some localized plastic deformation before machining took place. From figure 3.86(b), the formation of cracks could also be observed which lead to the abrasion of work surface finally. The experimental conditions in this case were corresponding to a moderate rate of energy input to the tool/abrasive; hence the proportion of brittle fracture was expected to

be larger than the previous case. The propagation of cracks was observed as shown in figure 3. 86(c).This propagation may be because of higher rate of machining.

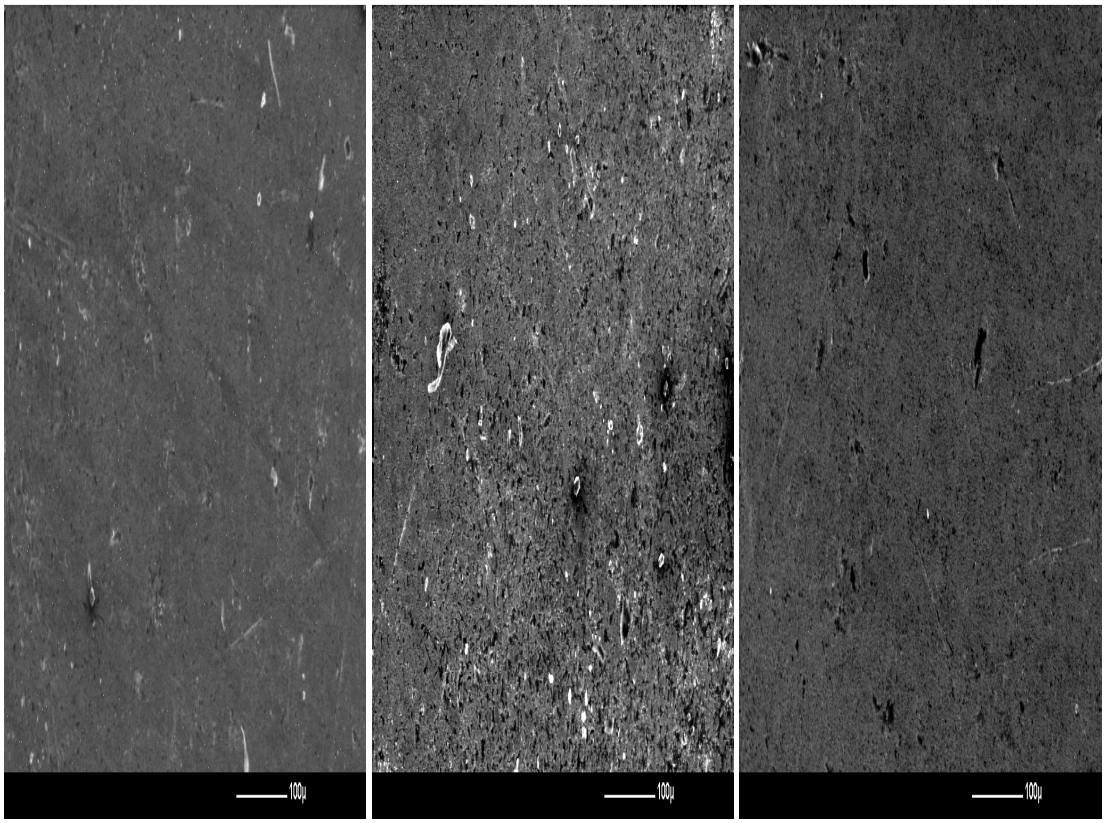

(a) **(b)** **(c)**

Figure 3.86 SEM Photograph for WC, Stellite and PCD (Expt No. 2)

3.8.4 Analysis of microstructure of WC, stellite and PCD (Expt. No.3)

Figure 3.87 presents the microstructure of tungsten carbide, stellite and diamond after ultrasonic machining, considering the experimental conditions as designed in experiment no. 3. The parameter settings corresponding to this case involve the use of abrasive slurry as extremely hard boron carbide with a higher level of power rating (75%), contributing to the ductile failure of the work surface. The increase in the surface hardness is quite small which could be contributed to extremely high rate of machining obtained , which results in very quick removal of work material by brittle fracture without undergoing significant amount of work hardening. From figure 3.87(a), It could be observed that ductile failure dominated the fracture of work surface, but some signs of brittle fracture were also observed in the form of sharp edges. Figure 3.87 (b) also suggests a mixed mode of material removal with greater contribution from ductile failure. From figure

3.87(c), the formation of very small pinholes was observed which could be due to the faster rate of energy input to the work surface.

3.8.5 Analysis of microstructure of WC, stellite and PCD (Expt. No.4)

Figure 3.88 presents the microstructure of tungsten carbide, stellite and diamond after ultrasonic machining, considering the experimental conditions as designed in experiment no. 4. From figure 3.88 (a), the occurrence of ductile shear failure could be observed .This may be attributed due to larger particle size. The parameter settings corresponding to this case involve the use of abrasive slurry as soft alumina with a higher level of power rating (75%), contributing to the ductile failure of the work surface. From figure 3.88(b), It could be observed that the material removal took place by a mixed mode, which is evident from the presence of dimples as well as sharp edges. From figure 3.88(c), the formation of very small pinholes was observed which could be due to the faster rate of energy input to the work surface.

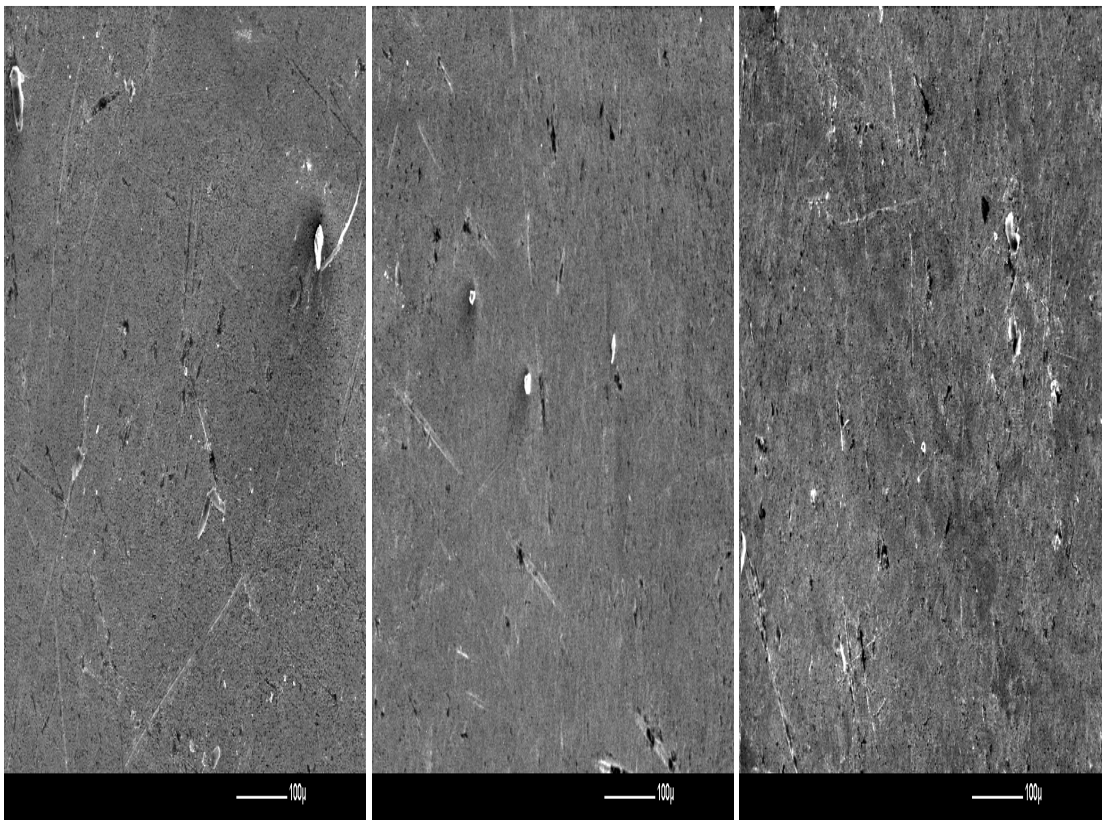

(a) **(b)** **(c)**

Figure 3.87 SEM Photograph for WC, Stellite and PCD (Expt No. 3)

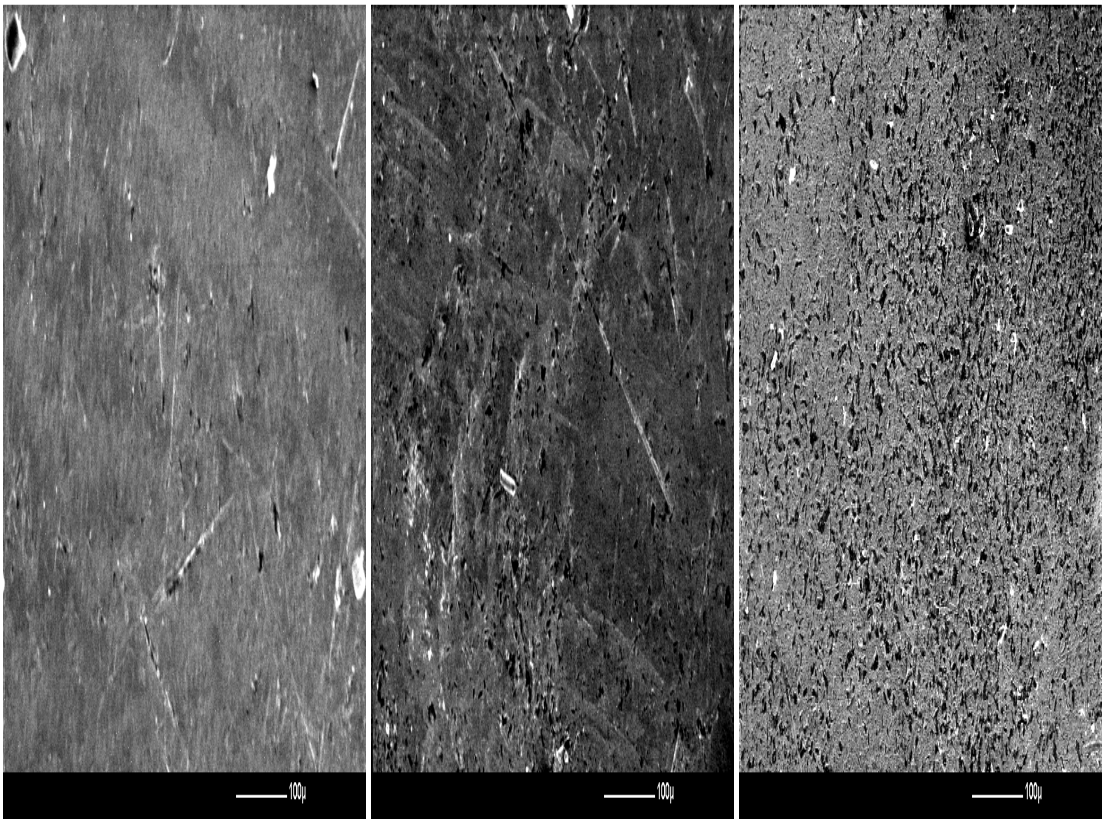

(a) **(b)** **(c)**

Figure 3.88 SEM Photograph for WC, Stellite and PCD (Expt No. 4)

3.8.6 Analysis of microstructure of WC, stellite and PCD (Expt. No.5)

Figure 3.89 presents the microstructure of tungsten carbide, stellite and diamond after ultrasonic machining, considering the experimental conditions as designed in experiment no. 5. From figure 3.89(a), the formation of very small pinholes was observed which could be due to the faster rate of energy input to the work surface. From figure 3.89 (b), the most visible features observed were internal cracks. The parameter settings corresponding to this experimental condition include silicon carbide as slurry which is comparatively harder and low level of power rating (25%); hence the cleavage type of fracture could be expected. Elongated projected regions were observed which suggest cleavage type of fracture as shown in figure 3.89(c).

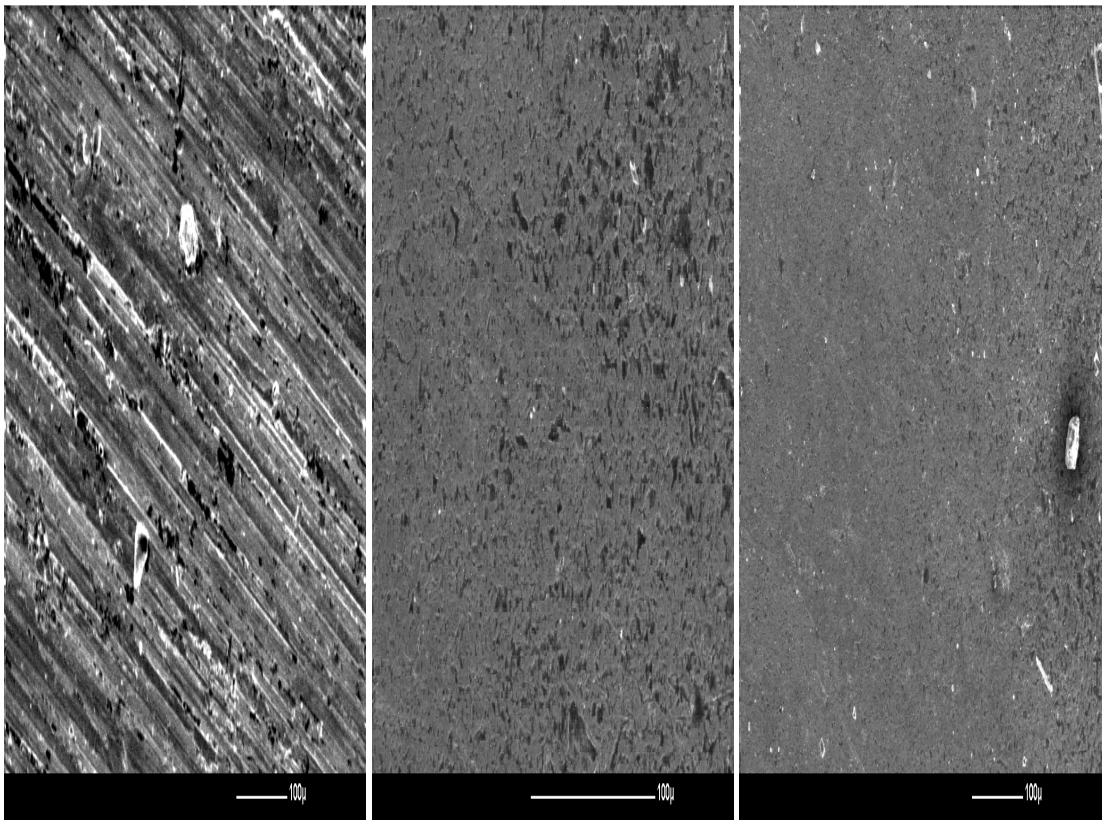

(a) **(b)** **(c)**

Figure 3.89 SEM Photograph for WC, Stellite and PCD (Expt No. 5)

3.8.7 Analysis of microstructure of WC, stellite and PCD (Expt. No.6)

Figure 3.90 presents the microstructure of tungsten carbide, stellite and diamond after ultrasonic machining, considering the experimental conditions as designed in experiment no. 6. There were no pinholes observed as shown in figure 3.90(a). From figure 3.90(b), the work surface experienced purely ductile failure as lots of dimples with uniform shape and distribution could be observed. The process settings for this experimental condition involve the use of a coarse grit size (220) and moderate level of power rating (50%) which results in very low rate of machining and hence the ductile failure could be expected. As the rate of machining was very low, it took a comparatively larger time period to machine the work surface to the desired depth .This may be attributed to as almost all the machining took place through continuous plastic deformation which sustained during the entire machining time . From figure 3.90 (c) the most visible features observed were internal cracks.

3.8.8 Analysis of microstructure of WC, stellite and PCD (Expt. No.7)

Figure 3.91 presents the microstructure of tungsten carbide, stellite and diamond after ultrasonic machining, considering the experimental conditions as designed in experiment no. 7. Elongated projected regions were observed which suggest cleavage type of fracture as shown in figure 3.91(a). The input parameter settings involve use of a abrasive as silicon carbide and moderate level of power rating (50%) while the grit size is fine (500). Hence, the rate of energy input to the tool and abrasive is high. From figure 3.91(b), the formation of very small pinholes was observed which could be due to the faster rate of energy input to the work surface.No cracks nor pinholes were observed as shown in figure 3.91(c).

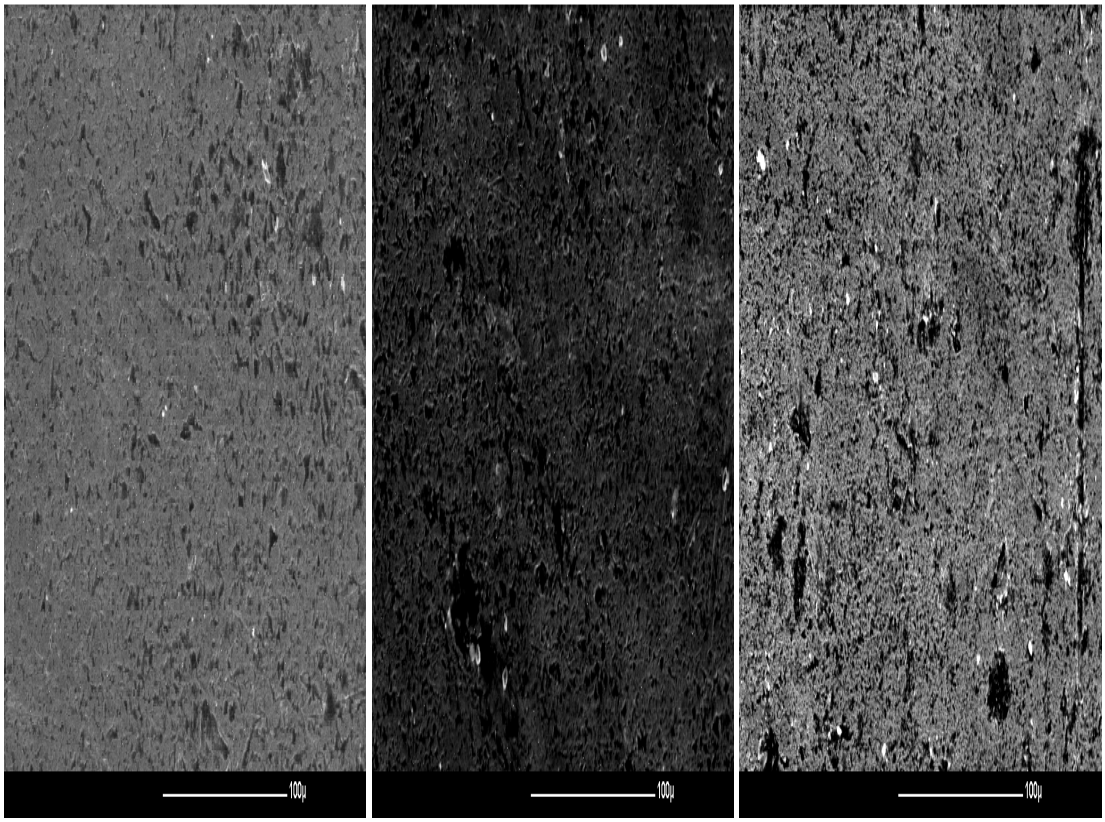

(a) **(b)** **(c)**

Figure 3.90 SEM Photograph for WC, Stellite and PCD (Expt No. 6)

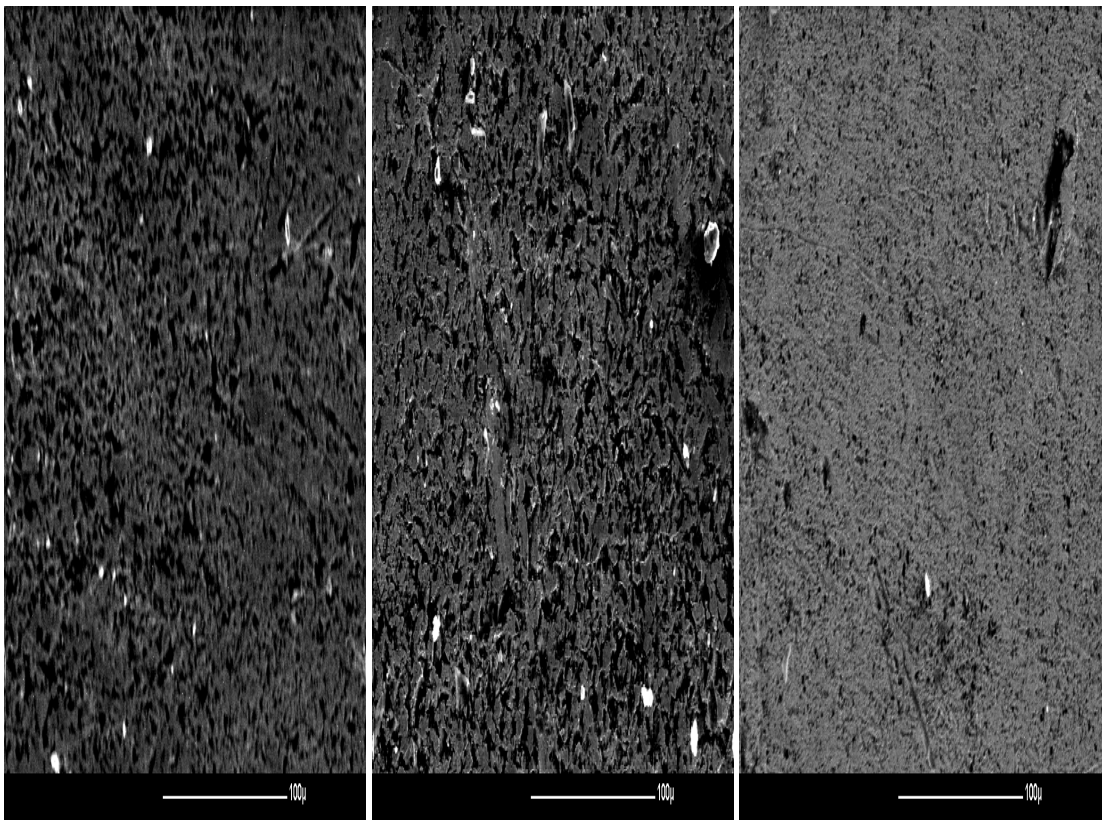

(a) **(b)** **(c)**

Figure 3.91 SEM Photograph for WC, Stellite and PCD (Expt No. 7)

3.8.9 Analysis of microstructure of WC, stellite and PCD (Expt. No.8)

Figure 3.92 presents the microstructure of tungsten carbide, stellite and diamond after ultrasonic machining, considering the experimental conditions as designed in experiment no. 8. The process settings include Boron carbide slurry with a coarse grit size (220) and high power input (75%). Hence, the rate of energy input to the tool or abrasive is moderately high. It can be observed from figure 3.92(a) that the cleavage type of fracture took place. In figure 3.92(b), no cracks were observed as surface was found to be smooth. In figure 3.92(c),the fractured surface shows white and dark contrast in which the brighter contrast is the projected portion of the fractured surface which is comparatively larger than that observed in case of high energy input conditions. This indicates ductile type of failure and slightly longer duration was required to fracture the surface.

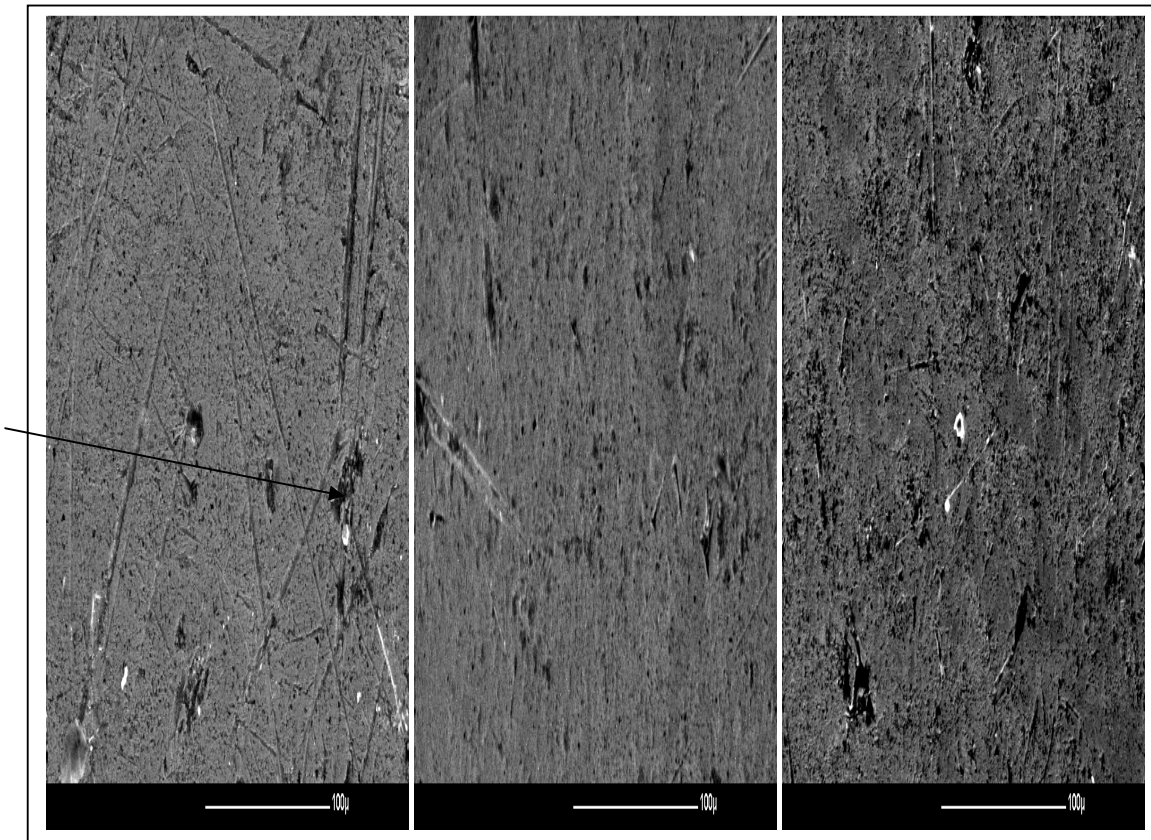

(a) **(b)** **(c)**

Figure 3.92 SEM Photograph for WC, Stellite and PCD (Expt No. 8)

3.8.10 Analysis of microstructure of WC, stellite and PCD (Expt. No.9)

Figure 3.93 presents the microstructure of tungsten carbide, stellite and diamond after ultrasonic machining, considering the experimental conditions as designed in experiment no. 9. The process settings include aluminum oxide as abrasive slurry with a medium grit size of 320 and low power input (25%). Hence, the rate of energy input to the tool or abrasive is extremely low. It can be observed from figure 3.93 (a) that purely ductile type of fracture took place, as a large number of dimples could be seen. From figure 3.93 (b) , the presence of some cleavage planes in addition to a large number of dimples distributed in the entire surface has been observed. Also, there is an evidence of inter-granular fracture. The area of workpiece which is directly under the center of the tool face also experiences significant amount of plastic deformation. Neither cracks nor pinholes were observed as shown in figure 3.93(c).

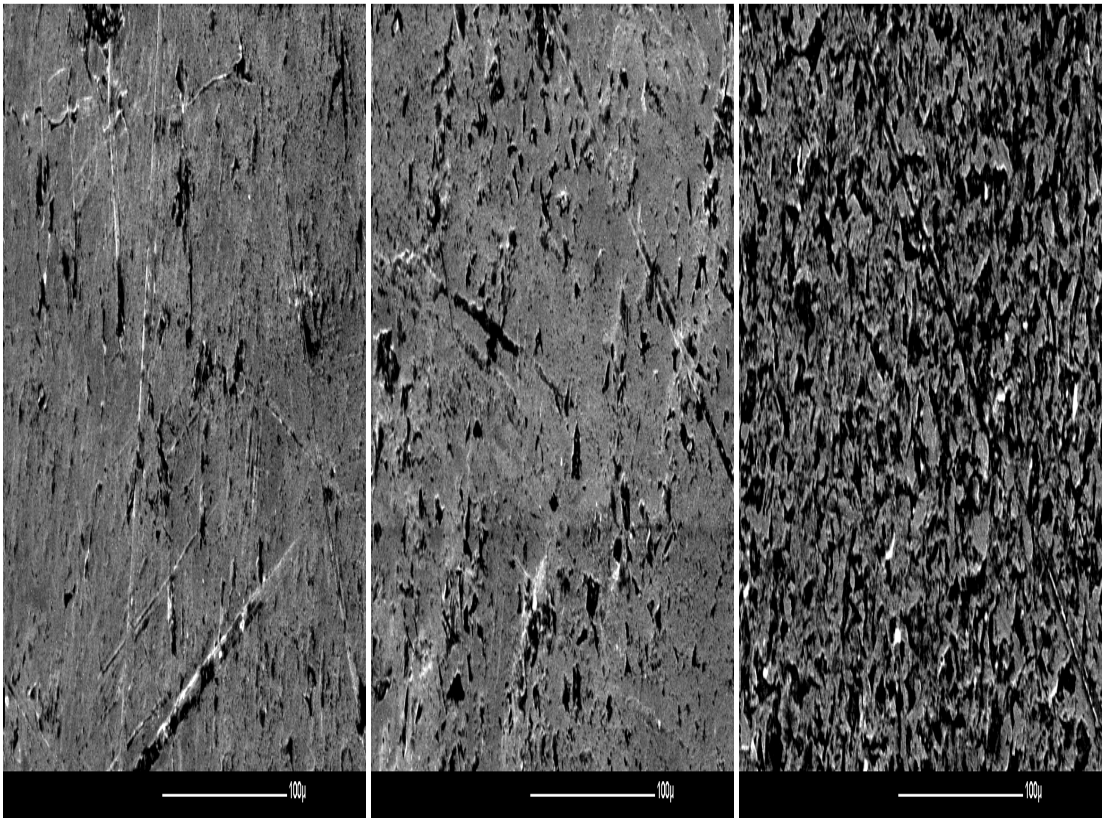

(a) **(b)** **(c)**

Figure 3.93 SEM Photograph for WC, Stellite and PCD (Expt No. 9)

3.8.11 Analysis of microstructure of WC, stellite and PCD (Expt. No.10)

Figure 3.94 presents the microstructure of tungsten carbide, stellite and diamond after ultrasonic machining as designed in experiment no. 10. The process settings include boron carbide as abrasive slurry with a medium grit size of 320 and moderate power input (50%). In figure 3.94 (a), a large number of longitudinal cracks could be observed which indicates brittle failure of the work surface. Neither cracks nor pinholes were observed as shown in figure 3.94(b).Figure 3.94 (c) gives evidence of a mixed mode of material removal, with predominant ductile failure of the work material. The contradiction regarding to the evidence of ductile failure at high energy input conditions was found to be due to the plastic deformation at the center of the tool face.

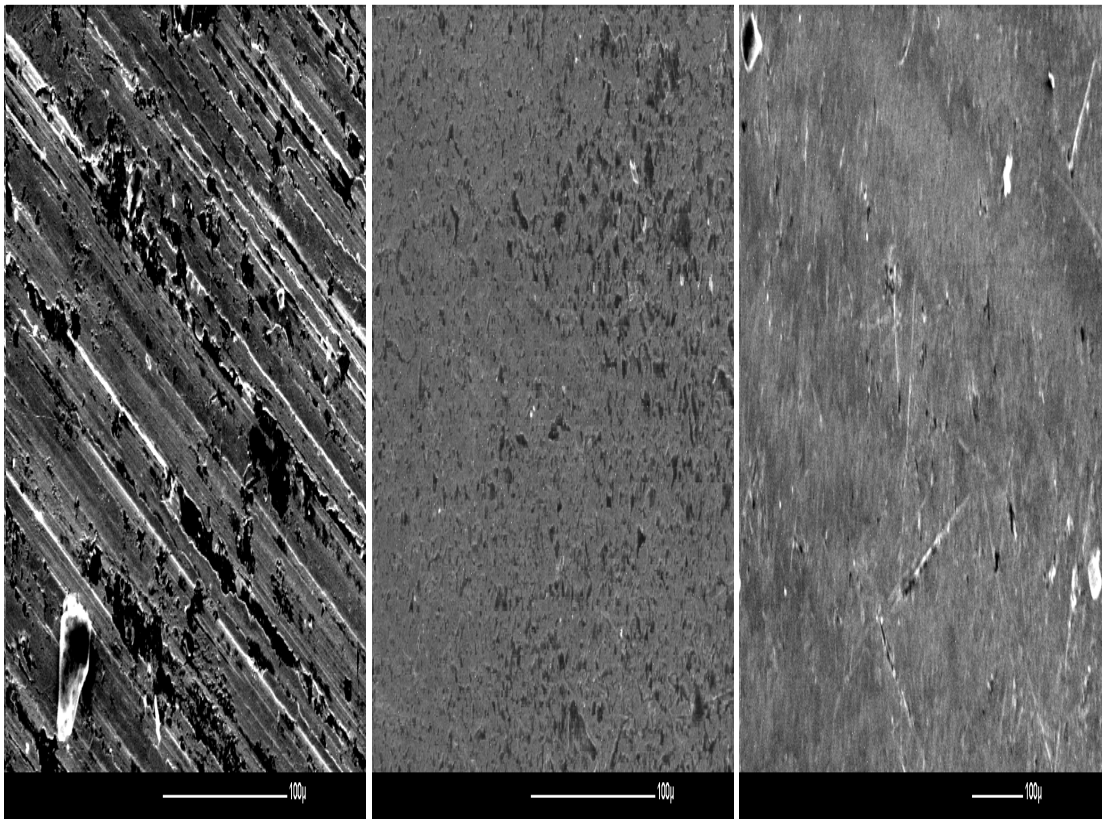

(a) **(b)** **(c)**

Figure 3.94 SEM Photograph for WC, Stellite and PCD (Expt No. 10)

3.8.12 Analysis of microstructure of WC, stellite and PCD (Expt. No.11)

Figure 3.95 presents the microstructure of tungsten carbide, stellite and diamond after ultrasonic machining, considering the experimental conditions as designed in experiment no. 11. The process settings include aluminum oxide as abrasive slurry with a fine grit size of 500 and high power input (75%).Hence, a high level of energy input can be assigned to this case. Neither cracks nor pinholes were observed as shown in figure 3.95(a). Figure 3.95 (b) gives evidence of a mixed mode of material removal with predominant brittle fracture of the work material, which could be due to the use of fine grit size. In figure 3.95 (c), a large number of cracks can be observed along the grain boundaries indicating inter-granular fracture.

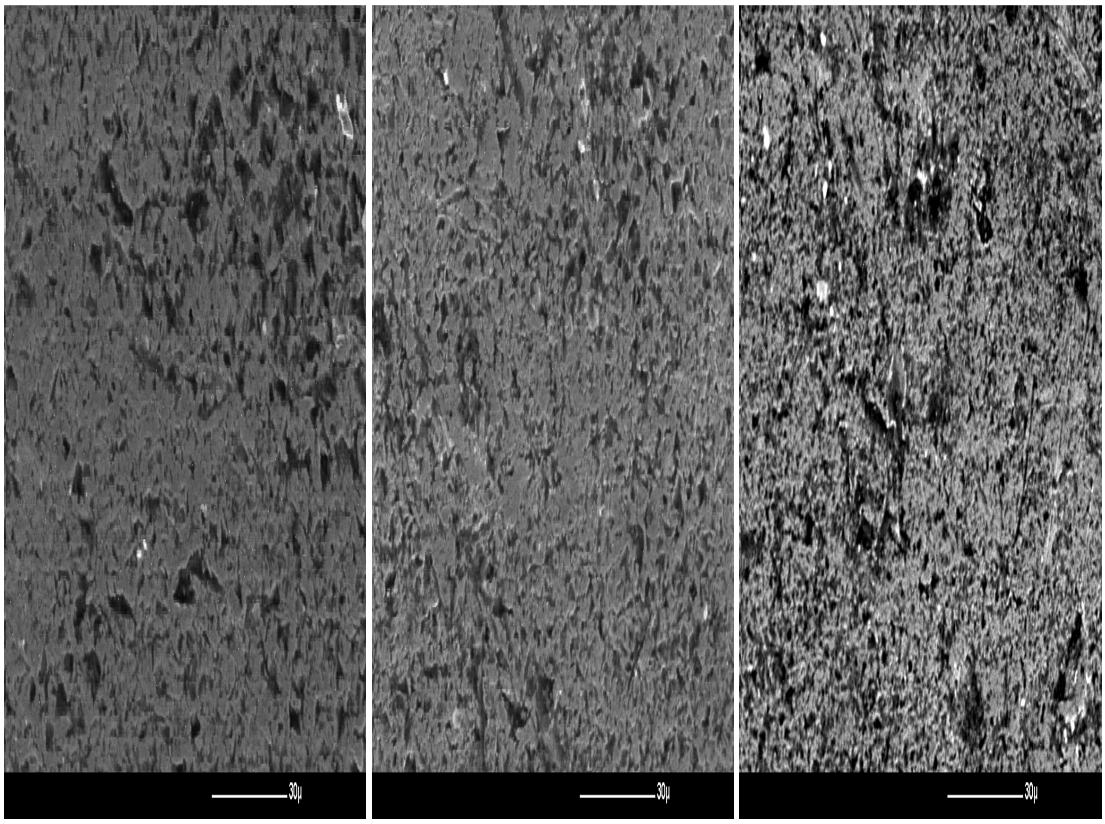

(a) **(b)** **(c)**

Figure 3.95 SEM Photograph for WC, Stellite and PCD (Expt No. 11)

3.8.13 Analysis of microstructure of WC, stellite and PCD (Expt. No.12)

Figure 3.96 presents the microstructure of tungsten carbide, stellite and diamond after ultrasonic machining as designed in experiment no. 12. The process settings include silicon carbide as abrasive slurry with a corse grit size of 220 and low power input (25%). Hence, the energy input for the tool and subsequently work surface can be termed as low. From figure 3.96 (a), a large number of cracks can be observed along the grain boundaries indicating inter-granular fracture. The figure 3.96 (b) suggests predominant brittle fracture (90-95%) with a very few localized ductile failure regions. Whereas figure 3.96 (c) indicates uniform abrasion of the work

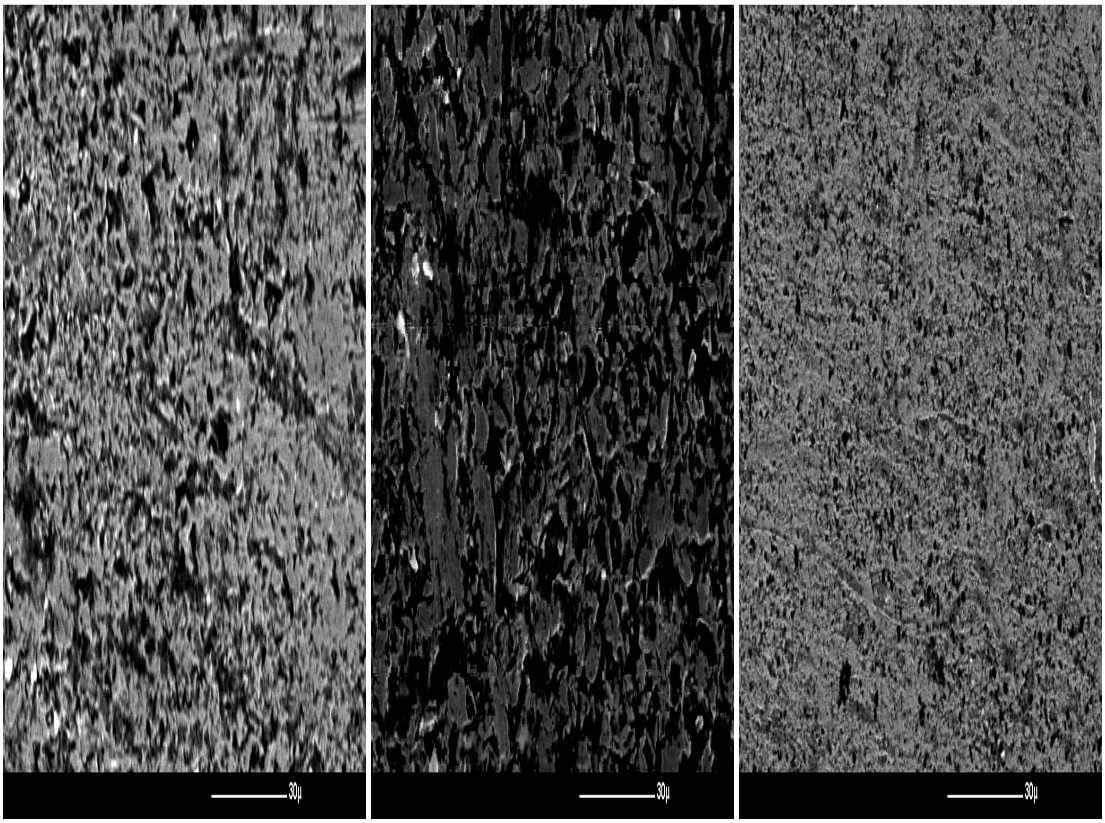

(a) **(b)** **(c)**

Figure 3.96 SEM Photograph for WC, Stellite and PCD (Expt No. 12)

3.8.14 Analysis of microstructure of WC, stellite and PCD (Expt. No.13)

Figure 3.97 presents the microstructure of tungsten carbide, stellite and diamond after ultrasonic machining as designed in experiment no. 13. The process settings include silicon carbide as abrasive slurry with a corse grit size of 220 and high power input (75%).Figure 3.97(a) gives evidence of a mixed mode of material removal with predominant ductile fracture of the work material, which could be due to the use of coarse grit size. From figure 3.97(b), purely brittle fracture is observed as the parameter settings indicate a high level of energy input into the work. Hence, the strain hardening of the work surface proceeds at a faster rate. In figure 3.97 (c), a large number of cracks can be observed along the grain boundaries indicating inter-granular fracture.

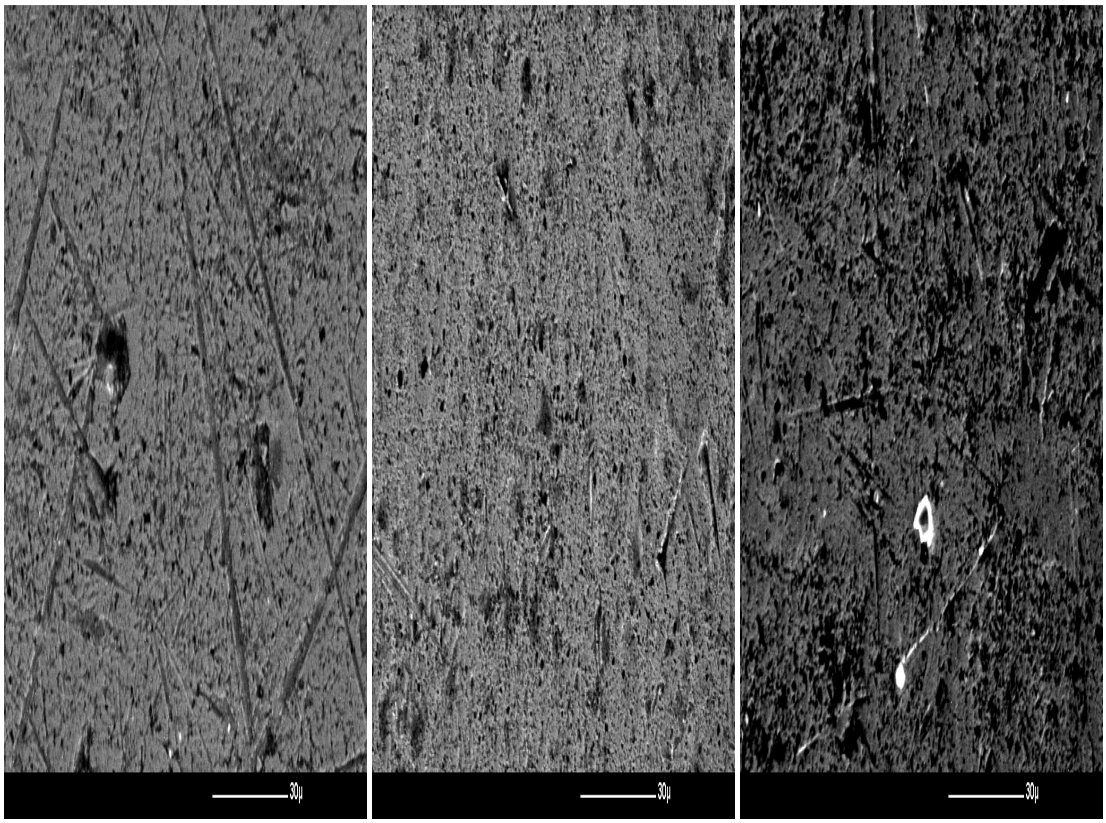

(a) **(b)** **(c)**

Figure 3.97 SEM Photograph for WC, Stellite and PCD (Expt No. 13)

3.8.15 Analysis of microstructure of WC, stellite and PCD (Expt. No.14)

Figure 3.98 presents the microstructure of tungsten carbide, stellite and diamond after ultrasonic machining, as designed in experiment no. 14. The process settings include low power input (25%). Hence, a very low machining rate was observed. The figure 3.98(a) presents the microstructure of the machined surface that indicates material failure by brittle fracture. It can be observed from figure 3.98 (b) that purely ductile type of fracture took place, as a large number of dimples could be seen. From figure 3.98 (c), the presence of some cleavage planes in addition to a large number of dimples distributed in the entire surface has been observed. Also, there is an evidence of inter-granular fracture.

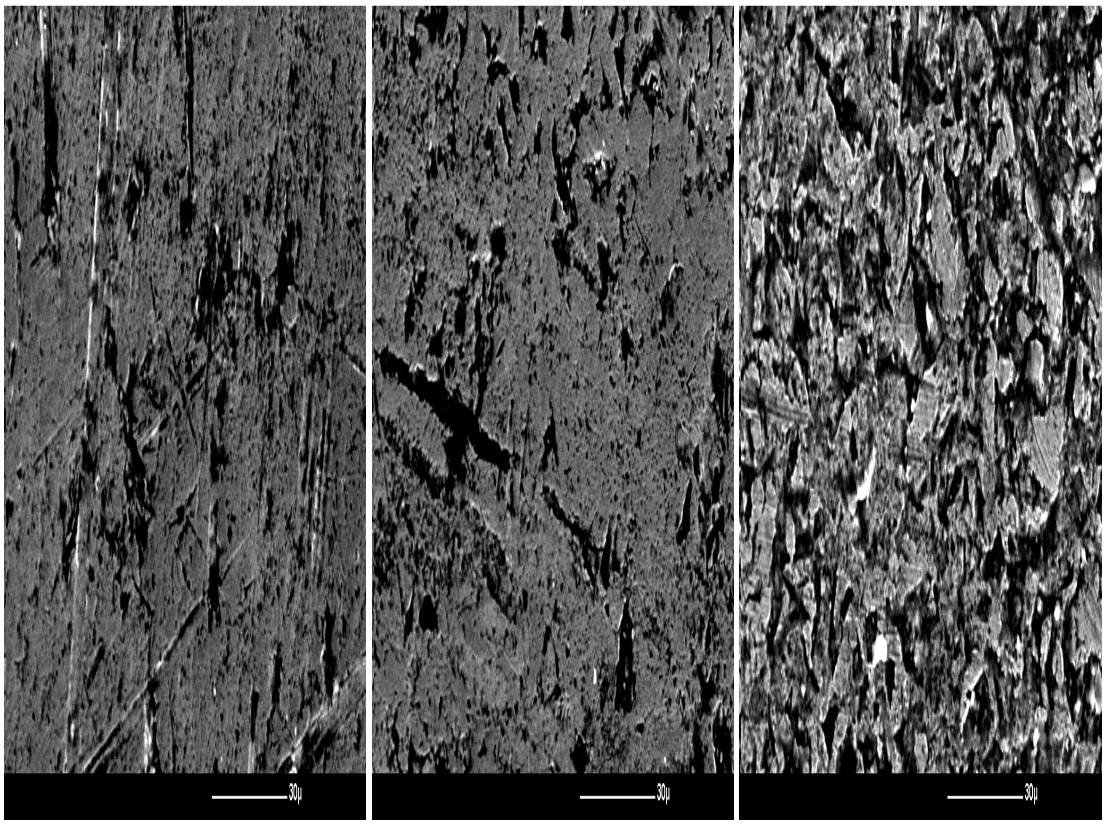

(a) **(b)** **(c)**

Figure 3.98 SEM Photograph for WC, Stellite and PCD (Expt No. 14)

3.8.16 Analysis of microstructure of WC, stellite and PCD (Expt. No.15)

Figure 3.99 presents the microstructure of tungsten carbide, stellite and diamond after ultrasonic machining, as designed in experiment no.15.The process settings corresponding to this trail condition provide a moderate level of energy input to the tool. From figure 3.99 (a) that the material fracture took place purely due to ductile failure of the surface, as large number of dimples of uniform size could be observed. This is due to the fact that the region under consideration in the former case belongs to the center of the work surface where rate of machining is comparatively low. Figure 3.99 (b) indicates presence of cleavage planes and dominant brittle fracture can be observed. From figure 3.99 (c), the pulling out of some grains due to propagation of cracks can also be observed.

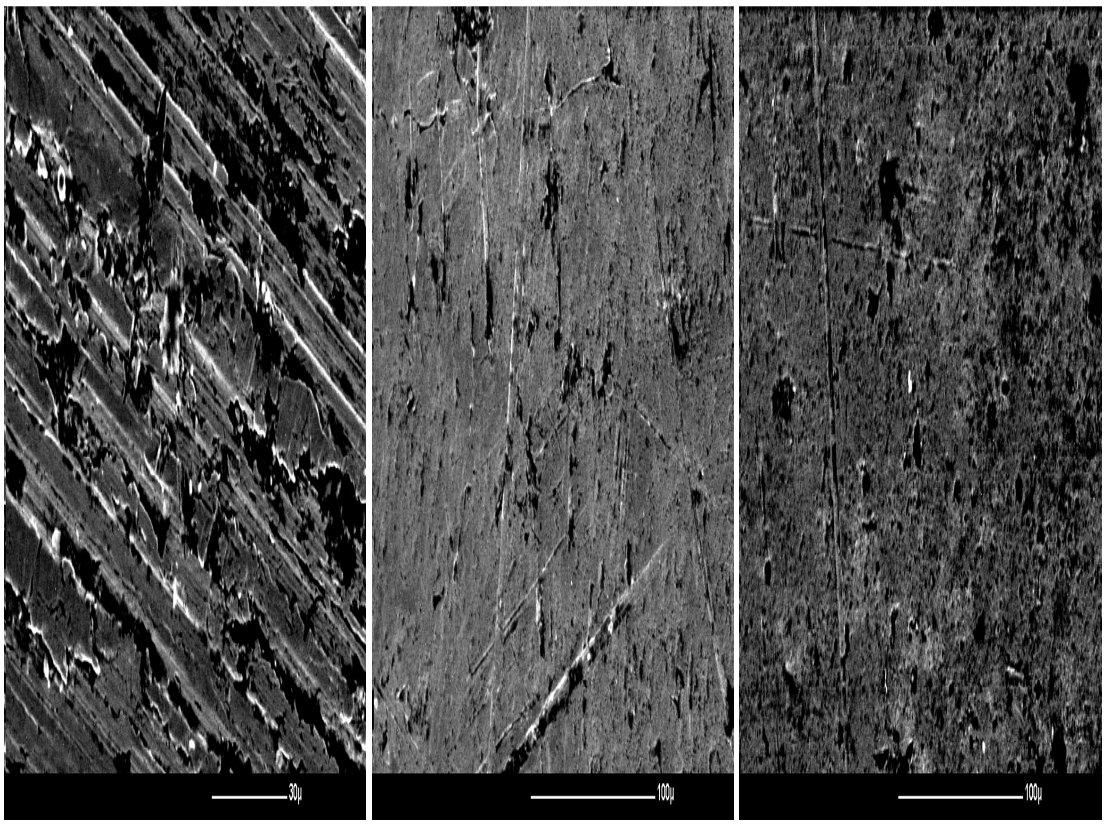

(a) **(b)** **(c)**

Figure 3.99 SEM Photograph for WC, Stellite and PCD (Expt No. 15)

3.8.17 Analysis of microstructure of WC, stellite and PCD (Expt. No.16)

Figure 3.100 presents the microstructure of tungsten carbide, stellite and diamond after ultrasonic machining, as designed in experiment no.16.The process settings provides a high level of energy input to the tool. Hence, a high machining rate was observed.From figure 3.100(a), the microstructure of the machined surface indicates material failure by brittle fracture. This might be due to the absence of plastic deformation in this case, which leads to lesser strain hardening. Figure 3.100 (b) indicates presence of cleavage planes and dominant brittle fracture can be observed. From figure 3.100 (c), the pulling out of some grains due to propagation of cracks can also be observed.

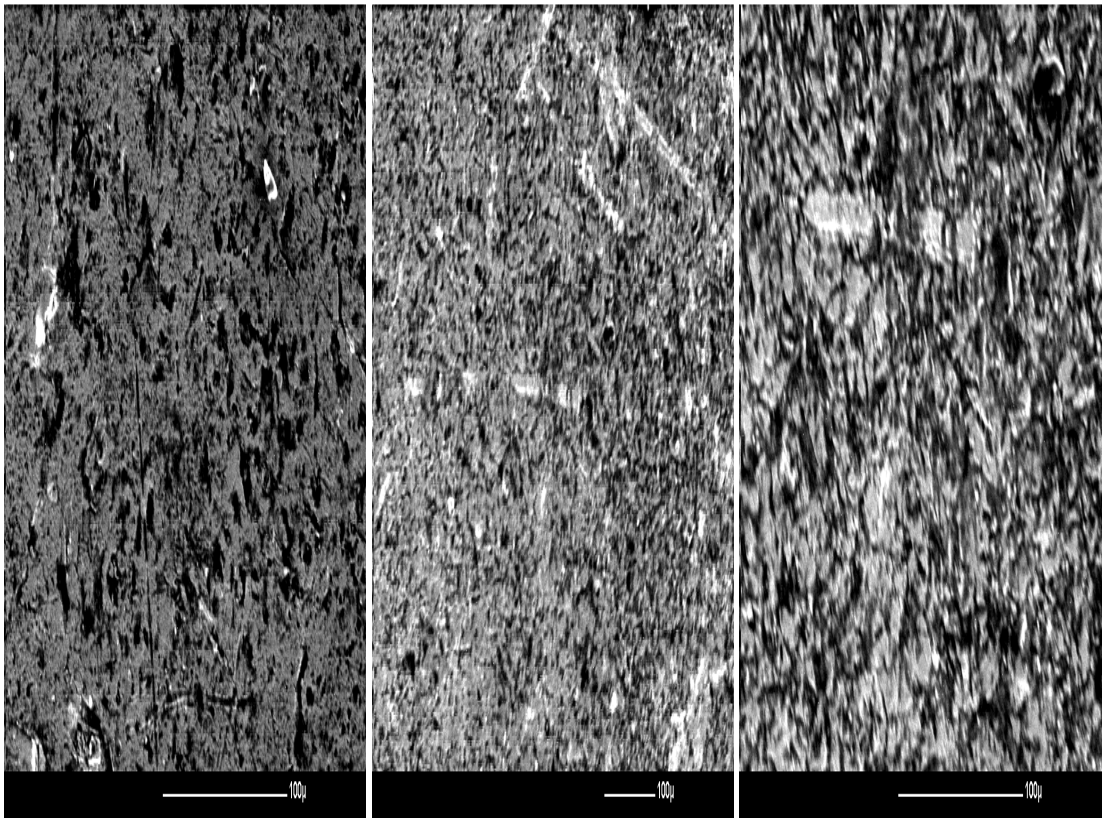

(a) **(b)** **(c)**

Figure 3.100 SEM Photograph for WC, Stellite and PCD (Expt No. 16)

3.8.18 Analysis of microstructure of WC, stellite and PCD (Expt. No.17)

Figure 3.101 presents the microstructure of tungsten carbide, stellite and diamond after ultrasonic machining as designed in experiment no. 17. The process settings include Al_2O_3 as abrasive slurry with a coarse grit size of 220 and moderate power input (50%). The process settings corresponding to this trail condition provide a moderate level of energy input to the tool. For the figure 3.101(a), the cleavage type of fracture can be observed. Figure 3.101 (b) presents the localized plastic deformation that can be seen in the form of a few round dimples. This is expected in this case as the rate of energy input into the tool or abrasive is moderate.

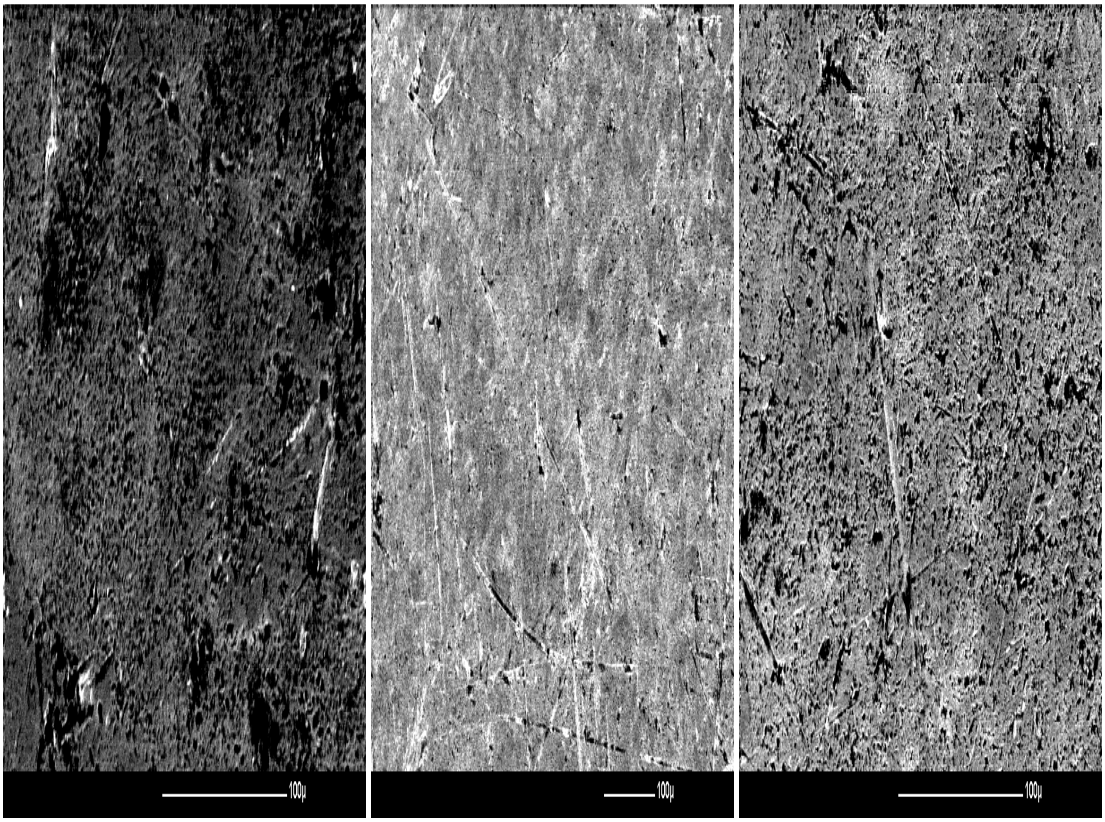

(a) **(b)** **(c)**

Figure 3.101 SEM Photograph for WC, Stellite and PCD (Expt No. 17)

3.8.19 Analysis of microstructure of WC, stellite and PCD (Expt. No.18)

Figure 3.102 presents the microstructure of tungsten carbide, stellite and diamond after ultrasonic machining, considering the experimental conditions as designed in experiment no. 18. The process settings include silicon carbide as abrasive slurry with a moderate grit size of 320 and high power input (75%). The process settings in this case render a high rate of energy input to the tool/abrasive, so purely ductile type of failure has been observed as in figure 3.102(a).

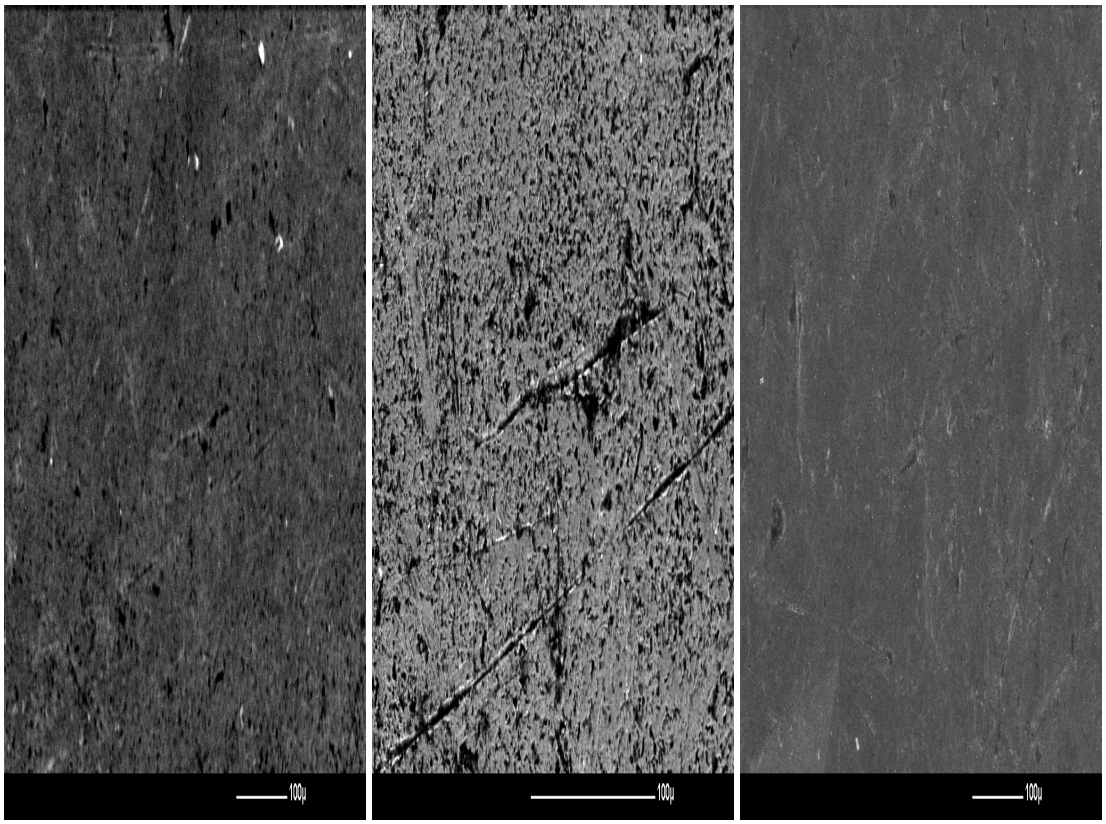

(a) **(b)** **(c)**

Figure 3.102 SEM Photograph for WC, Stellite and PCD (Expt No. 18)

There is no evidence of any brittle fracture of the work surface as sharp edges have not been observed. From figure 3.102 (b), the presence of some cleavage planes in addition to a large number of pin holes distributed in the entire surface has been observed. The area of workpiece which is directly under the center of the tool face also experiences significant amount of plastic deformation. Neither cracks nor pinholes were observed as shown in figure 3.102(c).

CHAPTER-IV

RESULTS AND DISCUSSION

4.1 INTRODUCTION

Experiments were conducted at various settings of abrasive slurry type, abrasive slurry concentration, abrasive slurry grit size, tool types and power ratings of USM. Material removal rate, tool wear rate and surface roughness has been measured and plotted as per taguchi design. Following are the results of experimentation.

4.2 ANALYSIS OF RESULTS

The statistica 7.0 software has been used for robust design and analysis of the results. Table 4.1 shows S/N ratio of MRR, SR and TWR for tungsten carbide.The analysis of variance of MRR for tungsten carbide is shown in figure 4.2 where symbols SS and P(%) presents the sum of squares and percentage of contribution of the factors.

Table 4.1 S/N ratio of MRR, SR, TWR for WC

S.No	S/N (MRR)	S/N (SR)	S/N (TWR)
1	25.589	16.569	17.887
2	26.927	18.923	12.060
3	21.724	24.659	11.602
4	30.016	26.416	10.194
5	23.678	17.017	16.953
6	27.949	21.489	10.387
7	18.990	15.565	8.795
8	19.987	14.807	11.250
9	21.250	7.969	11.438
10	17.700	22.442	14.279
11	28.130	18.151	18.155
12	27.776	20.112	23.607
13	26.167	19.114	18.847
14	30.466	22.787	25.109
15	26.355	17.983	26.362
16	23.253	16.374	11.140
17	25.501	16.796	10.954
18	25.713	17.190	9.311

Table 4.2 Analysis of variance of MRR for WC

Effect	Tool material	Abrasive slurry	Slurry concentration	Grit size	Power rating
SS	14.75	20.71	43.01	12.06	7.94
F value	0.38	0.53	1.11	0.31	0.20
P(%)	14.97	21.03	43.67	12.24	8.06

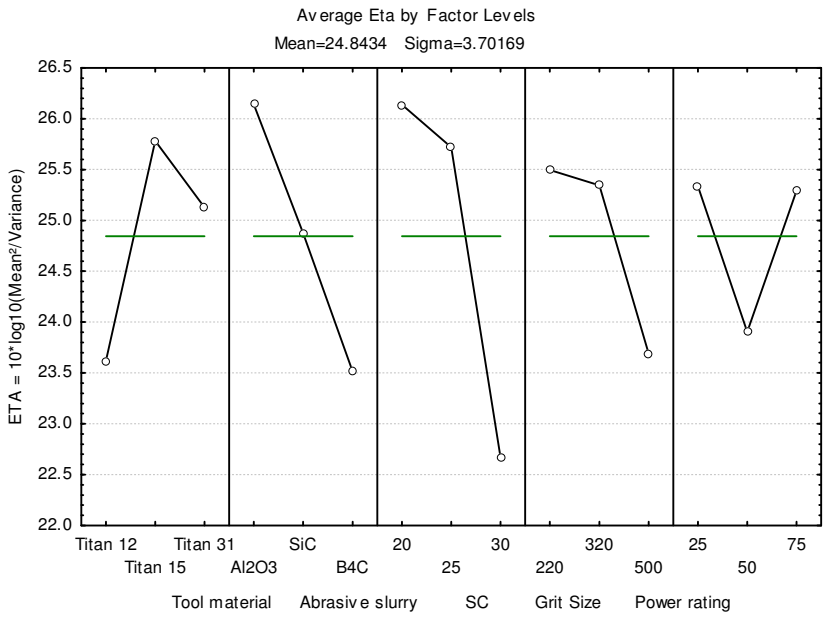

Figure 4.1 Effects of process parameters on S/N ratio of MRR for WC

Table 4.3 Analysis of variance of SR for WC

Effect	Tool material	Abrasive slurry	Slurry concentration	Grit size	Power rating
SS	6.38	32.18	3.67	4.62	32.48
F value	0.10	0.52	0.05	0.07	0.52
P(%)	8.04	40.56	4.62	5.82	40.94

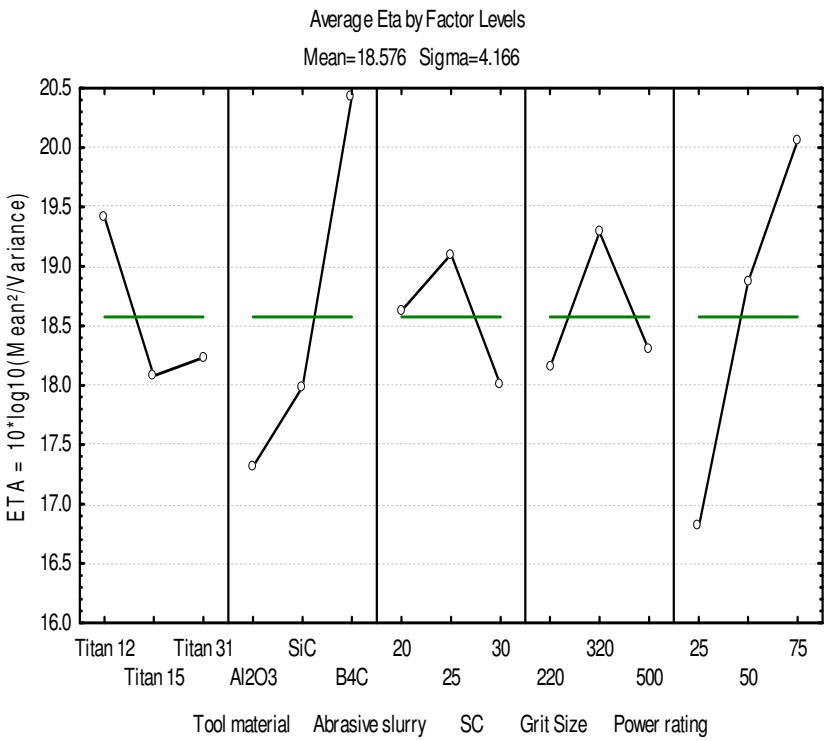

Figure 4.2 Effects of process parameters on S/N ratio of SR for WC

Table 4.4 Analysis of variance of TWR for WC

Effect	Tool material	Abrasive slurry	Slurry concentration	Grit size	Power rating
SS	17.49	10.49	9.26	12.43	70.65
F value	0.14	0.08	0.07	0.10	0.59
P(%)	14.53	8.71	7.69	10.33	58.71

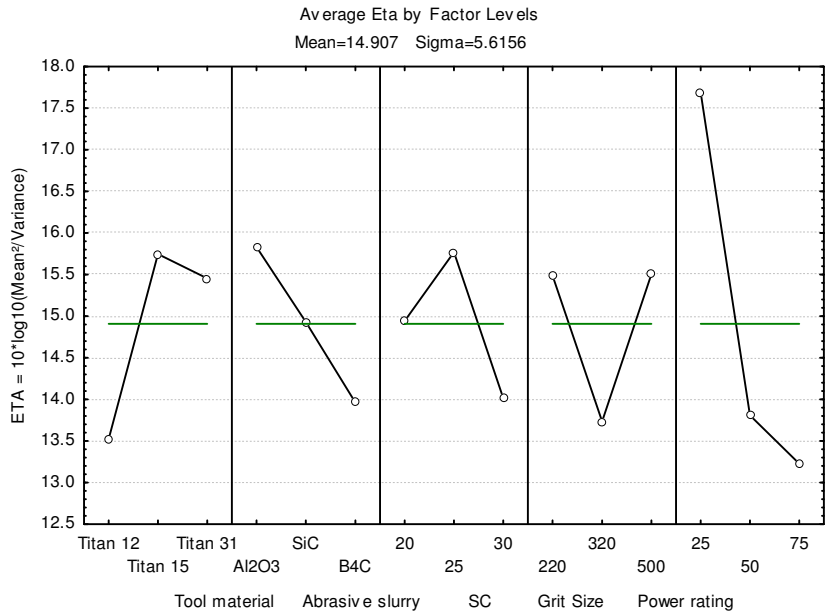

Figure 4.3 Effects of process parameters on S/N ratio of TWR for WC

Table 4.5 S/N ratio of MRR, SR, TWR for stellite

S.No	S/N (MRR)	S/N (SR)	S/N (TWR)
1	26.634	26.235	17.887
2	23.743	16.423	12.060
3	23.277	20.875	11.602
4	29.454	22.144	10.194
5	22.121	17.952	16.953
6	32.961	19.876	10.387
7	17.698	11.815	8.795
8	17.492	19.518	11.250
9	23.280	15.679	11.438
10	18.314	17.724	14.279
11	29.504	18.411	18.155
12	26.515	24.349	23.607
13	25.291	23.582	18.847
14	29.003	24.905	25.109
15	25.289	19.399	26.362
16	28.205	12.611	11.140
17	25.108	15.263	10.954
18	25.783	10.566	9.311

Table 4.6 Analysis of variance of MRR for stellite

Effect	Tool material	Abrasive slurry	Slurry concentration	Grit size	Power rating
SS	13.16	27.45	48.93	5.23	13.53
F value	0.23	0.48	0.86	0.09	0.23
P(%)	12.15	25.34	45.18	4.82	12.49

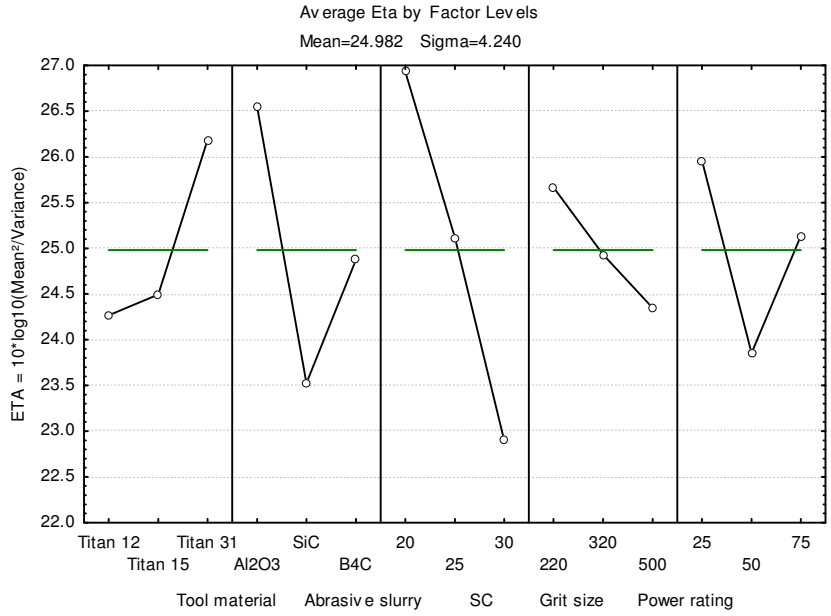

Figure 4.4 Effects of process parameters on S/N ratio of MRR for stellite

Table 4.7 Analysis of variance of SR for stellite

Effect	Tool material	Abrasive slurry	Slurry concentration	Grit size	Power rating
SS	0.94	15.25	1.04	70.47	39.32
F value	0.01	0.24	0.01	1.11	0.62
P(%)	0.74	12	0.81	55.47	30.95

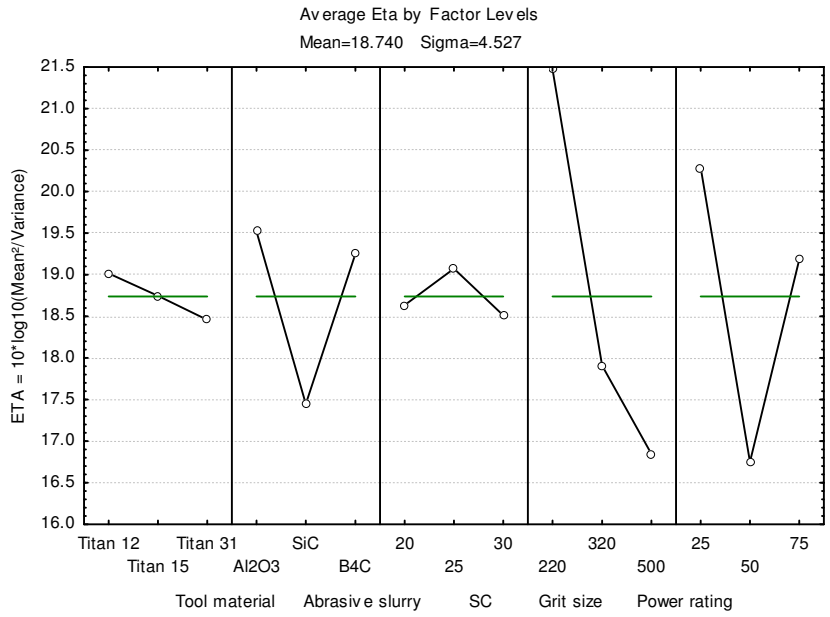

Figure 4.5 Effects of process parameters on S/N ratio of SR for stellite

Table 4.8 Analysis of variance of TWR for stellite

Effect	Tool material	Abrasive slurry	Slurry concentration	Grit size	Power rating
SS	21.04	13.32	9.08	14.61	67.74
F value	0.17	0.11	0.07	0.12	0.56
P(%)	16.72	10.58	7.21	11.61	53.85

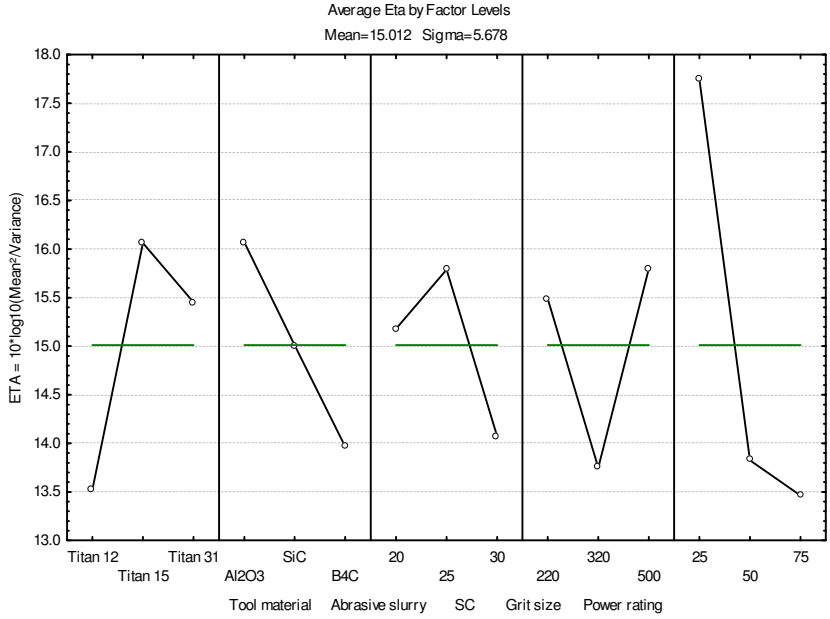

Figure 4.6 Effects of process parameters on S/N ratio of TWR for stellite

Table 4.9 S/N ratio of MRR, SR, TWR for PCD

S.No	S/N (MRR)	S/N (SR)	S/N (TWR)
1	31.588	15.660	5.644
2	24.771	12.632	5.674
3	22.827	12.656	2.145
4	14.777	16.636	3.973
5	15.641	8.662	6.036
6	14.274	6.990	12.512
7	18.358	11.481	7.473
8	17.000	7.860	7.178
9	19.427	10.717	8.154
10	17.324	8.578	5.076
11	16.719	15.890	1.034
12	14.261	10.734	6.675
13	15.357	11.597	4.824
14	14.249	5.235	7.785
15	15.401	9.597	8.089
16	15.048	10.882	6.993
17	20.485	5.570	5.551
18	16.375	11.848	19.714

Table 4.10 Analysis of variance of MRR for PCD

Effect	Tool material	Abrasive slurry	Slurry concentration	Grit size	Power rating
SS	8.34	28.59	11.25	6.97	6.02
F value	0.10	0.34	0.13	0.08	0.07
P(%)	13.63	46.73	18.39	11.39	9.84

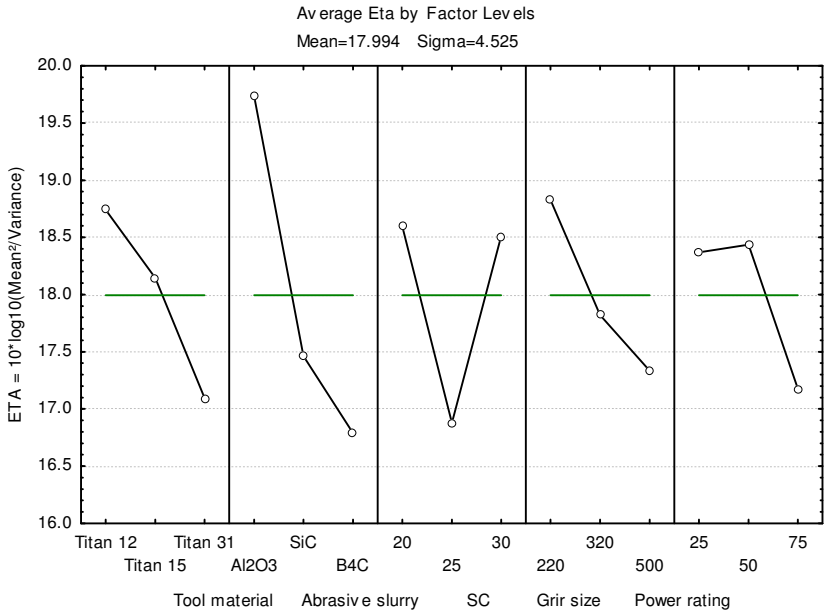

Figure 4.7 Effects of process parameters on S/N ratio of MRR for PCD

Table 4.11 Analysis of variance of SR for PCD

Effect	Tool material	Abrasive slurry	Slurry concentration	Grit size	Power rating
SS	76.48	19.38	49.51	46.08	89.90
F value	1.96	0.49	1.27	1.18	2.31
P(%)	27.18	6.88	17.59	16.37	31.95

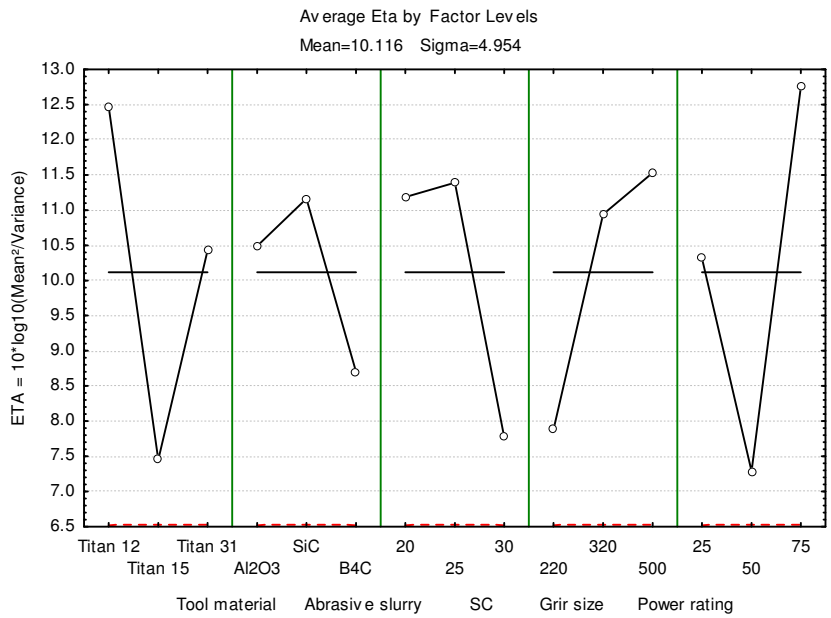

Figure 4.8 Effects of process parameters on S/N ratio of SR for PCD

Table 4.12 Analysis of variance of TWR for PCD

Effect	Tool material	Abrasive slurry	Slurry concentration	Grit size	Power rating
SS	62.28	26.86	43.86	29.04	2.53
F value	1.90	0.82	1.34	0.89	0.07
P(%)	37.84	16.32	26.65	17.64	1.53

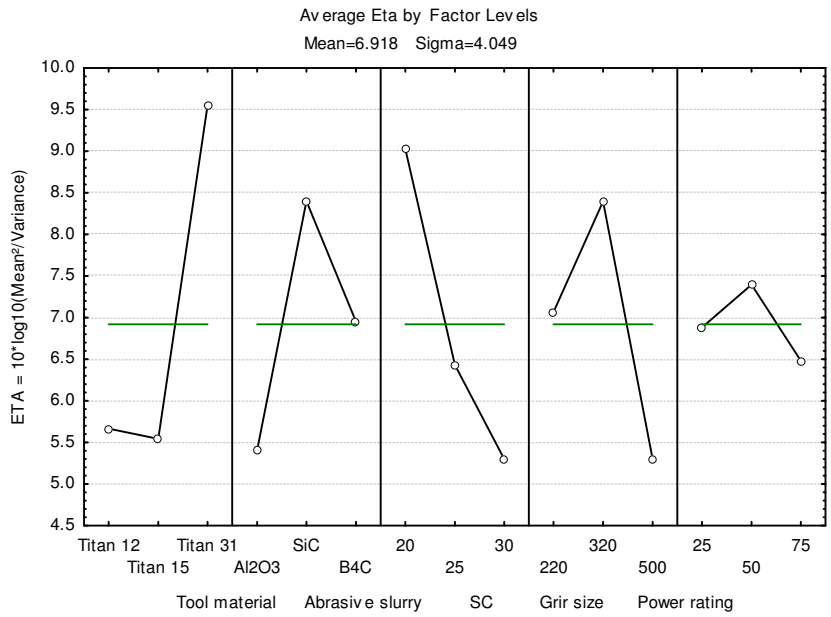

Figure 4.9 Effects of process parameters on S/N ratio of TWR for PCD

4.3 CONFIRMATORY EXPERIMENTATION

4.3.1 Performing the confirmatory experiments

Conducting a confirmation experiment is a final step of robust design project. Its purpose is to verify that the optimum conditions suggested by the matrix experiment improve the project output. If the observed S/N ratio under the optimum conditions is close to the respective predictions, then it was concluded that the additive model on which the matrix experiment was based is a good approximation of reality. Then, the recommended optimum conditions were adopted for the processing of the product, as the case may be. However, if the observed S/N ratios under the optimum conditions differ drastically from their respective predictions, there is an evidence of failure of the additive model. There can be many reasons for failure.The verification experiment has two aspects: The first is that the prediction must agree under the laboratory conditions; the second aspect is that the predictions should be valid under actual manufacturing conditions for the process design and under actual field conditions for the product design. A judicious choice of both the noise factors to be included in the experiment. The testing conditions are essentially for the predictions made through the laboratory experiment and that is to be valid for both manufacturing and field conditions. For the case study of tungsten carbide, stellite and diamond machining characteristics optimization, nine final observations were made for the initial and optimum conditions. The results are tabulated in tables 4.13-4.15 respectively. It is clear that the data agree very well with the predications about the improvement in the S/N ratios. So, we could adopt the optimum settings as the new process settings and proceed to implement these settings. The graphs 1, 3, 5 represents the initial conditions and 2, 4, 6 represent optimum conditions for the tungsten carbide, stellite and poly-crystalline diamond as shown in figures 4.10.

Table 4.13 Results of confirmatory experiments for tungsten carbide

Response type		Initial conditions	Optimum conditions	Improvement (%)
MRR	mm^3/min	0.162	0.214	32.09
TWR	mm^3/min	0.064	0.052	18.75
SR	microns	0.62	0.48	22.58

Table 4.14 Results of confirmatory experiments for stellite

Response type		Initial conditions	Optimum conditions	Improvement (%)
MRR	mm^3/min	0.158	0.182	15.18
TWR	mm^3/min	0.058	0.046	20.68
SR	microns	0.86	0.64	25.58

Table 4.15 Results of confirmatory experiments for PCD

Response type		Initial conditions	Optimum conditions	Improvement (%)
MRR	mm^3/min	0.178	0.186	4.49
TWR	mm^3/min	0.082	0.076	7.31
SR	microns	0.92	0.80	13.04

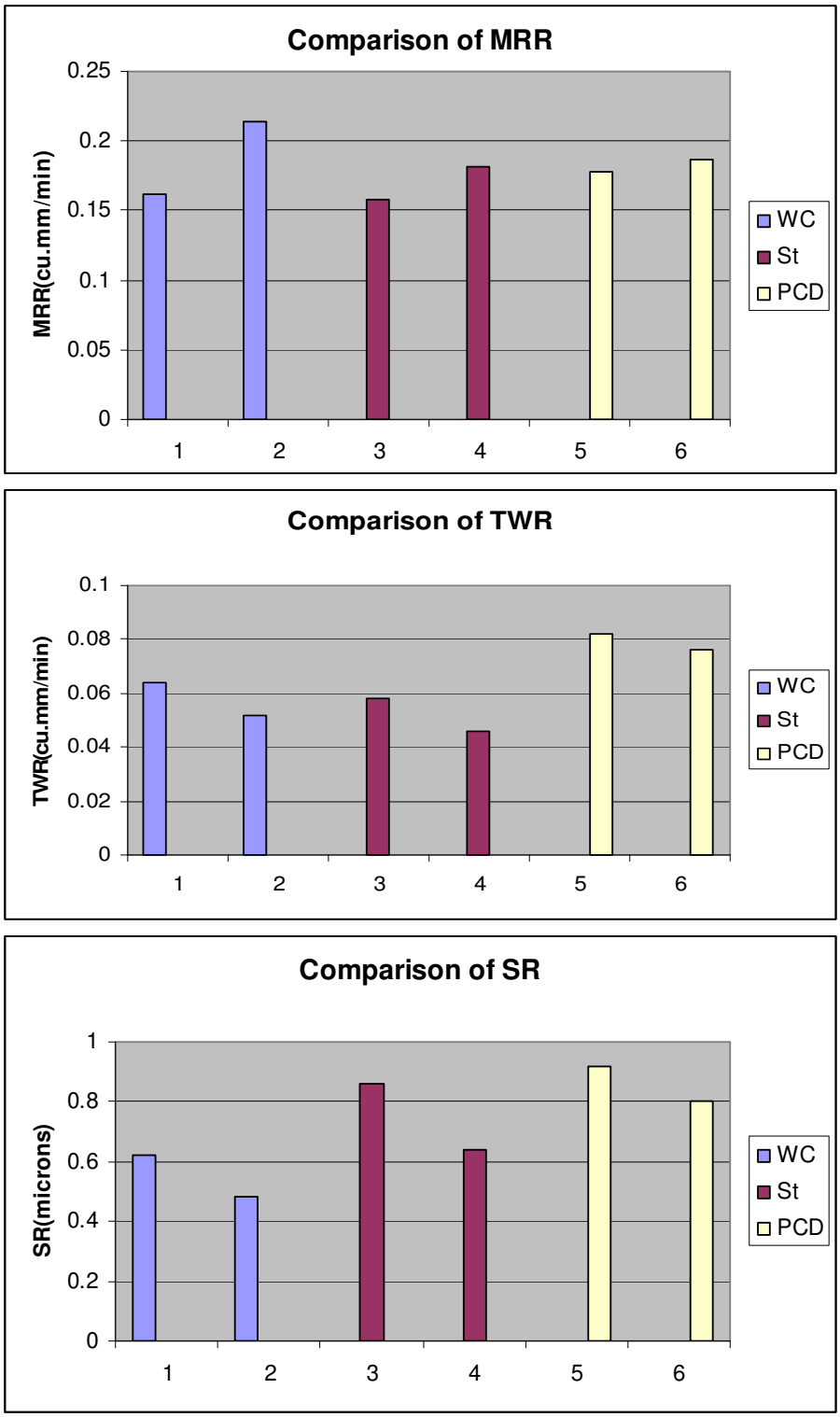

Figure 4.10 Comparison of initial Vs optimum conditions

4.3.2 Follow-up experiments

The optimization of a process or a product need not be completed in a single matrix experiment. Several matrix experiments may have to be conducted in sequence before completing a product or process design. The information learnt in one matrix experiment was used to plan the subsequent matrix experiments for achieving even more improvement in the process or the product. The factors studied in such subsequent experiments, or the levels of the factors, were typically different from those studied in the earlier experiments.

4.3.3 Range of applicability

In any development activity, it is highly desirable that the conclusions continue to be valid when one advances to a new generation technology. In the case study of the machining characteristics optimization, this means that once the process to machine tungsten carbide, stellite and diamond work pieces is developed , and it to be valid, when one advances to more grades of these materials.The present results are valid for (90-98%) confidence interval.

The process developed for one application should be valid for other applications also. The processes and products developed by the robust design method generally have these characteristics of design transferability. Thus a significant amount of development effort may be saved in transferring the process to new control factors that will handle new grades of given work-pieces.

CHAPTER V

MODELING OF RESULTS

5.1 INTRODUCTION

The two broad approaches for optimizing the machining characteristics have been used in the study.

1. Micro-modeling
2. Macro-modeling

1. Micro-modeling: This model is based on dimensional analysis according to Buckingham's Л– theorem. It begins by developing a mathematical model of the system, which, in this case, would be of the MRR of tungsten carbide, stellite and diamond. When systems are complex, as in the case study, we must make assumption that simplify the operation, as well as put forth considerable effort to develop the model. Furthermore, the more simplifying we do, the less realistic the model will be, and, hence, the less adequate it will be for precise optimization. But once an adequate model is constructed, a number of well known optimization methods, can be used to find the best system configuration.

2. Macro-modeling: This model is based on taguchi design for optimization.In this type of modeling, we bypass the step of building a mathematical model of the system. The concern is primarily with obtaining the optimum system configuration, not with obtaining a detailed understanding of the system itself. As such, macro-modeling gives faster and more efficient results. It gives the specific information needed for optimization with a minimum expenditure of experimental resources.

5.2 MACRO-MODEL FOR PREDICTING MACHINING CHARACTERISTICS OF TUNGSTEN CARBIDE, STELLITE AND DIAMOND

The case study under consideration deals primarily with obtaining the optimum system configuration in terms of response parameters with minimum expenditure of experimental resources. The best settings of control factors have been determined through experiments

as shown in tables 5.1, 5.2 & 5.3 for tungsten carbide, stellite and diamond as macro model.

Table 5.1 Optimized Process Settings (Macro-model) for WC

Optimized MRR conditions	
Tool material	TITAN 15
Grit size	220
Abrasive slurry	Alumina
Power rating	25 % i.e.125W
Slurry concentration	20%
Optimized TWR conditions	
Tool material	TITAN 15
Grit size	500
Abrasive slurry	Alumina
Power rating	25 % i.e.125W
Slurry concentration	25%
Optimized SR conditions	
Tool material	TITAN 12
Grit size	320
Abrasive slurry	Boron carbide
Power rating	75% i.e.375W
Slurry concentration	25%

Table 5.2 Optimized Process Settings (Macro-model) for stellite

Optimized MRR conditions	
Tool material	TITAN 31
Grit size	220
Abrasive slurry	Alumina
Power rating	25 % i.e.125W
Slurry concentration	20%
Optimized TWR conditions	
Tool material	TITAN 15
Grit size	220
Abrasive slurry	Alumina
Power rating	25 % i.e.125W
Slurry concentration	25%
Optimized SR conditions	
Tool material	TITAN 12
Grit size	220
Abrasive slurry	Alumina
Power rating	25% i.e.125W
Slurry concentration	25%

Table 5.3 Optimized Process Settings (Macro-model) for PCD

Optimized MRR conditions	
Tool material	TITAN 12
Grit size	220
Abrasive slurry	Alumina
Power rating	50 % i.e.250W
Slurry concentration	20%
Optimized TWR conditions	
Tool material	TITAN 31
Grit size	320
Abrasive slurry	SiC
Power rating	50 % i.e.250W
Slurry concentration	20%
Optimized SR conditions	
Tool material	TITAN 12
Grit size	500
Abrasive slurry	SiC
Power rating	75% i.e.375W
Slurry concentration	25%

5.3 MICRO-MODEL FOR PREDICTING MACHINING CHARACTERISTICS OF TUNGSTEN CARBIDE, STELLITE AND DIAMOND

The micro model has been developed using dimensionless approach (Buckingham's Л – theorem). The Buckingham's Л-theorm states that, in a physical problem including "n" quantities in which there are "m" dimensions, the quantities can be arranged into "n-m" independent dimensionless parameters. The following assumptions have been made while developing the mathematical micro-model for the given situation.

1. Frequency of ultrasonic vibration is fixed through out the experimentation and it is of the order of 20 kHz + 200 Hz.

2. Amplitude of vibration is constant throughout the experimentation and it of the order of 0.0253-0.0258mm.

3. Feed force is also constant and maintained equal to 1.724 kg throughout the experiment.

5.3.1 Micro-model for predicting material removal rate

MRR "Z" depends upon five input parameters namely ultrasonic power, elastic modulus of tool, slurry hardness factor, slurry concentration and grit size of slurry. Now on selecting M (mass), L (length) and T (time) as basic dimensions, the dimensions of the following parameters are given by:

1. MRR "Z" (mm^3/min) $M^0L^3T^{-1}$
2. Power rating "P" (W) $M L^2 T^{-3}$
3. Elastic modulus of tool "E" (G Pa) $M L^{-1} T^{-2}$
4. Slurry hardness factor "μ_s" (kgf/mm^2) $M L^{-1} T^{-2}$
5. Slurry concentration " λ" (gm/mm^3) $M L^{-3} T^0$
6. Slurry grit size "ρ" (mm) M^0LT^0

$$Z = f(P, E, \mu_S, \lambda, \rho)$$

In this case,n=6 and m=3, therefore there are (n-m) ,three dimensionless groups. These are π_1, π_2, π_3 .Assuming Z,P and E as the quantities which directly goes in π_1, π_2, π_3 respectively.

$$\pi_1 = Z(\mu_s)^{\alpha_1}(\lambda)^{\gamma_1}(\rho)^{\delta_1}$$

$$\pi_2 = P(\mu_s)^{\alpha_2}(\lambda)^{\gamma_2}(\rho)^{\delta_2}$$

$$\pi_3 = E(\mu_s)^{\alpha_3}(\lambda)^{\gamma_3}(\rho)^{\delta 3}$$

On substituting the dimensions of each quantity and equating to zero,the exponent of each basic dimension is obtained.

$$\pi_1 = \left(L^3T^{-1}\right)\left(ML^{-1}T^{-2}\right)^{\alpha_1}\left(ML^{-3}\right)^{\gamma_1}(L)^{\delta_1}$$

$$0 = \alpha_1 + \gamma_1$$

$$0 = 3 - \alpha_1 - 3\gamma_1 + \delta_1$$

$$0 = -1 - 2\alpha_1$$

$$\alpha_1 = -1/2\,, \quad \gamma_1 = 1/2 \quad , \quad \delta_1 = -2$$

$$\pi_1 = Z\lambda^{1/2}/\mu_s^{1/2}\rho^2$$

Similarly

$$\pi_2 = \left(ML^2T^{-3}\right)\left(ML^{-1}T^{-2}\right)^{\alpha_2}\left(ML^{-3}\right)^{\gamma_2}(L)^{\delta_2}$$

$$0 = 1 + \alpha_2 + \gamma_2$$

$$0 = 2 - \alpha_2 - 3\gamma_2 + \delta_2$$

$$0 = -3 - 2\alpha_2$$

$$\alpha_2 = -3/2\,, \quad \gamma_2 = 1/2\,, \quad \delta_2 = -2$$

$$\pi_2 = P\lambda^{1/2}/\mu_s^{3/2}\rho^2$$

Similarly

$$\pi_3 = \left(ML^{-1}T^{-2}\right)\left(ML^{-1}T^{-2}\right)^{\alpha_3}\left(ML^{-3}\right)^{\gamma_3}(L)^{\delta_3}$$

$$0 = 1 + \alpha_3 + \gamma_3$$

$$0 = -1 - \alpha_3 - 3\gamma_3 + \delta_3$$

$$0 = -2 - 2\alpha_3$$

$$\alpha_3 = -1, \quad \gamma_3 = 0 \ , \ \delta_3 = 0$$

$$\pi_3 = E/\mu_s$$

The relationship can be assumed to be of the form

$$\pi_i = f\left(\pi_j, \pi_k\right)$$

On assuming i=1,j=2 and k=3,the functional relationship is of the form

$$\pi_1 = f\left(\pi_2, \pi_3\right)$$

$$Z\lambda^{1/2}/\mu_s^{1/2}\rho^2 = f\left(P\lambda^{1/2}/\mu_s^{3/2}\rho^2, E/\mu_s\right)$$

This has been found experimentally that Z directly goes with P.Therefore the equation becomes

$$Z\lambda^{1/2}/\mu_s^{1/2}\rho^2 = P\lambda^{1/2}/\mu_s^{3/2}\rho^2 f\left(E/\mu_s\right)$$

$$Z = K\left(PE/\mu_s^2\right)$$

Where K is a constant of proportionality.

Calculation of K:

On keeping E/μ_s^2 fixed, experiments were performed for different values of P to calculate the value of Z. The actual experimental data has been collected and plotted in figures 5.1-5.9 respectively. The data collected has been further used for finding the best fitting

curve.The second degree polynomial equation is coming out to be the best fitted curve using the regression analysis.

Case 1 (TITAN12 tool, WC work material, aluminium oxide slurry, 220 abrasive grit size)

The governing equation of MRR is given as:

$$Z = (-10^{-6} P^2 + 4*10^{-4} P + 0.1556)\left(PE/\mu_s^2\right)$$

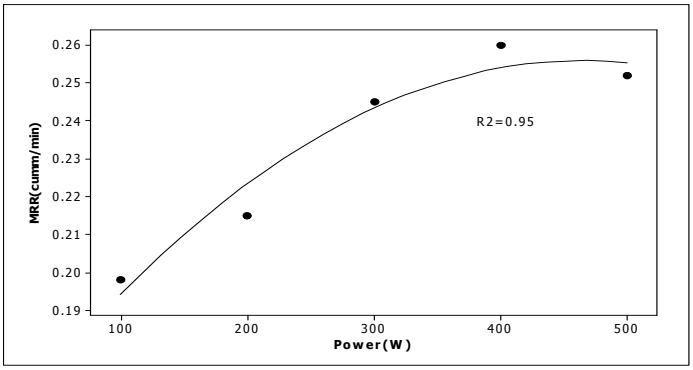

Figure 5.1 MRR Vs Power (TITAN12 tool, WC work material)

Case 2 (TITAN15 tool, WC work material, aluminium oxide slurry, 220 abrasive grit size

$$Z = (-10^{-6} P^2 + 4*10^{-3} P + 0.168)\left(PE/\mu_s^2\right)$$

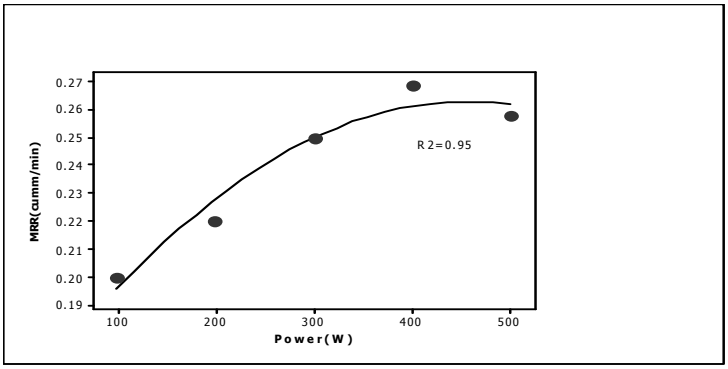

Figure 5.2 MRR Vs Power (TITAN15 tool, WC work material)

Case 3 (TITAN31 tool, WC work material, aluminium oxide slurry, 220 abrasive grit size,)

$$Z = (-10^{-6} P^2 + 4*10^{-3} P + 0.1776)\left(PE/\mu_s^2\right)$$

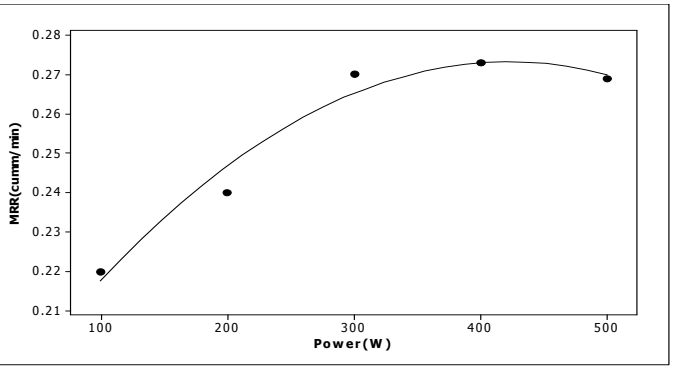

Figure 5.3 MRR Vs Power (TITAN31 tool, WC work material)

Case 4 (TITAN12 tool, stellite work material, aluminium oxide slurry, 220 abrasive grit size)

$$Z = (-10^{-6} P^2 + 4*10^{-4} P + 0.1504)\left(PE/\mu_s^2\right)$$

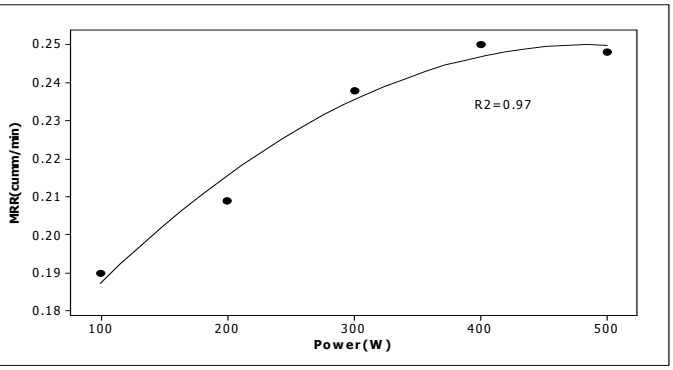

Figure 5.4 MRR Vs Power (TITAN12 tool, stellite work material)

Case 5 (TITAN15 tool, stellite work material, aluminium oxide slurry, 220 abrasive grit size)

$$Z = (-10^{-6} P^2 + 4*10^{-4} P + 0.1518)\left(PE/\mu_s^2\right)$$

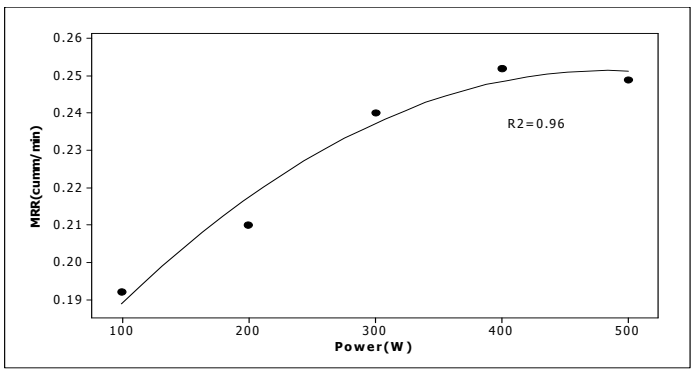

Figure 5.5 MRR Vs Power (TITAN15 tool, stellite work material)

Case 6 (TITAN31 tool, stellite work material, aluminium oxide slurry, 220 abrasive grit size)

$$Z = (-10^{-6} P^2 + 4*10^{-4} P + 0.1526)\left(PE/\mu_s^2\right)$$

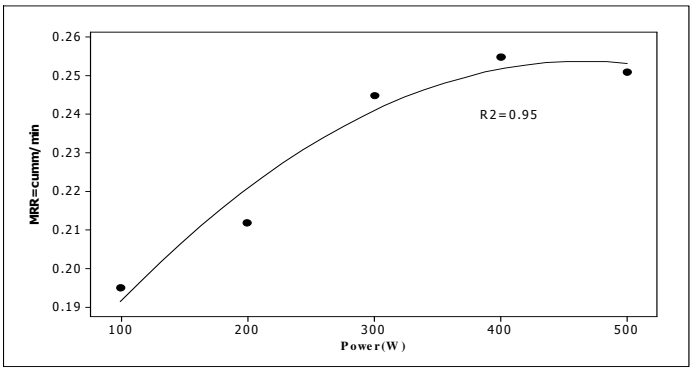

Figure 5.6 MRR Vs Power (TITAN31 tool, stellite work material)

Case 7 (TITAN12 tool, PCD work material, aluminium oxide slurry, 220 abrasive grit size)

$$Z = (-10^{-6} P^2 + 2*10^{-4} P + 0.1992)\left(PE/\mu_s^2\right)$$

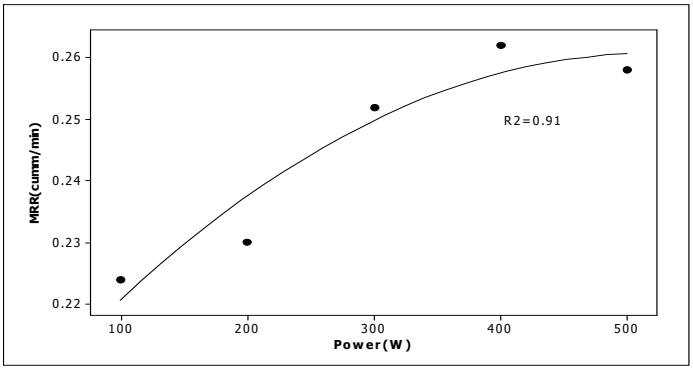

Figure 5.7 MRR Vs Power (TITAN12 tool, PCD work material)

Case 8 (TITAN15 tool, PCD work material, aluminium oxide slurry, 220 abrasive grit size)

$$Z = (-10^{-6} P^2 + 2*10^{-4} P + 0.2020)\left(PE/\mu_s^2\right)$$

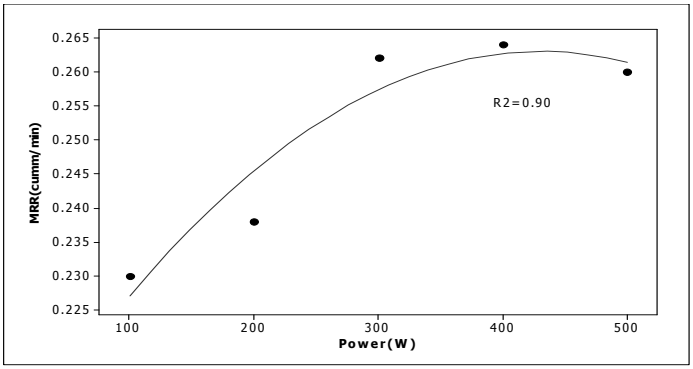

Figure 5.8 MRR Vs Power (TITAN15 tool, PCD work material)

Case 9(TITAN31 tool, PCD work material, aluminium oxide slurry, 220 abrasive grit size)

$$Z = (-10^{-6} P^2 + 2*10^{-4} P + 0.2068)\left(PE/\mu_s^2\right)$$

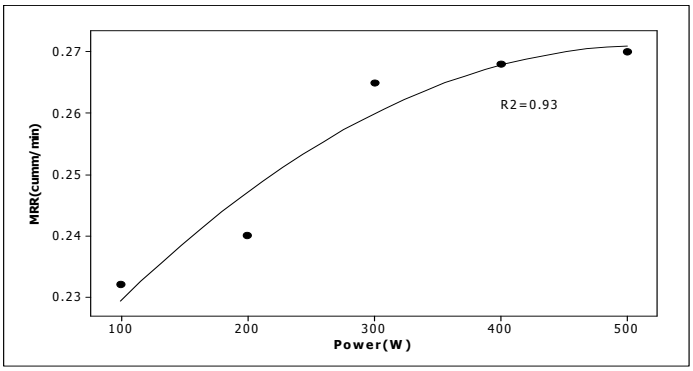

Figure 5.9MRR Vs Power (TITAN31 tool, PCD work material)

5.3.2 Micro-model for predicting tool wear rate

Tool wear rate"V" depends upon five input parameters namely ultrasonic power, tool hardness factor, slurry hardness factor, slurry concentration and grit size of slurry. Now

on selecting M (mass), L (length) and T (time) as basic dimensions, the dimensions of the following parameters are given by:

1. TWR "V" (mm^3/min) $M^0L^3 T^{-1}$
2. Power rating "P" (W) $M L^2 T^{-3}$
3. Tool hardness factor "H" (kgf/mm^2) $M L^{-1} T^{-2}$
4. Slurry hardness factor "μ_s" (kgf/mm^2) $M L^{-1} T^{-2}$
5. Slurry concentration " λ" (gm/mm^3) $M L^{-3} T^0$
6. Slurry grit size "ρ" (mm) M^0LT^0

$$V = f(P, H, \mu_S, \lambda, \rho)$$

The equation for TWR has been derived by applying the Buckingham's theorm as discussed in the article 5.3.1

$V = K\left(PH/\mu_s^2 \right)$ Where K is constant of proportionality.

Calculation of K:

On keeping H/μ_s^2 fixed, experiments were performed for different values of P to calculate the value of V. The actual experimental data has been collected and plotted in figures 5.10-5.18 respectively. The data collected has been further used for finding the best fitting curve.The second degree polynomial equation is coming out to be the best fitted curve using the regression analysis.

Case 1(TITAN12 tool, WC work material, aluminium oxide slurry, 220 abrasive grit size)

$$V = (7*10^{-3}H^2 - 0.04H + 0.137)\left(PH/\mu_s^2 \right)$$

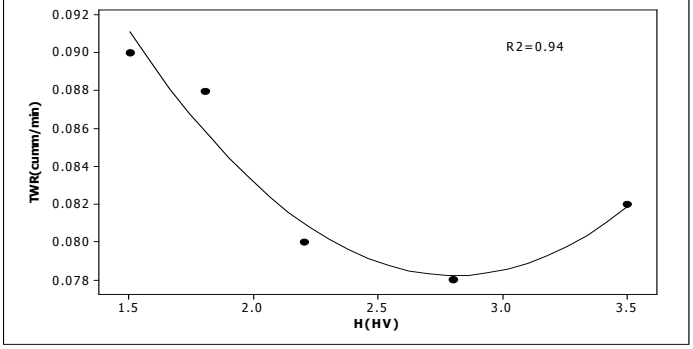

Figure 5.10 TWR Vs Power (TITAN12 tool, WC work material)

Case 2 (TITAN15 tool, WC work material, aluminium oxide slurry, 220 abrasive grit size)

$$V = (8*10^{-3}H^2 - 0.04P + 0.1413)\left(PH/\mu_s^2\right)$$

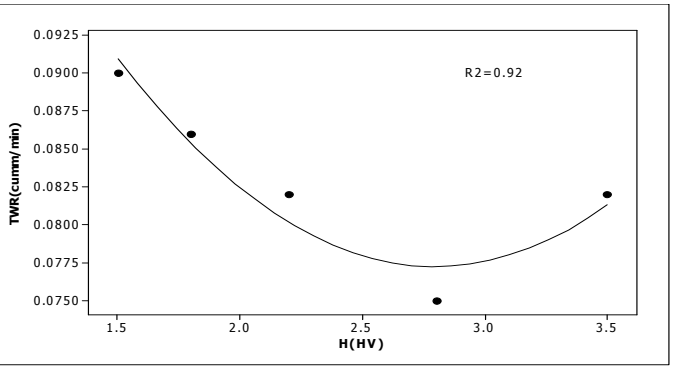

Figure 5.11TWR Vs Power ((TITAN15 tool, WC work material)

Case 3 (TITAN31 tool, WC work material, aluminium oxide slurry, 220 abrasive grit size)

$$V = (8*10^{-3}H^2 - 0.04P + 0.1312)\left(PH/\mu_s^2\right)$$

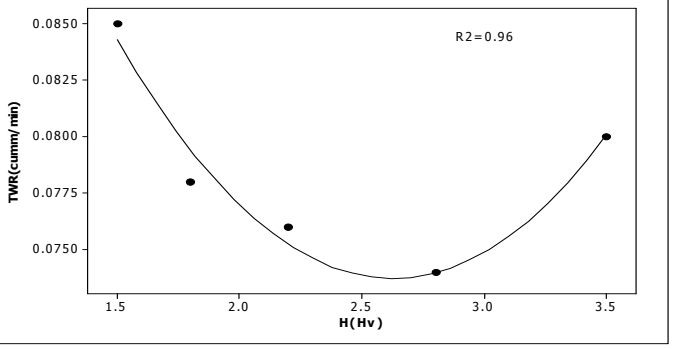

Figure 5.12 TWR Vs Power (TITAN31 tool, WC work material)

Case 4 (TITAN12 tool,stellite work material, aluminium oxide slurry, 220 abrasive grit size)

$$V = (5*10^{-2} H^2 - 0.027P + 0.129)\left(PH/\mu_s^2\right)$$

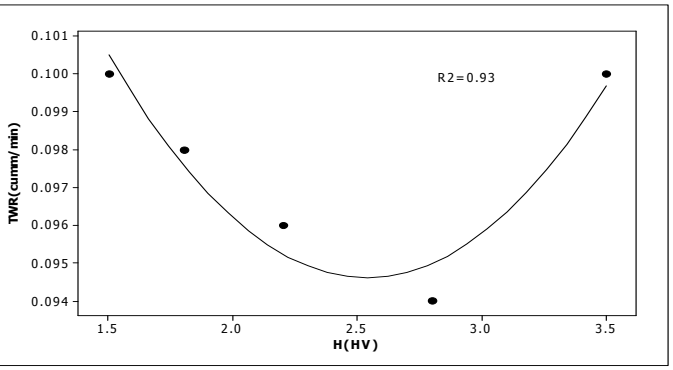

Figure 5.13 TWR Vs Power (TITAN12 tool,stellite work material)

Case 5 (TITAN15 tool,stellite work material, aluminium oxide slurry, 220 abrasive grit size)

$$V = (6*10^{-3} H^2 - 0.03P + 0.142)\left(PH/\mu_s^2\right)$$

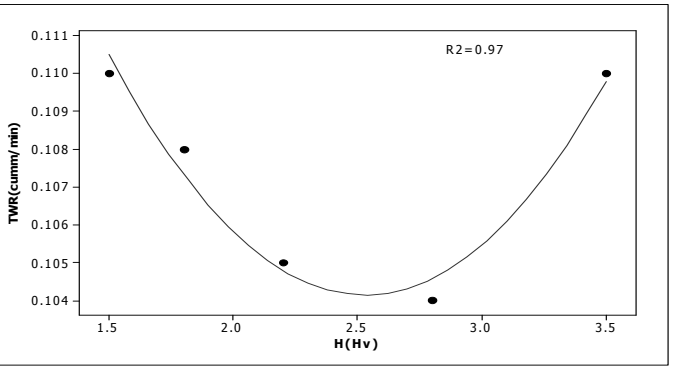

Figure 5.14 TWR Vs Power (TITAN15 tool, stellite work material)

Case 6 (TITAN31 tool, stellite work material, aluminium oxide slurry, 220 abrasive grit size)

$$V = (5*10^{-3} H^2 - 0.028H + 0.145)\left(PH/\mu_s^2\right)$$

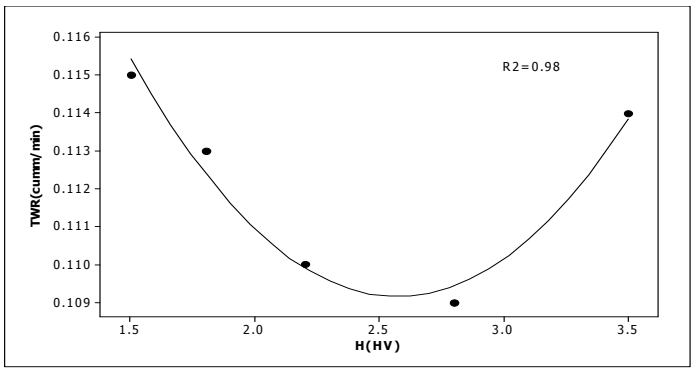

Figure 5.15 TWR Vs Power (TITAN31 tool, stellite work material)

Case 7 (TITAN12 tool,PCD work material, aluminium oxide slurry, 220 abrasive grit size)

$$V = (5*10^{-3}H^2 - 0.028H + 0.1552)\left(PH/\mu_s^2\right)$$

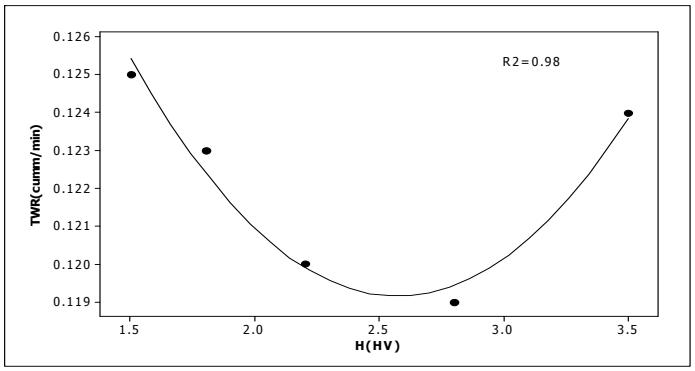

Figure 5.16 TWR Vs Power (TITAN12 tool, PCD work material)

Case 8 (TITAN15 tool, PCD work material, aluminium oxide slurry, 220 abrasive grit size)

$$V = (5*10^{-3}H^2 - 0.03H + 0.1619)\left(PH/\mu_s^2\right)$$

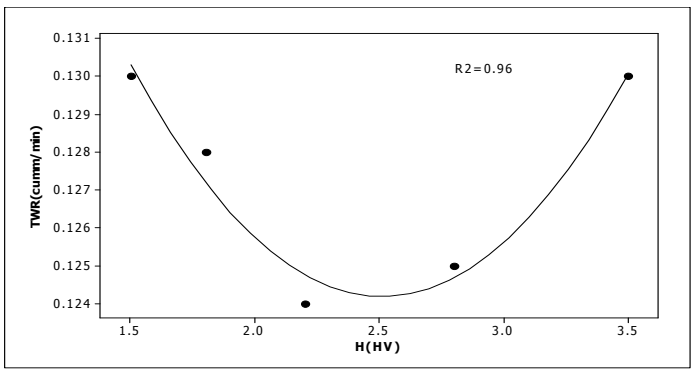

Figure 5.17 TWR Vs Power (TITAN15 tool, PCD work material)

Case 9 (TITAN31 tool, PCD work material, aluminium oxide slurry, 220 abrasive grit size)

$$V = (5*10^{-3} H^2 - 0.04H + 0.1728)$$

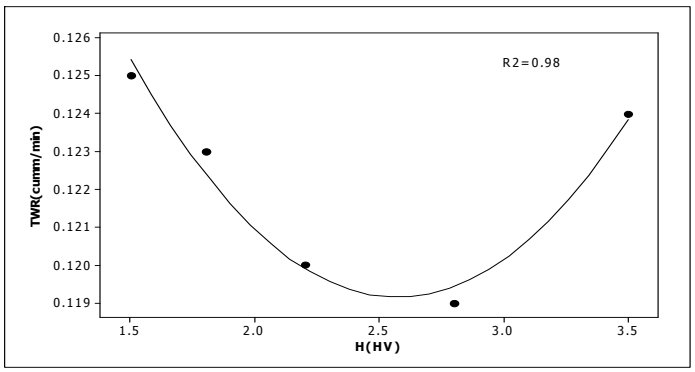

Figure 5.18 TWR Vs Power (TITAN31 tool, PCD work material)

It has been concluded from the above figures that the second degree polynomial equation is coming out to be the best fitted curve using the regression analysis.

CHAPTER-VI

CONCLUSIONS AND SCOPE OF FUTURE WORK

6.1 CONCLUSIONS

Based on the experiments conducted in the present study, the following conclusions have been drawn.

1. The tool material, type of abrasive used, slurry concentration and slurry grit size significantly affect the MRR in ultrasonic machining of tungsten carbide. With regard to S/N response, slurry concentration factor has emerged as most significant with a percent contribution of 43.67 % followed by abrasive slurry type (21.03%), tool material (14.97%) and grit size (12.24%) (table 4.2). Power rating factor can be termed as the least significant for MRR with a percent contribution of 8.06 %. **It has been concluded from the results that "input parameters settings of power rating at 125W, with TITAN 15 tool and aluminium oxide slurry with a coarse grit size of 220 and slurry concentration of 20% have given the optimum results for MRR as shown in figure 4.1; when tungsten carbide was machined".**
2. The type of abrasive slurry and power rating of the ultrasonic machine have been identified as the significant factors as far as surface quality in USM of tungsten carbide is concerned. Other factors such as slurry concentration and abrasive grit size used have been found to be relatively least significant. Power rating has emerged as the most significant factor with a percent contribution of the order of 40.94 %, whereas abrasive slurry factor also contributes 40.56 % to the variation in surface roughness (table 4.3). **It has been concluded that "input parameters settings of power rating at 375W, with TITAN 12 tool and boron carbide slurry with abrasive grit size of 320 and slurry concentration of 25% have given the optimum results for SR as shown in figure 4.2; when tungsten carbide was machined.**
3. The slurry grit size, tool material and power rating significantly affect the TWR in ultrasonic machining of tungsten carbide. With regard to S/N response, power rating factor has emerged as most significant with a percent contribution of 58.71% followed by tool material (14.53%), grit size (10.33%), abrasive slurry

type (8.71%) and slurry concentration factor can be termed as the least significant for TWR with a percent contribution of 7.69 % (table 4.4). **It has been concluded from the results that "input parameters settings of power rating at 125W, with TITAN 15 tool and aluminium oxide slurry with abrasive grit size of 500 and slurry concentration of 25% have given the optimum results for TWR as shown in figure 4.3; when tungsten carbide was machined".**

4. Power rating, type of abrasive used, slurry concentration significantly affects the MRR in ultrasonic machining of stellite. With regard to S/N response, slurry concentration factor has emerged as most significant with a percent contribution of 45.18% followed by abrasive slurry type (25.34%), power rating (12.49%) and tool material (12.15%) (table 4.6).The grit size can be termed as the least significant for MRR with a percent contribution of 4.82 %. **It has been concluded from the results that "input parameters settings of power rating at 125W, with TITAN 31 tool and aluminium oxide slurry with a coarse grit size of 220 and slurry concentration of 20% have given the optimum results for MRR as shown in figure 4.4; when stellite was machined".**
5. The abrasive grit size and power rating of the ultrasonic machine have been identified as the significant factors as far as surface quality in USM of stellite is concerned. Other factors such as tool material, abrasive slurry concentration used have been found to be relatively least significant. Abrasive grit size has emerged as the most significant factor with a percent contribution of the order of 55.47 %, whereas power rating factor also contributes 30.95 % to the variation in surface roughness (table 4.7). **It has been concluded that "input parameters settings of power rating at 125W, with TITAN 12 tool and aluminium oxide slurry with abrasive grit size of 220 and slurry concentration of 25% have given the optimum results for SR as shown in figure 4.5; when stellite was machined.**
6. The tool material, slurry grit size and power rating significantly affect the TWR in ultrasonic machining of stellite. With regard to S/N response, power rating factor has emerged as most significant with a percent contribution of 53.85% followed by tool material (16.72%) and grit size (11.61%) and abrasive slurry type (10.58%) and slurry concentration factor can be termed as the least significant for TWR with a percent contribution of 7.21 % (table 4.8). **It has been concluded from the results that "input parameters settings of ultrasonic power rating at 125W, with TITAN 15 tool and aluminium oxide slurry with abrasive grit**

size of 500 and slurry concentration of 25% have given the optimum results for TWR as shown in figure 4.6; when stellite was machined".

7. Type of abrasive used, slurry concentration and tool material significantly affect the MRR in ultrasonic machining of poly-crystalline diamond. With regard to S/N response, type of abrasive slurry factor has emerged as most significant with a percent contribution of 46.73% followed by abrasive slurry concentration (18.39%), tool material (13.63%) and grit size (11.39%).The power rating can be termed as the least significant for MRR with a percent contribution of 9.84 % (table 4.10). **It has been concluded from the results that "input parameters settings of power rating at 250W, with TITAN 12 tool and aluminium oxide slurry with a coarse grit size of 220 and slurry concentration of 20% have given the optimum results for MRR as shown in figure 4.7; when poly-crystalline diamond was machined".**
8. The tool material and power rating of the ultrasonic machine have been identified as the significant factors as far as surface quality in USM of poly-crystalline diamond is concerned. Other factors such as abrasive slurry and grit size used have been found to be relatively least significant. The power rating has emerged as the most significant factor with a percent contribution of the order of 31.95 %, whereas tool material factor also contributes 27.18 % to the variation in surface roughness (table 4.11). **It has been concluded that "input parameters settings of ultrasonic power rating at 375W, with TITAN 12 tool and silicon carbide slurry with abrasive grit size of 500 and slurry concentration of 25% have given the optimum results for SR as shown in figure 4.8; when poly-crystalline diamond was machined.**
9. The tool material, slurry concentration and grit size significantly affect the TWR in ultrasonic machining of poly-crystalline diamond .With regard to S/N response, tool material factor has emerged as most significant with a percent contribution of (37.84%) followed by slurry concentration (26.65%), grit size (17.64%) and abrasive slurry (16.32%) and power rating factor can be termed as the least significant for TWR with a percent contribution of 1.53 % (table 4.12). **It has been concluded from the results that "input parameters settings of ultrasonic power rating at 250W, with TITAN 31 tool and silicon carbide slurry with abrasive grit size of 320 and slurry concentration of 20% have**

given the optimum results for TWR as shown in figure 4.9; when poly-crystalline diamond was machined".

10. It has been investigated from the experimental observations that even minor fluctuations of abrasive slurry concentration can affect the response to considerable extent. Hence, a large volume of the slurry must be used to minimize the effect of variations in the input parameters. Also, the tool may crack if slurry flow rate is inadequate.
11. Tungsten carbide, stellite and poly-crystalline diamond exhibits fair machinability while machined with USM process. The surface roughness of the machined surface has been found to be better than most of the other non-conventional machining processes such as electric discharge machining (EDM), laser beam machining (LBM), plasma arc machining (PAM) etc.There is no evidence of any surface damage in form of micro cracking or heat affected zone. The relative toughness of work and tool plays an important role in ultrasonic machining of above said work materials.
12. The tool surface undergoes a change in shape with the progress in machining. The tendency of dish formation at the centre of the tool face has been found to be more prevalent in tungsten carbide and diamond as compared to stellite. It is necessary to restore the shape of the tool before performing another experiment.
13. The selection of tool materials and design of the tools are very critical from point of view of MRR and TWR in ultrasonic machining. Initial weight of the tool is another important factor. Tool weight should not exceed the maximum limit of 50 g for optimum performance in USM for the present set-up. Improper design and excessive length of the tool leads to high temperature generation at the tool face and may also lead to fatigue failure.

6.2 LIMITATIONS

1. The results are valid within the specified range of the process parameters. In the present work, 500W piezoelectric transducer based USM apparatus was used. The depth of cut was limited as excessive length of the tool was adding to the tool weight.The tool weight more than 50g resulted in auto-cut of machine. Hence results are limited in present form to machine comparatively small sized work pieces.

2. The use of solid tool leads to the problem of flushing of slurry particles from the machined surface after a certain depth of cut. Because of this reason, the depth of cut was limited in the present work.

6.3 SCOPE OF FUTURE WORK

1. In the present investigation, only five process parameters viz. tool material, abrasive type, slurry grit size, slurry concentration and power rating were included as input factors. Study of other process parameters such as amplitude of vibration, tool geometry, flow rate of abrasive slurry, temperature of the abrasive slurry, static load and type of tool horn can be included.
2. Further study can be focused on rotary usm or hybrid USM-EDM processes that may involve five or six times superior efficiency in terms of MRR as compared to static USM used for the present investigation. Also, the flow of slurry can be magnetized while machining with static usm on tungsten carbide, stellite and Poly-crystalline diamond.
3. Although effect of power rating on the machining performance of USM has been investigated in this study, it can be further investigated with different work-tool combinations on high power ultrasonic machines.
4. The study can be extended to other tougher and harder materials such as copper alloys, titanium and their alloys etc for their application in manufacturing industry.

REFERENCES

1. Scott, A .C. and Yung,C.S. (1996), In-process control of surface roughness due to tool wear using a new ultrasonic system, International Journal of Machine Tools and Manufacture, Vol. 36, pp. 411-422.
2. Kumar, P.and Singh.H. (2006), Optimising feed force for turned parts through taguchi technique, Sadhna-Academy, Proceedings in Engg. Sciences,Vol.31,pp. 671-681
3. Leung, T.K. (1996), A critical look at taguchi modeling approach for robust design, Journal of Applied Statistics, Vol. 23, pp. 81- 95.
4. Younes, L. D., Tehranpars, T. and Iran, A.J. (2002), A new insight into the taguchi method, Quality Assurance, Vol. 9, pp. 55–62.
5. Akbari, J., Borzoi, H.and Mamduhi, M. (2008), Using ultrasonic vibration for increasing the performance of grinding process of fine ceramics, Proceedings of International Conference on Processing and Fabrication of Advanced Materials (XVII), Delhi, pp. 207-219.
6. Adithan, M. and Venkatesh,V.C.(1975), Study of the performance characteristics of an ultrasonic drilling head,Wear,Vol.33,pp. 261-270.
7. Aspinwall, D.K.,Thoe,T.B.and Wise,M.L.(1998), Review of ultrasonic machining, International Journal of Machine Tools and Manufacture, Vol.38, pp. 239–255.
8. Liao,Y.S., Chen,Y.C. and Lin, M.H. (2007), Feasibility study of the ultrasonic vibration assisted drilling of inconel super alloy ,International Journal of Machine Tools and Manufacture, Vol. 47, pp. 2-13.
9. George, P.M., Raghunath, B.K., Manocha, L.M. and Warrier, A.M. (2004), EDM machining of carbon-carbon composite- a taguchi approach, Journal of Materials Processing Technology, Vol.145, pp.66-71.
10. Simon, S.F., Chang, G. and Bone, M. (2005), Burr size reduction in drilling by ultrasonic assistance, Robotics and Computer Integrated Manufacturing, Vol.21, pp. 442–450.
11. Aspinwall,D.K.,Kasuga,Y.and Mantle,A.L.(2001),The use of ultrasonic machining for the production of holes in γ-trial , Proceedings of the 13th International Symposium for Electromachining, ISEM XVIII, Spain, pp .925-936.
12. Chang,C.W. and Chun, P.K.(2007), Evaluation of surface roughness in laser-assisted machining of aluminum oxide ceramics with taguchi method,

International Journal of Machine Tools and Manufacture, Vol. 47 ,pp.141–147

13. Jain,V.K., Koshy,P., and Lal,G.K.(1996),Mechanism of material removal in electrical discharge diamond grinding, International Joural of Machine Tools and Manufacture,Vol.36,pp.1173-1185.
14. Liu,K., Li,X.P., Rahman,M. and Liu,X.D.(2004), Study of ductile mode cutting in grooving of tungsten carbide with and without ultrasonic vibration assistance, International Journal of Advance Manufacturing Technology, Vol.24, pp. 389–394.
15. Ramakrishnan, N. and Brahmankar, P.K.(2005), On the fatigue characteristics of electrodischarge machined alumina particulate reinforced aluminium matrix composites, International Journal of Manufacturing Technology and Management, Vol.7, pp. 342-351.
16. Majeed, M.A., Vijayaraghavan, L., Malhotra, S.K. and Krishnamurthy,S. (2008), Ultrasonic machining of Al_2O_3/laPO_4 composites, International Journal of Machine Tools and Manufacture,Vol. 48, pp. 40–46.
17. Pei, Z.J. and Ferreira, P.M. (1998), Modeling of ductile-mode material removal in rotary ultrasonic machining, International Journal of Machine Tools and Manufacture, Vol.38, pp. 1399-1418.
18. Lin, S. (1996), Study on the longitudinal torsional composite mode exponential ultrasonic horns, Ultrasonic, Vol. 34, pp. 757-762.
19. Wang, A.C., Biing Y.H. , Xiang,T.L. and Fuang Y.H. (2002), Use of micro ultrasonic vibration lapping to enhance the precision of micro holes drilled by micro electric-discharge machining, International Journal of Machine Tools and Manufacture, Vol.42, pp. 915-923.
20. Babitsky, V.I., Kalashnikov, A.N., Meadows, A. and Wijesundara, P. (2003), Autoresonant control of ultrasonically assisted cutting, International Journal of Machine Tools and Manufacture, Vol.14, pp. 91-114.
21. Margaret,S. G., Anatol B., Lloyd B., Leonard,J.B.and Mazon,H. (2004), Ultrasonic diffraction gratting spectroscopy and characterization of fluids and slurries, Ultrasonics, Vol. 42, pp. 531-536.
22. Makarov, P.V., Romanova,V.A. and Balokhonov, R.R.(1997), Plastic deformation behavior of mild steel subjected to ultrasonic treatment, Theoretical and Applied Fracture Mechanics, Vol. 28, pp. 141-146.

23. Jones, A.R. and Hull,J.B. (1998), Ultrasonic flow polishing, Ultrasonics, Vol. 36, pp. 97-101.
24. Dhar,S., Purohit,R., Saini,N., Sharma,A. and Kumar,G.H.(2007), Mathematical modeling of electric discharge machining of cast Al–4Cu–6Si alloy–10 wt.% SiC_P composites, Journal of Materials Processing Technology, Vol. 194, pp. 24-29.
25. Pei, Z.J. and Ferreira, P.M. (1999), An experimental investigation of rotary ultrasonic face milling , International Journal of Machine Tool and Manufacture, Vol.39, pp. 1327-1344.
26. Hocheng,H. and Kuo, K.L.(2001),Fundamental study of ultrasonic polishing of mild steel, International Journal of Machine Tools and Manufacture, Vol.42, pp.7-13.
27. Kazantsev, V.F. and Rozenberg, L.D. (1965), The mechanism of ultrasonic cutting, Ultrasonics, Vol.3, pp. 166-172.
28. Taichiu,L. and Jianxin,D.(2002), Mechanical surface treatments of electro-discharge machined (EDMed) ceramic composite for improved strength and reliability, Journal of the European Ceramic Society ,Vol. 22, pp. 545-550
29. Jianxin,D. and Taichiu,L. (2002), Ultrasonic machining of alumina based ceramic composites, Journal of the European Ceramic Society, Vol. 22, pp. 1235-1241.
30. Lee, T.C. and Chan, W. (1997), Mechanism of the ultrasonic machining of ceramic composites, Journal of Materials Processing Technology, Vol 71, pp.195-201.
31. Adithan, M. and Venkatesh, V.C. (1974), Parameter influence on tool wear in ultrasonic drilling, Tribology, Vol.7, pp.260-264.
32. Rama, A., Krishnamurthy, R. and Gokularathnam, C.V. (1989), Machining performance of toughened ceramic and cold compact alumina in ultrasonic drilling, Journal of Mechanical Working Technology, Vol.20, pp. 365-375.
33. Spur, G., Brueker, T., and Holl, S.E. (1997), Ultrasonic machining of ceramics, Industrial Ceramics, Vol.17, pp. 29-34.
34. Guzzo, P. L., Raslan, A., De, M. and Jose, D. B. (1999), Relationship between quartaz crystal orientation and the surface quality obtained by the ultrasonic machining, Proceedings of Annual IEEE International Frequency Control Symposium, Vol.2, pp. 792-795.
35. Kainth,G.S., Nandy,A.and Singh,K.(1979), On the mechanics of material removal

in ultrasonic machining , International Journal of Machine Tool Design and Research, Vol. 19, pp. 33-41.

36. Hocheng, H. and Hsu, C.(1995), Preliminary study of ultrasonic drilling of fiber reinforced plastics , Journal of Materials Processing Technology ,Vol. 48, pp. 255-266.
37. Wong, Y.S.,Seah, W.K., Loh, H.T.,Teng ,C.S.and Lee,L.C.(1995), Approximation of exponential curves for CNC machining of tool holders used in ultrasonic machining, Journal of Materials Processing Technology ,Vol. 48, pp. 713-719.
38. Dam,H.,Quist, P. and Schreiber, M.P. (1995), Productivity, surface quality and tolerances in ultrasonic machining of ceramics, Journal of Materials Processing Technology , Vol. 51, pp. 358-368.
39. Amin ,S.G., Ahmed ,M.H. and Youssef,A.H. (1995), Computer-aided design of acoustic horns for ultrasonic machining using finite element analysis, Journal of Materials Processing Technology ,Vol. 55, pp. 254-260.
40. Komaraiah, M.and Narasimha,P. R.(1993), A study on the influence of workpiece properties in ultrasonic machining, International Journal of Machine Tools and Manufacture ,Vol.33, pp. 495-505.
41. Hahn, R. and Schulze, P. (1994), A new ultrasonic machining route to create complex ceramic components, Ultrasonics Symposium, Proceedings, IEEE ,Vol. 3 ,pp. 1389 – 1392
42. Goetze,D.(1954),Ultrasonic machining of tungsten carbide, Ultrasonic Engineering,Transactions of the IRE Professional Group on , Vol. 2, pp.19 – 22.
43. Gan,J., Wang, X., Zhou, M., Ngoi ,B. and Zhong, Z.(2003), Diamond turning of glass with ultrasonic vibration, International Journal of Advanced Manufacturing Technology, Vol.21,pp 952-955.
44. Fang, F.Z., Liu,L.D. and Lee, L.C. (2003),Micro-machining of optical glasses-A review of diamond-cutting glasses, Sadhana, Vol. 28, pp. 945–955.
45. Skiedraite,I., Grazeviciute,J., Ostasevicius, V., Jurenas,V.and Bubulis,A.(2007), Ultrasonic application in turning process of different types of metals , Ultragaras,Vol.62, pp. 1392-2114.
46. Guzzo,P.L.,Raslan,A.A.,Shinohara,A.H.,Suzuki,C.K.andMikawa,Y.(2001), Characterization of synthetic quartz crystals grown from cylindrical seeds produced by ultrasonic machining, Journal of Crystal Growth, Vol. 229, pp. 275–

282.

47. Lia, Z.C., Jiaoa, Y., Deinesa, T.W., Pei, Z.J., and Treadwell, C. (2005), Rotary ultrasonic machining of ceramic matrix composites: feasibility study and designed experiments, International Journal of Machine Tools and Manufacture, Vol.45, pp.1402–1411.
48. Guzzo, P.L., Raslan, A.A., and Mello, D. (2003), Ultrasonic abrasion of quartz crystals, Wear, Vol. 255, pp. 67–77.
49. Sagar, R. and Sahu,P.(2006), Development of abrasive cut off wheel having side grooves, International Journal of Advanced Manufacturing Technology Vol.31,pp.37-40.
50. Wang, X., Zhou, M., Gan, G.K. and Ngoi,B.(2002),Theoretical and experimental studies of ultraprecision machining of brittle materials with ultrasonic vibration, International Journal of Advanced Manufacturing Technology, Vol. 20, pp. 99–102.
51. Hocheng, H., Tai, H.N. and Liu, C.S. (2000), Assessment of ultrasonic drilling of C/SiC composite material,Composites Part A: Applied Science and Manufacturing ,Vol. 31, pp. 133-142.
52. Adithan, M. and Venkatesh, V.C. (1976), Production accuracy of holes in ultrasonic drilling**,** Wear , Vol. 40, pp. 309-318.
53. Khairy, A.B.E. (1990), Assessment of some dynamic parameters for the ultrasonic machining process, Wear , Vol. 137, pp. 187-198.
54. Komaraiah,M., Manan,A., Reddy,N, and Victor,S.(1988), Investigation of surface roughness and accuracy in ultrasonic machining, Precision Engineering , Vol.10, pp. 59-65.
55. Palanikumar,K. (2006),Application of taguchi and response surface methodologies for surface roughness in machining glass fiber reinforced plastics by PCD tooling, International Journal of Advanced Manufacturing Technology, Vol. 36, pp. 19–27.
56. Singh, R. and Khamba, J. S. (2007), Macromodel for ultrasonic machining of titanium and its alloys: designed experiments, Proceedings of the I MECH E Part B Journal of Engineering Manufacture, Vol. 221, pp. 221-229.
57. Jadoun.R.S.,Kumar,P.and Mishra, B.K.(2006),Manufacturing process optimization for tool wear rate in ultrasonic drilling of engineering ceramics using the taguchi

method ,International journal of Machining and Machinability of Materials, Vol.1, pp.94-114.

58. Zeng, W.M., Li, Z.C., Pei, Z.J. and Treadwell,C.(2005), Experimental observation of tool wear in rotary ultrasonic machining of advanced ceramics,International Journal of Machine Tools and Manufacture,Vol.45,pp.1468-1473.
59. Wang,L. and Li, D.Y.(2003), Effects of yttrium on microstructure, mechanical properties and high-temperature wear behavior of cast stellite 6 alloy,Wear,Vol. 225,pp. 535-544
60. Hsu,C.Y., Lin,Y.Y., Lee,W.S. and Lo,S.P.(2008), Machining characteristics of inconel 718 using ultrasonic and high temperature-aided cutting **,** Journal of Materials Processing Technology ,Vol. 198 , pp. 359-365.
61. Singh, R.and Khamba, J.S. (2008), Comparison of slurry effect on machining characteristics of titanium in ultrasonic drilling, Journal of Materials Processing Technology, Vol. 1, pp. 200-205.
62. Shabgard, M.R., Ivanov, A. and Rees, A.(2006),Influence of EDM machining on surface integrity of WC-Co, Second International Conference on Multi-Material Micro Manufacture, pp. 331-334.
63. Choi,J.P.,Jeon,B.H.and Kim,B.H.(2007), Chemical-assisted ultrasonic machining of glass,Journal of Materials Processing Technology,Vol. 191 , pp. 153-156 .
64. Singh,R. and Khamba,J.S.(2007), Investigation for ultrasonic machining of titanium and its alloys,Journal of Materials Processing Technology, Vol.183, pp. 363-367.
65. Neugebauer,R. and Stoll,A.(2004), Ultrasonic application in drilling, Journal of Materials Processing Technology, Vol. 149, pp. 633-639,
66. Babitsky, V.I., Kalashnikov, A.N., Meadows and .Wijesundara, P.(2004), Ultrasonically assisted turning of aviation materials, Journal of Materials Processing Technology,Vol. 132 , pp. 157-167 **.**
67. Seah, K.H.., Wong,Y.S. and Lee, L.C. (1993), Design of tool holders for ultrasonic machining using FEM, Journal of Materials Processing Technology, Vol. 37, pp. 801-816.
68. Tsutsumi,C., Okano,K. and Suto,T.(1993), **,**High quality machining of ceramics**,** Journal of Materials Processing Technology,Vol. 37 , pp. 639-654.
69. Tuersley,I.P.,Jawaid,A.and Pashby,I.R.(1994), Review: Various methods of

machining advanced ceramic materials,Journal of Materials Processing Technology,Vol. 42 , pp. 377-390.

70. Pei, Z.J., Ferreira, P.M. and Haselkorn, M. (1995), Plastic flow in rotary ultrasonic machining of ceramics, Journal of Materials Processing Technology, Vol. 48, pp. 771-777.
71. Tosun,N., Cogun,C. and Tosun ,G.(2004), A study on kerf and material removal rate in wire electrical discharge machining based on taguchi method, Journal of Materials Processing Technology, Vol.152, pp.316-322.
72. Zhixin,J.,Jianhua,Z. and Xing,A.(1995),Ultrasonic vibration pulse electro-discharge machining of holes in engineering ceramics, Journal of Materials Processing Technology,Vol. 53, pp. 811-816.
73. Mult,H.C., Spur,G., Ing,D. and Holl, S.E.(1996), Ultrasonic assisted grinding of ceramics, Journal of Materials Processing Technology, Vol. 62, pp. 287-293.
74. Guo,Z.N., Lee, T.C., Yue,T.M. and Lau,W.S.(1997), A study of ultrasonic aided wire electrical discharge machining , Journal of Materials Processing Technology, Vol. 63, pp.823-828.
75. Kim, J.D. and Choi, H. (1997), Micro surface phenomenon of ductile cutting in the ultrasonic vibration cutting of optical plastics, Journal of Materials Processing Technology, Vol. 68, pp. 89-98.
76. Zhang, J.H., H., Lee, T.C., Lau, W.S. and Ai, X. (1997), Spark erosion with ultrasonic frequency, Journal of Materials Processing Technology, Vol. 68, pp. 83-88.
77. Guo, Z.N., Lee, T.C., Yue, T.M. and Lau, W.S. (1997), Study on the machining mechanism of WEDM with ultrasonic vibration of the wire, Journal of Materials Processing Technology, Vol. 69, pp. 212-221.
78. Lin,Y.C., Yan ,B.H. and Chang, Y.S.(2000), Machining characteristics of titanium alloy (Ti–6Al–4V) using a combination process of EDM with USM, Journal of Materials Processing Technology,Vol. 104, pp. 171-177.
79. Nath, C. and Rahman, M. (2008), Effect of machining parameters in ultrasonic vibration cutting, International Journal of Machine Tools and Manufacture, Vol. 48, pp.965-974.
80. Ghahramani, B. and Wang, Z.Y.(2001), Precision ultrasonic machining process: a case study of stress analysis of ceramic (Al_2O_3), International Journal of Machine

Tools and Manufacture, Vol. 41, pp. 1189-1208.

81. Chunxiang,M.,Shamoto,E., Moriwaki,T. and Wang, L.(2004), Study of machining accuracy in ultrasonic elliptical vibration cutting , International Journal of Machine Tools and Manufacture , Vol. 44 , pp. 1305-1310.
82. Akbari, J.and Azarhoushang, B.,(2007), Ultrasonic-assisted drilling of Inconel 738-LC, International Journal of Machine Tools and Manufacture, Vol.47, pp. 1027-1033.
83. Wiercigroch,M., Neilson,R.D.and Player,M.A.(1999), Material removal rate prediction for ultrasonic drilling of hard materials using an impact oscillator approach, Physics Letters A, Vol. 259, pp. 91-96.
84. Klopfstei ,M.J., Ghisleni,R., Lucca,D.A. and Brinksmeier, E.(2008), Surface characteristics of micro-ultrasonically machined silicon ,International Journal of Machine Tools and Manufacture , Vol. 48, pp. 473-476.
85. Soundararajan, V. and Radhakrishnan, V. (1986), An experimental investigation on the basic mechanism involved in ultrasonic machining, International Journal of Machine Tool Design and Research, Vol. 26, pp. 307-321.
86. Moriwaki,T., Shamoto,E. and Inoue,K.(1992), Ultraprecision ductile cutting of glass by applying ultrasonic vibration ,CIRP Annals–Manufacturing Technology, Vol. 41, pp. 141-144**.**
87. Zhou,M.,Wang, X.J., Ngoi,B.K. and Gan,J.G.(2002), Brittle ductile transition in the diamond cutting of glasses with the aid of ultrasonic vibration , Journal of Materials Processing Technology, Vol. 121, pp. 243-251.
88. Jin,M. and Murakawa, M.(2001), Development of a practical ultrasonic vibration cutting tool system , Journal of Materials Processing Technology, Vol. 113, pp. 342-347.
89. Lee, J.S., Lee, D.W.,Jung,Y.H. and Chung, W.S.(2002),A study on micro-grooving characteristics of planar lightwave circuit and glass using ultrasonic vibration cutting , Journal of Materials Processing Technology, Vol. 130, pp. 392-396.
90. Egash,K., Mizutani,K. and Nagao,T.(2002), Ultrasonic vibration drilling of microholes in glass , CIRP Annals – Manufacturing Technology, Vol. 51 , pp. 339-342.
91. Jain, N.K. and Jain, V.K. (2001), Modeling of material removal in mechanical type

advanced machining processes: a state-of-art review, International Journal of Machine Tools and Manufacture, Vol. 41, pp.1573-1635.

92. Moriwaki,T. and Shamot,E.(1995), Ultrasonic elliptical vibration cutting , CIRP Annals Manufacturing Technology, Vol. 44, pp. 31-34.

93. Kumabe,J., Fuchizawa, K., Soutome,T. and Nishimoto,Y.(1989), Ultrasonic superposition vibration cutting of ceramics , Precision Engineering, Vol 11, pp. 71-77.

94. Skelton, R.C. (1969), Effect of ultrasonic vibration on the turning process, International Journal of Machine Tool Design and Research, Vol. 9, pp. 363-374.

95. Xiao ,M., Wang,Q.M., Sato,K., Karube, S., Soutome,T. and Xu, H.(2006), The effect of tool geometry on regenerative instability in ultrasonic vibration cutting , International Journal of Machine Tools and Manufacture, Vol. 46, pp. 492-499.

96. Adithan, M. and Krishnamurthi, R.(1978), Structural alterations in the workpiece by ultrasonic drilling,Wear, Vol. 46, pp. 327-334.

97. Chunxiang,M.,Shamoto,E., Moriwaki,T., Wang, L.,Zhang ,Y.and Wang,L.(2005), Suppression of burrs in turning with ultrasonic elliptical vibration cutting , International Journal of Machine Tools and Manufacture, Vol. 45, pp. 1295-1300.

98. Nath, C., Rahman,M. and Andrew, S.S.(2007), A study on ultrasonic vibration cutting of low alloy steel ,Journal of Materials Processing Technology, Vol.192, pp. 159-165.

99. Onikura,H., Ohnishi,O., Take,Y. and Kobayashi, A.(2000), Fabrication of micro carbide tools by ultrasonic Vibration Grinding ,CIRP Annals-Manufacturing Technology, Vol. 49, pp. 257-260.

100. Kremer,D.,Lhiaubet, C. and Moisan,A.(1991), A study of the effect of synchronizing ultrasonic vibrations with pulses in EDM ,CIRP Annals – Manufacturing Technology,40, pp. 211-214.

101. Balamuth,L.(1966), Ultrasonic assistance to conventional metal removal, Ultrasonics,Vol. pp. 125-130.

102. Davim, J.P. (2003), Design of optimization of cutting conditions for turning metal matrix composites based on the orthogonal arrays, Journal of Materials Processing Technology, Vol.132, pp. 340-344.

103. Zaho J.,Wang L., and Li, H.(1991), A new side clamped ultrasonic vibration in cutting system with two stage amplification ,International Journal of Machine

Tools and Manufacture,Vol. 31,pp 249-256.

104. Rajukar, K.P., Wang, Z.Y. and Kuppattan, A. (1999), Micro removal of ceramic material (Al_2O_3) in the precision ultrasonic machining, Precision Engineering, Vol. 23, pp 73-78.

105. Chiang, K.T.and Tsai, D.C.(2008), Effect of silicon particles on the rapidly resolidified layer of Al-Si alloys in the electro discharge machining process, Int J Adv Manuf Technol,Vol. 36, pp.707–714.

106. Singh,R.,and Khamba,J.S. (2006), Investigation for ultrasonic machining of titanium and its alloys, International Journal of Machine Tools and Manufacture, Vol. 47, pp. 1027-1033.

107. Kremer, D. (1981), The state of the art of ulrtrasonic machining, Annals of the CIRP, Vol. 30, pp. 107-110.

108. Lee, W.M. and Liao, Y.S. (2007), Adaptive control of the WEDM process using a self-tuning fuzzy logic algorithm with grey prediction, Int J Adv Manuf Technol Vol. 34, pp.527–537.

109. Lia,Z.C., Liang,W.C., Pei, Z.P. and Treadwell,C. (2005), Edge chipping reduction in rotary ultrasonic machining of ceramics:finite element analysis and experimental verification, International Journal of Machine Tools and Manufacture , Vol.46,pp. 1469–1477.

110. Mohammadi, T., Ahmad, M., Sadrzadeh, M. and Razm,A.(2004), Separation of copper ions by electrodialysis using taguchi experimental design, Desalination ,Vol.169 ,pp. 21-31

111. Babitskya, V.I., Astashevb, V.K. and Meadowsa,A.(2007),Vibration excitation and energy transfer during ultrasonically assisted drilling, Journal of Sound and Vibration, Vol. 308, pp. 805–814.

112. Miller, G.E.(1957),Special theory of ultrasonic machining, Journal of Applied Physics,Vol.28,pp. 149-156.

113. Guzzo,P.L.,Shinohara,A.H.and Ralsan,A.(2004),A comparative study on ultrasonic machining of hard and brittle materials,Journal of Brazil Society of Mechanical Sciences and Engineering, Vol.26,pp 56-61.

114 Chiang, K.T.(2008), Modeling and analysis of the effects of machining parameters on the performance characteristics in the EDM process of Al_2O_3+TiC mixed ceramic, Int J Adv Manuf Technol,Vol. 37, pp.523–533. .

115 Anantha, R., Krishnamurthy, R., and Gokularathnam, C. (1989), Machining performance of toughened ceramic and cold compact alumina in ultrasonic drilling, Journal of Mechanical Working Technology, Vol.20, pp 365-375.

116 Singh, R. and Khamba, J., (2007), Taguchi technique for modeling material removal rate in ultrasonic machining of titanium, Materials Science and Engineering, Vol. 460, pp. 365-369.

117 Zhixin, J., Zhang and Xing, A.(1997), Study of a new kind of machining technology of USM and EDM, International Journal of Machine Tools and Manufacture, Vol.37, pp. 193-199.

118 Kumar,V. and Khamba, J.(2008), Statistical analysis of experimental parameters in ultrasonic machining of tungsten carbide using taguchi approach, Journal of the American Ceramic Society,Vol. 91, pp. 92-96.

119 Kumar,V. and Khamba, J.(2006), Experimental Investigation of ultrasonic machining of alumina-based ceramic composite, journal of the American Ceramic Society, Vol. 89, pp. 2413-2417.

120 Kumar,V. and Khamba, J.(2008), Optimization and modeling of process parameters in ultrasonic machining process, Proceedings of International conference on Processing and fabrication of Advanced materials XVII ,USA , pp. 242-252.

121 Kumar,V.,Khamba,J. ,Mohapatra,S. and Kumar,J.(2005), Ultrasonic machining (USM)and its application to machining of tough materials-A Review, Proceedings of International conference on Advances in Materials, Product Design & Manufacturing Systems (ICMPM), TamilNadu , pp. 837-843.

122 Kumar,V., Mohapatra,S. and Singh,P.(2006), Experimental investigation and optimization of performance characteristics of an ultrasonic machining (USM) process, Proceedings of International conference on Global manufacturing and Innovation (An advanced Optimization Technology approach,GMI) ,Coimbatore ,pp 1-9.

123 Kumar,V., Mohapatra,S. and Kumar,D.(2007), Surface modification in electric discharge machining with powder mixed fluid, Proceedings of International conference on “Recent Advances in Composite Materials (ICRACM), Varanasi.,pp. 1067-1072.

124 Zhang, Q.H.,Zhang, J.H., Jia,Z.X. and Ai,X.(1998), Fracture at the exit of the hole

during the ultrasonic drilling of engineering ceramics, Journal of Materials Processing Technology, Vol. 84, pp. 20-24.

125 Chen, Y.H., Tam,S.C.,Chen,W.L. and Zheng, H.Y.(1996), Application of taguchi method in the optimization of laser micro-engraving of photomasks,International Journal of Materials and Product Technology, Vol.11,pp. 333-344.

126 Mohan,B.,Rajadurai, A. and Satyanarayana,K.G.(2002), Effect of SiC and rotation of electrode on electric discharge machining of Al–SiC composite, Journal of Materials Processing Technology, Vol.124, pp. 297-304.

127 Gilmore,R.(1991),Ultrasonic machining:a case study, J Mater Process Technology, Vol.28, pp. 139–148.

128 Pei, Z.J., Khanna, N. and Ferreira, P.M. (1995) An investigation into rotary ultrasonic machining of structural ceramics- a review, Ceramic Engineering, Vol.16, pp.259–278.

129 Ya,G., Qin, H.W.,Yang,S.G. and Xu, Y.W.(2002) Analysis of the rotary machining mechanism, J Mater Process Technology, Vol.129,pp.182–185.

130 Yu, Z.Y., Rajurkar, K.P.and Tandon, A. (2004) Study of 3D micro-ultrasonic machining, Journal of Manufacturing Science and Engineering, Vol.126, pp.721-727.

131 Gilmore, R. (1995) Ultrasonic Machining and Polishing, Proc. Int. Symposium for Electro Machining, Switzerland, pp. 941–951.

132 Cano, T.D., Sansano, A., Rodriguez, M.A. Gonzalez, A. and Saja, J. (2002) Implement of a CCD spectrometer as experimental set-up to evaluate the emission of an electroluminescent device using the taguchi methodology, Measurement, Vol.35, pp. 257–268.

133 Chao, P.Y. and Hwang, Y.D. (1997) An improved taguchi's method in design of experiments for milling CFRP composite, INT. J. PROD. RES., Vol 35, pp 51-66.

134 Forouraghi, B. (1999), On utility of inductive learning in multi-objective robust design,Artificial Intelligence for Engineering Design, Analysis and Manufacturing, Vol 13, pp. 27–36.

135 Hunga, Y.H., et al. (2006) Optimizing the controller IC for micro HDD process based on taguchi method, Microelectronics Reliability ,Vol. 46, pp.1183–1188.

136 Lin, T.R. (2002) Optimization technique for face milling stainless steel with multiple performance characteristic, International Journal of Advanced

Manufacturing Technology, Vol.19, pp. 330-335.

137 Mertol, A. (2000) Application of the taguchi method to chip scale package (CSP) design, IEEE Trans Adv Package, Vol. 23, pp.266-276.

138 Ramulu, M. (2005) Ultrasonic machining effects on the surface finish and strength of silicon carbide ceramics, International Journal of Technology and Management, Vol.7, pp. 107-126.

139 Roy, R.K. (1990) A premier on the taguchi method, Van Nostrand Reinhold New York.

140 Sanchez, J.A., et al. (2006) Study on gap variation in multi-stage planetary EDM, International journal of machine tools and manufacture, Vol. 46, pp. 1598 1603.

141 Wang, H. and Wu, C.L. (2000) The mechanism of material removal in ultrasonic drilling of engg. ceramics, Proceeding of Institution of mechanical engineers, Vol.214, pp.805-810.

142 Kim, J. and Choi, H. (1998), Characteristics of chip generation by ultrasonic vibration cutting with extremely low cutting velocity, International Journal of Advanced Manufacturing Technology, Vol.14, pp 2-6.

143 Adithan, M.(1988),The hardening mechanism of tools in ultrasonic drilling-an investigation by an X-ray diffraction technique,Tribology International, Vol. 21, pp.163-168.

144 Teng,S.Y.,Hwang,S.J.(2007),Predicting the process induced warpage of electronic packages using the P–V–T–C equation and the taguchi method,Microelectronics Reliability ,Vol.47 , pp 2231–2241

145 Yang,S.C ., Huanga,K.S. and Lin ,Y.C.(2007), Optimization of a pulsed carbon dioxide snow jet for cleaning CMOS image sensors by using the taguchi method,Sensors and Actuators ,Vol. 139,pp 265–271

146 Weng, F.T.(2005),A study of cathode agitation in ultrasonic-aided micro electroforming, Int J Adv Manuf Technol,Vol. 25,pp 909–912

147 Zhong,Z.W. and Lin, G.(2006), Ultrasonic assisted turning of an aluminium-based metal matrix composite reinforced with SiC particles, Int J Adv Manuf Technol, Vol. 27,pp1077–1081

148 Abdullah,A. and Shabgard,M.R.(2007) Effect of ultrasonic vibration of tool on electrical discharge machining of cemented tungsten carbide (WC-Co), Int J Adv Manuf Technol , Vol.38, pp. 1137-1147.

149 Chang ,H.(2008) A data mining approach to dynamic multiple responses in taguchi experimental design, Expert Systems with Applications ,Vol. 35 ,pp 1095–1103

150 Brahim, T.R., Ru, S.G. and Cafer,C. (2008) A taguchi approach for investigation of some physical properties of concrete produced from mineral admixtures, Building and Environment ,Vol. 43 ,pp 1127–1137.

151 Sheng,J.W, Wua, Kwan,O. and Sheau,W.S.(2008) Robust design of micro bubble drag reduction in a channel flow using the taguchi method, Ocean Engineering Vol. 35,pp 856–863

152 Zhao,W.,Wang,Z.,Di,S.,Chi,G.and Wei,H.(2002),Ultrasonic and electric discharge machining to deep and small hole on titanium alloy,Journal of Materials Processing Technology, Vol. 120,pp 101-106

153 Phadke, M.S. (1989), Quality engineering using robust design, Prentice Hall Englewood cliffs, NJ.

154 Bagchi,T.P.(1993),Taguchi methods explained-Practical steps to robust design, Prentice Hall of India Pvt. Ltd

155 Ross, P.J. (1988), Taguchi techniques for quality engineering, Mcgraw Hill Book Company,New york.

156 Ezugwa,E and Wang,Z.(1997),Titanium alloys and their machinability-A review, Journal of Materials Processing Technoloy,Vol. 68,pp 262-274.

157 Jain, V.K. (2004), Advanced machining processes, Allied publishers, pp.28-55.

158 Gary F.(1987), Non traditional manufacturing processes,Marcel Dekker,Inc.,pp. 67-86.

159 Zahra,A., Nidal,H. and Taysir,N.H.(1997), Calibrated methods for ultrasonic on line monitoring of gradual wear during turning operation,International Jounal of Machine Tools and Manufactire,Vol.37,pp 1475- 1484.

160 McGeough J.A. (1988) Advanced methods of machining, Chapman and Hall, London,pp 170-198.

161 Frederick J.R. (1965) Ultrasonic engineering, John Wiley and Sons Inc., New York.

162 Shaw M.C.(1956) Ultrasonic grinding, Microtechnic,Vol.10,pp.257-265.

163 Xiao,M., Sato,R., Karube,S. and Soutome,T. (2006), The effect of tool nose radius in ultrasonic vibration cutting of hard metal, International Journal of Machine Tools and Manufacture, Vol. 43, pp. 1375-1382.

164 Ozgedik,A. and Cogun, C.(2006), An experimental investigation of tool wear in electric discharge machining, Int J Adv Manuf Technol, Vol.27, pp. 488–500.

APPENDIX I

Introduction of tungsten carbide

Tungsten carbide as a super hard and high wear-resistant material has been used widely in industries. The common method for producing tungsten carbide components is by powder metallurgy technology. However, for small quantity production, such as product prototyping, this method is obviously too costly and time consuming. It is expected to make the prototypes by material removal process, such as cutting, if the ductile cutting of tungsten carbide can be achieved. To increase the life of carbide tools, these are sometimes coated. Two such coatings are TiN (titanium nitride) and TiC (titanium carbide). Most coatings generally increase a tool's hardness and or lubricity. A coating allows the cutting edge of a tool to cleanly pass through the material without having the material stick to it. Tungsten Carbide has hardness close to diamond. This makes it a commonly used material for applications requiring high strength and wear resistance. Tungsten carbide is harder than sapphire and retains a superior edge after extensive use. Tungsten carbide is not a metal alloy but, as it is the product of powder metallurgy so very fine grains of two materials are mixed and fused under high temperature and pressure. While the fine knife edge is vulnerable to chipping under lateral forces, this composite material is exceptionally strong in compression, which is the dominant force applied during sectioning. The hardness of tungsten carbide contributes greatly to its durability when sectioning. Durability depends on many factors including types of sample being cut, frequency of use and care taken in handling the blades.

Properties of tungsten carbide

Molar mass (g/mol)	195.86
Appearance	grey-black solid
Density (g/cm^3) and phase	15.8 , solid
Solubility in water	Insoluble
Melting point (°C)	2870
Boiling point (°C)	6000
Thermal conductivity (W/(m K)	84.02
Tensile strength (GPa)	0.3448

Applications of tungsten carbide

Military use: Tungsten carbide is often used in armor-piercing ammunition, especially where depleted uranium is not available. The first use of W_2C projectiles occurred in Luftwaffe tank-hunter squadrons, which used 37 mm auto cannon equipped Ju-87G Stuka attack planes to destroy soviet T-34 tanks in WWII. Owing to the limited german reserves of tungsten, W_2C material was reserved for making machine tools and small numbers of projectiles for the most elite combat pilots, like Hans Rudel.Tungsten carbide ammunition can be of the sabot type (a large arrow surrounded by a discarding push cylinder) or a sub caliber ammunition, where copper or other relatively soft material is used to encase the hard penetrating core, the two parts being separated only on impact. The latter is more common in small-caliber arms, while sabots are usually reserved for artillery use.

Sports: Hard carbides, especially tungsten carbide, are used by athletes, generally on poles which impact hard surfaces. Trekking poles used by many hikers for balance and to reduce pressure on leg joints, generally used carbide tips in order to gain traction when placed on hard surfaces. This is because such carbide tips last much longer than other types of tips.

APPENDIX II

Introduction of stellite

Stellite is the most generally useful cobalt alloy, having excellent resistance to many forms of mechanical and chemical degradation over a wide temperature range.It retains a reasonable level of hardness up to above 800°C. Stellite is a commercial wear-resistant cobalt-based alloy that has found many applications against wear in different environments and at elevated temperatures. Its high resistance to mechanical attack and chemical degradation over a wide temperature range results in its wide use as a valve seat material. The good performance of stellite at elevated temperatures is attributed to its high-temperature abrasion resistance. However, when subjected to the attack combining heat, oxidation and wear, the oxide film could fail by hard particle abrasion and thus increasing the wear rate. The mechanical properties of the oxide film are important. In addition, the interfacial bonding strength of the oxide film is also an important factor affecting the overall resistance to wear at elevated temperatures. Considerable efforts

have been made to improve the oxide scale adherence for Co and Cr based alloys in order to control friction and wear at high temperatures. Oxygen-active elements such as yttrium, when alloyed into Co or Cr based alloys, may improve the high-temperature wear resistance of the alloys.

Properties of stellite

Hardness (HRC)	43.3
Density (g/cm^3)	0.87
Specific gravity	8.46
Solidus (^0F)	2340
Liquidus (^0F)	2540
Electrode potential (V)	0.25
Electrical resistivity (micro Ω -inch)	41.73
Thermal expan. coefficient ($10^{-6}/K$)	11.34
Thermal conductivity (W/mk)	14.82

APPENDIX III

Introduction of Diamond

The diamond finds increasing use as a thermal management material in electronic packaging of high power laser diodes, multi-chip modules, and other microelectronic devices. Numerous development tests using diamond heat spreaders have confirmed the enhanced ability to reject heat provided by diamond. For microprocessors, diamond heat spreaders can deliver increased clock rates. In airborne electronics, diamond heat spreaders can increase device packing density, simplify cooling system design, and provide increased MTBF with reduced weight and volume. Laser diodes mounted on diamond heat spreaders deliver higher output power, enhancing throughput in material processing and direct-to-plate printing operations. Thicker diamond will improve thermal performance to a diminishing extent, and will add to the cost of the component. The diamond heat spreader should ideally have length and width dimensions at least 5 times those of the heat source at the point of attachment to the heat spreader. The diamond components or coatings can be used as wear resistant elements in paper mills, high speed fabric mills, and other extremely abrasive manufacturing environments and processes. Both thick-film and coated PCD cutting tools are used to good advantage in non-ferrous

machining operations. The diamond wear elements can be attached to base materials using conventional epoxy or silicone adhesives.

Properties of Diamond

Tensile strength (Gpa)	1.2
Compressive trength (Gpa)	110
Sound velocity (m/s)	$18x10^3$
Density (g/cm^3)	3.52
Young's modulus(Gpa)	1.22
Poisson's ratio	0.2
Thermal expansion coefficient (/k)	$11\ x10^{-5}$
Thermal shock parameter (W/m)	$3\ x10^7$
Dielectric constant	5.7
Dielectric strength (V/cm)	10^7
Bandgap (eV)	5.45
Resistivity (Ω -cm)	10^{13}-10^{16}

APPENDIX IV

Introduction of titanium

Titanium got its name from "TITAN", a giant greek mythology. Titanium is a light metal .It is strong and highly resistant to corrosion. Titanium is bio-compatible because it is non allergenic. Its melting point is higher than that of steel. Although heat conductivity of titanium is almost the same as that of stainless steel, its weight is almost half of stainless steel. Titanium is non-toxic and easy to clean.

Properties of titanium alloy (TITAN15)

Density(g/cm3)	4.51
Melt range (^{0}C+15)	1677
Specific heat (J/gmK)	0.54
Electric resistivity(μ Ω -cm)	56
Yield stress/density ($*10^6$Nm/kg)	78
UTS(MPa)	491
Thermal cond.(W/mk)	16.3
Beta trans(^{0}C+15)	913
0.2% proof (MPa)	276
Th. exp. coeff. 0-100^{0}C($10^{-6}K^{-1}$)	8.6
Th. exp. coeff .0-300^{0}C($10^{-6}K^{-1}$)	9.2

Elong.(%)	20
Fatigue limit (% of tensile strength)	50
Tensile strength. (MPa)	345
Poisson's ratio	0.36
Tensile str./density (*10^6Nm/Kg)	107

Properties of titanium alloy (TITAN31)

Density(g/cm3)	4.42
Melt range (^{0}C+15)	1649
Specific heat (J/gmK)	0.56
Electric resistivity(μ Ω -cm)	170
Yield stress/density (*10^6Nm/kg)	206
UTS(MPa)	994
Thermal cond.(W/mk)	7.2
Beta trans(^{0}C+15)	999
0.2% proof (MPa)	828
Th. exp. coeff.0-100^{0}C(10^{-6}K^{-1})	8.8
Th. exp. coeff.0-300^{0}C(10^{-6} K^{-1})	9.2
Elongantion(%)	10
Fatigue limit (% of tensile strength)	55-60
Tensile strength (MPa)	345
Poisson's ratio	0.31
Tensile str./density (*10^6Nm/Kg)	226
Fracture toughness (Mpa-m$^{1/2}$)	75